PNNL-13400

Groundwater Flow and Transport Calculations Supporting the Immobilized Low-Activity Waste Disposal Facility Performance Assessment

M. P. Bergeron
S. K. Wurstner

December 2000

Prepared for
the U.S. Department of Energy
under Contract DE-AC06-76RLO 1830

Pacific Northwest National Laboratory
Richland, Washington 99352

PACIFIC NORTHWEST NATIONAL LABORATORY
operated by
BATTELLE MEMORIAL INSTITUTE
for the
UNITED STATES DEPARTMENT OF ENERGY
under Contract DE-AC06-76RLO 1830

Printed in the United States of America

Available to DOE and DOE contractors from the
Office of Scientific and Technical Information, P.O. Box 62, Oak Ridge, TN 37831;
prices available from (865) 576-8401.

Available to the public from the National Technical Information Service,
U.S. Department of Commerce, 5285 Port Royal Rd., Springfield, VA 22161

PNNL-13400

Groundwater Flow and Transport Calculations Supporting the Immobilized Low-Activity Waste Disposal Facility Performance Assessment

M. P. Bergeron
S. K. Wurstner

December 2000

Prepared for
the U.S. Department of Energy
under Contract DE-AC06-76RLO 1830

Pacific Northwest National Laboratory
Richland, Washington 99352

Summary

This report summarizes the Hanford Site-Wide Groundwater Model and its application to the Immobilized Low-Activity Waste (ILAW) Disposal Facility Performance Assessment (PA). The site-wide model and supporting local-scale models are used to evaluate impacts from the transport of contaminants at a hypothetical well 100 m downgradient of the disposal facilities and to evaluate regional flow conditions and transport from the ILAW disposal facilities to the Columbia River. These models were used to well-intercept factors (WIFs) or dilution factors from a given areal flux of a hypothetical contaminant released to the unconfined aquifer from the ILAW disposal facilities for two waste-disposal options: 1) a remote-handled trench concept and 2) a concrete-vault concept. The WIF is defined as the ratio of the concentration at a well location in the aquifer to the concentration of infiltrating water entering the aquifer. These WIFs are being used in conjunction with calculations of released contaminant fluxes through the vadose zone to estimate potential impacts from radiological and hazardous chemical contaminants within the ILAW disposal facility at compliance points.

Transport model calculations for a basecase considered a six trench configuration representing a remote-handled-trench concept and were based on local-scale flow conditions postulated after site-closure. These conditions were developed based on boundary conditions provided by the steady-state simulation of Post-Hanford flow conditions performed with the site-wide model.

Regional and local-scale flow results for the base case show that groundwater beneath the ILAW site moves in a southeasterly direction and then an easterly direction over about 15 km before reaching the Columbia River. For the six remote-handled trench configuration examined in the base case, predicted concentration profiles reach steady state within about 10 yr after the start of source release at the water table.

Concentration levels, based on an assumed infiltration rate of 4.2 mm/yr and input concentration of 1 Ci/m^3 at the source release area, reach a maximum value of 1.1 x 10^{-3} Ci/m^3 at a hypothetical 100-m well downgradient of the site and 7.8 x 10^{-4} Ci/m^3 at a 1-km well. For this assumed recharge rate (4.2 mm/yr), the calculated WIFs would be 1.1 x 10^{-3} at the 100-m well and 7.8 x 10^{-4} at the 1-km well.

Calculations of the WIFs in this analysis in general yielded different levels of dilution than those developed in previous calculations of an ILAW disposal-facility performed by Lu (1996). The differences in the calculated WIFs can be attributed to a number of factors.

The Lu (1996) analysis estimated the water table beneath the facility to be at about the same level considered in this analysis, but assumed that the water table would be situated in the Ringold Formation. The current model predicted that the water table would largely be along the edge of a buried channel containing very permeable Hanford Formation. The difference in the distribution and

hydraulic properties between the two conceptual models has led to higher levels of dilution using the current model. Additional work with the current model will be needed to evaluate the predictability of the WIF as a function of the hydraulic properties of the major hydrogeologic units beneath the facility.

Differences in the conceptual model of the unconfined aquifer used in the current analysis resulted in differences in the simulated direction of flow. The analysis by Lu (1996) predicted an easterly flow direction. The current local-scale model predicts a southeasterly flow direction. This difference in flow direction may be primarily attributable to including the highly permeable ancestral channel of the Columbia River, which contains the Hanford Formation in this analysis. The differences may also be a function of including natural recharge in the current regional-scale and local-scale analysis. Further work with the local-scale model will be needed to evaluate the predictability of the WIF as a function of the direction of flow.

Key factors affecting the current calculations appear to be related to the use of higher estimated hydraulic conductivities and groundwater velocities beneath the facility by the current model. The hydraulic conductivities used by the current model and the previous model used by Lu (1996) for the Ringold Formation are on the same order of magnitude (between 40 and 300 m/day in the current model; between 70 and 245 m/day in the model used by Lu [1996]). However, the current model contains areas of the Hanford formation beneath the facility and as a result has areas of very high permeability (between 2,200 and 30,000 m/day) in the area of the source release.

Uncertainties in the following key factors affecting calculated WIFs were investigated with sensitivity analyses:

- the source-release area at the water table
- the vertical position of the post-closure water table and the associated direction of groundwater flow
- the lateral position of the Hanford-Ringold Formation contact
- the hydraulic properties of Hanford and Ringold sediments.

Results of these analyses suggested that calculated WIFs are linearly related to the source-release area over the range of assumed surface areas of release. Calculated WIFs are also affected by the long-term predicted position of the water table and the resulting estimated distribution of hydraulic properties underlying the ILAW disposal facilities. The new facility is located in an area of the Hanford Site where it is underlain by an ancestral channel of the Columbia River that consists of highly permeable sediments of the Hanford Formation. For the predicted water table position used in this analysis, the current interpretation places the contact between the Hanford Formation and the underlying less-permeable Ringold Formation along the south edge of the new ILAW disposal facility area.

Assumptions made about long-term regional natural recharge rates and boundary conditions are uncertain and can also change the predicted position of the water table and the position of the contact between the Hanford and Ringold sediments. Higher assumed rates of recharge can increase the water-table elevation and the level of saturation in the Hanford-formation sediments, leading to lower calculated WIFs (i.e., higher levels of dilution) from releases from the ILAW facilities.

Estimates of the hydraulic properties used in this assessment are based on past calibration of the site-wide model that provides a reasonable approximation of the regional observations and trends. Estimates of these properties on the local-scale model used in this analysis are uncertain and can affect calculated WIFs. Reducing the estimated hydraulic conductivities of the Hanford formation underlying the disposal facilities to those estimated for the Ringold Formation resulted in an order of magnitude increase in the WIFs (i.e., less dilution) from releases from the ILAW disposal facilities.

Reference

A. H. Lu. 1996. *Contaminant Transport in the Unconfined Aquifer, Input to the Low Level Tank Waste Interim PA*, WHC-SD-WM-RPT-241, Westinghouse Hanford Company, Richland, Washington.

Acronyms

CFEST	Coupled Fluid, Energy, and Solute Transport
Dl	longitudinal dispersivity
DOE	U.S. Department of Energy
DOE-RL	DOE-Richland Operations
Dt	transverse dispersivity
HPDE	high density polyethylene
ILAW	Immobilized Low-Activity Waste
LLW	low-level waste
PA	Performance Assessment
PUREX	Plutonium-Uranium Extraction
RCRA	Resource Conservation and Recovery Act
RI/FS	Remedial Investigation/Feasibility Study
RL	Richland Operations Office
WIF	Well Intercept Factor

Contents

Figures

Tables

1.0 Introduction

This report summarizes methods and results of groundwater flow and transport analyses used to support the Immobilized Low Activity Waste (ILAW) disposal facility performance assessment (PA). The waste stored in the ILAW disposal facility will migrate downward through the vadose zone into the underlying unconfined aquifer system. Contaminants entering into the unconfined aquifer will migrate laterally within the aquifer until they are discharged into the Columbia River downgradient of the disposal facilities.

The flow and transport analysis applied to this assessment used site-wide and local-scale models. A regional scale site-wide groundwater model was used to evaluate regional flow conditions and transport from the ILAW disposal facility to the Columbia River. Local-scale models were used to evaluate impacts from the transport of contaminants at a hypothetical well 100 m downgradient of the disposal facility.

The development and calibration of the site-wide model that was used are described in detail in Wurstner et al. (1995) and Cole et al. (1997). The primary objectives in using the site-wide model to support the ILAW PA are to 1) develop a conceptual model describing the general flow regime for post-Hanford conditions following the cessation of past and current liquid-waste discharges to the vadose zone and groundwater systems at the Hanford Site, 2) ensure that hydraulic properties used for both the site-wide groundwater model and local-scale models are consistent and adequately simulate local-scale conditions, and 3) evaluate the regional distribution and concentration trends of contaminant plumes that could potentially develop beneath the ILAW disposal facility.

Section 2.0 of this report provides an overview of the Hanford Site and describes the disposal-facility design. Section 3.0 describes the relation of the groundwater modeling component of the ILAW disposal facility PA to other model components used in the analysis. Section 4.0 provides a brief history and chronology of the development of the site-wide conceptual and numerical model framework used in the analysis, and the data and methods used in performing the groundwater analysis within the overall ILAW PA methodology. Section 5.0 provides groundwater flow and transport calculations. Section 6.0 provides the results from applying the groundwater flow and transport analysis of well intercept factors (WIFs) calculated using both the local-scale and site-wide scale models. Section 7.0 provides results of a series of sensitivity analyses that were performed to evaluate the effect of several factors on modeling results, and conclusions are provided in Section 8.0.

2.0 Disposal Facility And Site Information

2.1 Geography of the Hanford Site

The Hanford Site is a 1450-km^2 (560-mi^2) area of semiarid land located in south-central Washington State (Figure 2.1). The Hanford Site is owned by the U.S. Government and restricted to uses approved by the U.S. Department of Energy (DOE). The major cities in the region are Seattle, Portland, and Spokane, which are more than 160 km (100 mi) away from the Hanford Site.

The major geographical features of the region are the nearby rivers and mountains. The Columbia River, which forms the eastern boundary of the Hanford Site, is an important source of water and hydroelectric power for the region. Other important rivers near the Hanford Site are the Yakima River to the southwest and the Snake River to the east. The Cascade Mountains, about 160 km (100 mi) to the west, have an important effect on the climate of the area.

Figure 2.2 shows the locations of two disposal sites that have been considered in the 1998 ILAW PA: the ILAW disposal site (located southwest of the Plutonium-Uranium Extraction [PUREX] Plant) and the existing vaults (located east of the PUREX plant and formerly known as the Grout Vaults). Both sites are located in the 200 East Area within the Hanford Site. The current plan is to use the ILAW disposal site as the primary site for disposal of ILAW waste.

2.2 Disposal Facility Design

According to Mann et al. (2000), the ILAW disposal plan is to use the existing disposal vaults from the grout program, suitably modified to receive ILAW packages, and build a new disposal facility of concrete vaults that is currently in the early design phase. In December 1999, DOE identified the remote-handled trench as the baseline concept for ILAW disposal at Hanford (Taylor 1999).

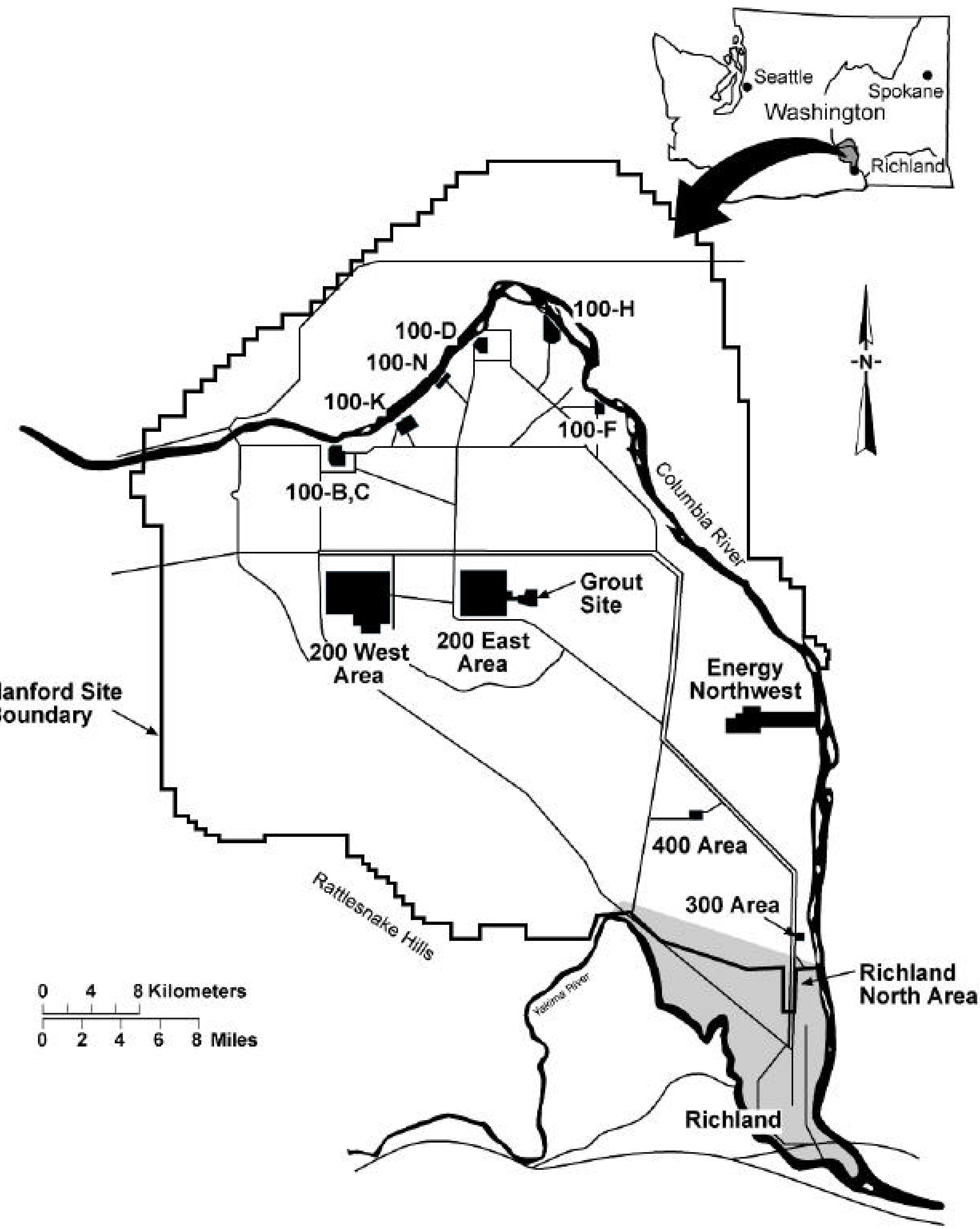

Figure 2.1. Map of the Hanford Site and Its Location Within Washington

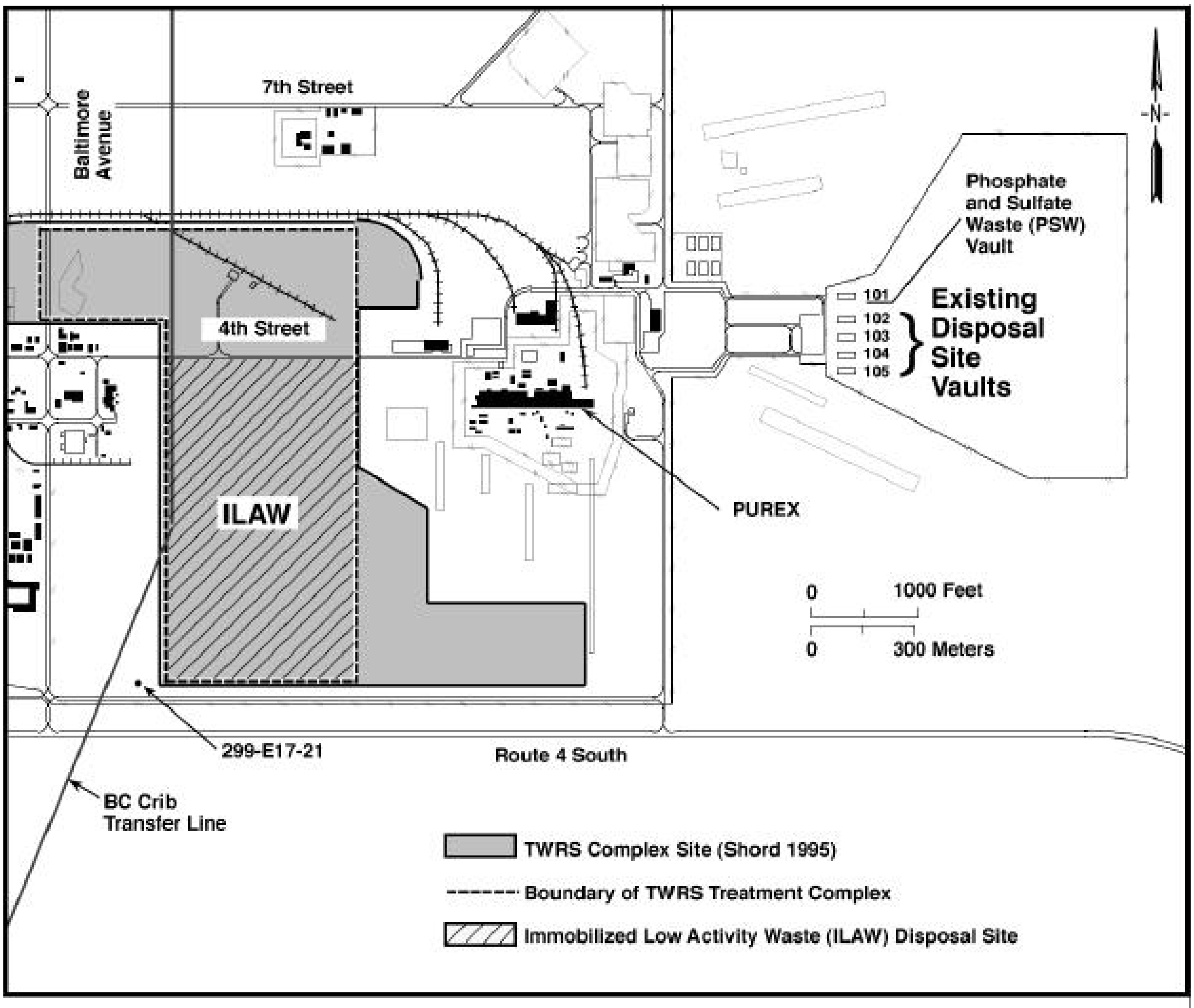

Figure 2.2. Location of the ILAW Disposal Site in the 200 East Area

2.2.1 New ILAW Disposal Area

2.2.1.1 Remote-Handled Trench Pre-Conceptual Design

The remote-handled trench concept has been chosen as the baseline for the ILAW Disposal Project (Taylor 1999). This trench concept is similar to the Radioactive Mixed Waste Burial Trench that was designed and constructed to accept solid waste at Hanford. Under the ILAW disposal plan described below, the disposal facility is a Resource Conservation and Recovery Act (RCRA)-compliant landfill (i.e., double-lined trench with leachate collection system). Many operational aspects and ancillary activities of the landfill (e.g., leachate collection and disposition, stormwater control, installation of surface barrier at closure, etc.) would be similar to those incorporated into the Radioactive Mixed Waste Burial Trench. However, operational activities for receiving ILAW packages and placing them in the trench would be modified to accommodate the different package sizes of remote-handled ILAW packages.

The conceptual-design layout of the six remote-handled trenches conceptualized for the ILAW disposal site is shown schematically in Figure 2.3. The trench side slopes are in a ratio of 3:1. The dimensions shown in Figure 2.3 represent the inner trench dimensions. Figure 2.4 shows the conceptual-design layout for the waste package loading into the remote-handled trench.

The design of the closure cover shown in Figure 2.4 is not yet complete. For this report, the closure cap (surface barrier) is assumed to have the same relative thickness, materials, and slope as the modified RCRA subtitle C closure cap defined in Puigh (2000, Section 4). A capillary break is assumed to consist of a 1-m-thick sand layer immediately below the surface barrier and gravel between the top of the trench and the sand layer. The sand and gravel layers together are 4 m over the center of the trench and have a 2% slope toward the long edge of each trench.

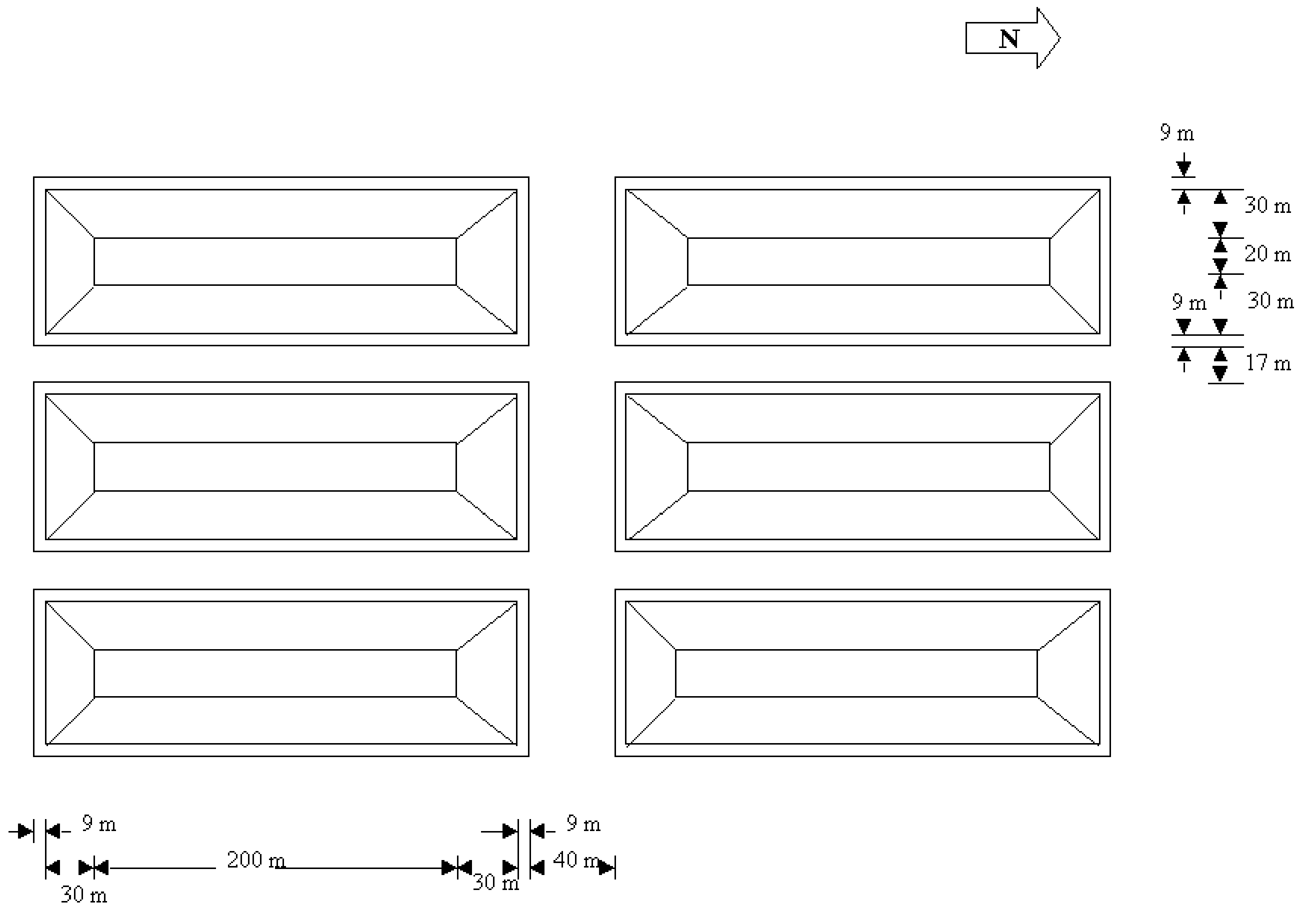

Figure 2.3. Remote-Handled Trench Pre-Conceptual Layout at the ILAW Disposal Site

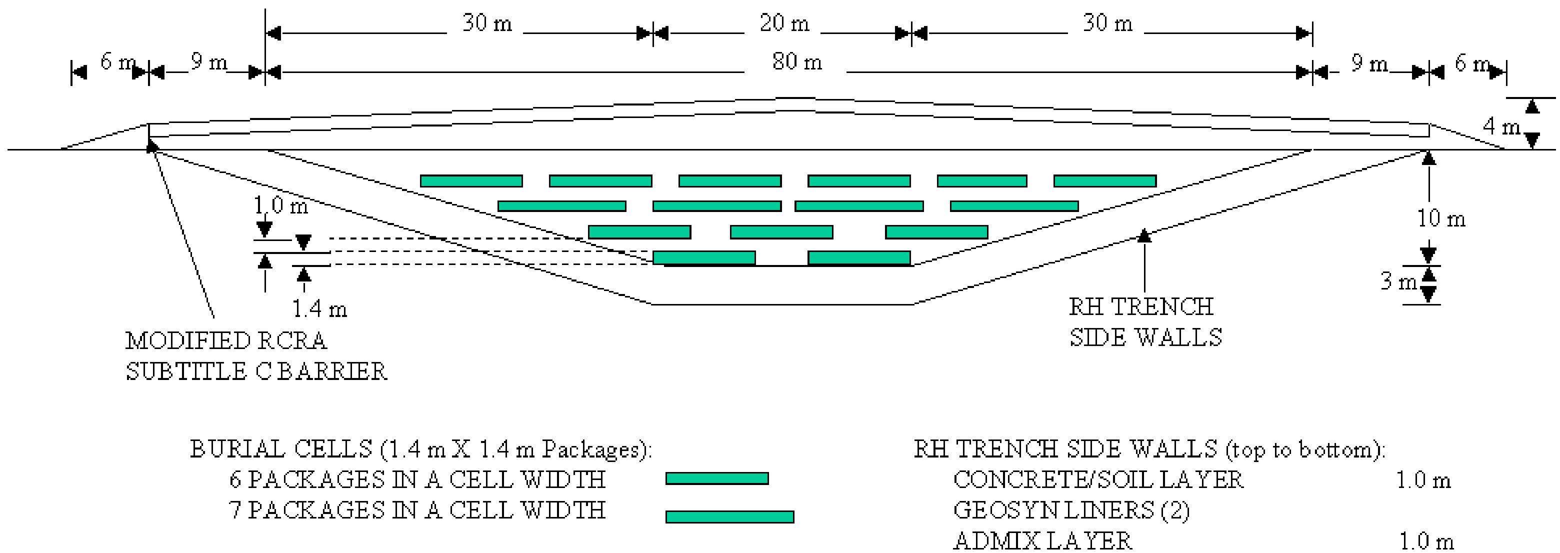

Figure 2.4. Remote-Handled Trench Pre-Conceptual Design

2.2.1.2 Concrete-Vault Conceptual Design

An alternate set of calculations for a concrete-vault design is based on an earlier conceptual design for the new ILAW disposal facility (Pickett 1998) that uses a long concrete-vault concept divided into cells. Each vault is an underground, open-topped, concrete vault approximately 23 m (76 ft) wide, 207.8 m (686 ft) long, and 11.0 m (26.7 ft) high. The top of the vault walls extends 1 m (3.3 ft) above grade. Each vault is divided into 11 cells, separated by concrete partition walls (0.45 m [1.5 ft] thick). Each vault can accommodate six layers of waste packages with 168 waste packages in each layer. Assuming that the waste package geometry is 1.4 m^3, the spacing between each waste package (including the walls) is 9.3 cm (3.7 in.) along the width, 11.5 cm (4.5 in.) along the length, and 10 cm (4 in.) between each layer of waste packages. Based on the Kirkbride (1999) estimate of approximately 70,000 packages needed for disposal of all planned ILAW waste, only seven new disposal vaults would be required to complete the disposal of all ILAW (assuming the existing vaults are not used).

Each vault is built above a RCRA-compliant leak detection and collection system. It consists of a cast-in-place reinforced concrete basin approximately 209.5 m (687.0 ft) long and 24.7 m (81 ft) wide with walls 1.07 m (3.5 ft) high. The basin floor is 0.6 m (2 ft) thick and contains steel reinforcing bars within. The catch basin is lined with two flexible membrane liners, and on top of these lies a layer of gravel with a perforated collection pipe routed to sumps, one at each end of a vault. Liquids entering the sump can be removed by using a portable pump lowered down a riser pipe.

Interim closure for each filled cell in the new disposal facility will consist of placing concrete shield covers (assumed to be 1.4 x 1.4 x 0.3 m [4.6 x 4.6 x 1 ft]) on the top layer of waste packages. The filler-material layer is assumed to have a depth of 0.3 m (1 ft) above the concrete shield covers. A "controlled density fill" consisting of a mixture of Portland cement, fly ash, aggregate, water, and admixtures is then placed on top of the filler-material layer. The depth of the "controlled density fill" is 0.45 m (1.5 ft). A waterproof membrane layer (assumed to be 60 mil, high-density polyethylene [HPDE]) is placed over the interim-closed vault. After all cells in the vault have been filled and interim-closed, a closure cap consisting of a capillary break followed by a modified RCRA subtitle C surface barrier will be placed over the entire vault (Puigh 2000). Again, it is assumed that the capillary break consists of a 1-m-thick sand layer immediately below the surface barrier and gravel between the top of the concrete vault and the sand layer. The sand and gravel layers together are assumed to be 4 m (13 ft) over the center of the trench and to have a 2% slope towards the long edge of each vault.

2.2.2 Existing Disposal Area

According to Puigh (1999), current disposal plans will use disposal vaults at the existing ILAW disposal facility (Figure 2.2), suitably modified to receive ILAW waste packages. The existing disposal vaults were originally constructed by a previous waste program in the late 1980s and early 1990s. They were designed to contain a liquid low-level waste (LLW) grout mixture during a curing and solidification period and to serve as a disposal structure for the resulting grouted waste monolith. Five vaults were originally constructed. One of the vaults was filled before the program was terminated, leaving four empty vaults available for use.

According to Puigh (1999), each vault is 37.6 m (123.5 ft) long and 15.4 m (50.5 ft) wide, with a roof clearance of 10.4 m (34.0 ft), providing 5,579 m^2 (6,236 ft^2) of floor space. The vaults are constructed of reinforced concrete and are designed and constructed in compliance with RCRA requirements for both hazardous waste surface impoundments and land disposal units. Each vault is built above a RCRA-compliant leak-detection and collection system. The leak-detection system consists of a sealed concrete slab sloped to a collection sump fitted with a riser pipe to the land surface and is capable of collecting, detecting, sampling, and removing any leachate that might escape from the primary structure.

A conceptual design activity has been performed to modify the existing disposal vaults to accept and serve as a disposal facility for the ILAW wastes (Pickett 1998). The modifications will consist of the following elements:

- Existing asphalt layer and concrete topping layer above the precast concrete roof slabs will be removed from all vaults.
- Side wall and wall extensions 1.8 m (6.0 ft) high will be added to the original top of the side and end walls in each vault.
- Rails for a gantry crane will be placed on the top of the side-wall extensions along the full length of the vaults to support the unloading of ILAW waste disposal packages from transportation vehicles.

3.0 Relation of Groundwater Modeling to Performance Assessment Modeling of ILAW Disposal System

This section of the report summarizes the relationship of groundwater modeling calculations described in this report to the overall performance assessment of the ILAW disposal facility. Topics covered include:

- Overall Strategy for Disposal Facility Assessment
- Integration of Results of Individual Model Components

3.1 Overall Strategy for Disposal Facility Assessment

In Mann et al. (2000), the overall strategy for looking at the long-term performance of the ILAW disposal facility involves a conceptual model that considers the following eight processes or steps as illustrated in Figure 3.1:

- The movement of infiltrating water as it leaves the very-near-surface soil region above the proposed disposal facility

- The movement and diversion of water as it migrates downward and interacts with an intact capillary barrier situated above the disposed wastes

- For water that is not diverted away by the capillary barrier, the chemical interaction of infiltrating water as it is modified by the local geochemical environment and waste form, accumulating contaminants.

- The movement of contaminant-laden water as it leaves the disposal facility, carrying contaminants with it. Some contaminants may interact with the material in the disposal facility, slowing the release of the contaminants to the surrounding natural environment.

- The movement of contaminated water as it moves through the undisturbed, unsaturated zone (vadose zone) below the disposal facility down to the unconfined aquifer. Some of the contaminants in the water undergo some geochemical sorption as they are transported through the vadose zone.

- The movement and mixing of contaminated water in the vadose zone with the water in the unconfined aquifer. Resultant contaminated groundwater migrates laterally to the point of water use where it is extracted from the aquifer by wells and brought to the surface, or until it reaches the Columbia River.

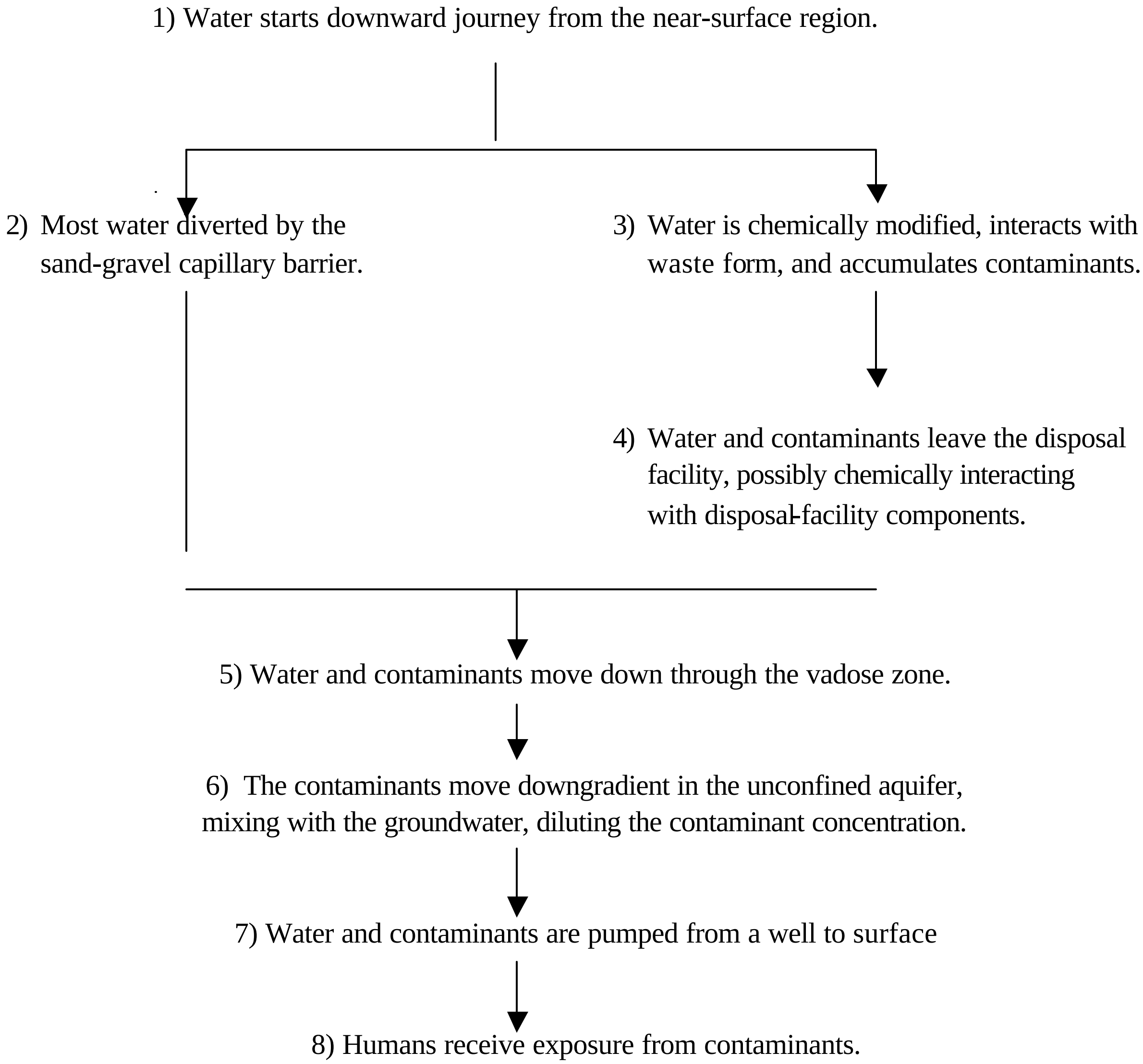

Figure 3.1. Eight Sequential Steps for the Groundwater Pathway

- The use of water containing radionuclides or other hazardous chemical contaminants then results in human exposure through a variety of pathways (ingestion, inhalation, and external radiation).

According to Mann et al. (2000), each component of the conceptual model of the ILAW disposal-facility PA was analyzed separated as illustrated in Figure 3.2 using a variety of component-specific computational models. A coupled, unsaturated flow, and reactive contaminant-transport model of the near field in the vicinity of the disposal facility was used to analyze the near-field interaction of infiltrating water with the ILAW disposal facilities and the proposed glass waste form. This model was based on the STORM code (Bacon et al. 1999). An unsaturated flow and transport model of the vadose zone above and below the disposal facility was used to estimate the moisture flow into the disposal facility and the moisture flow and contaminant transport from the disposal facility into groundwater. This model was based on the VAM3DF code (Huyakon et al. 1999)

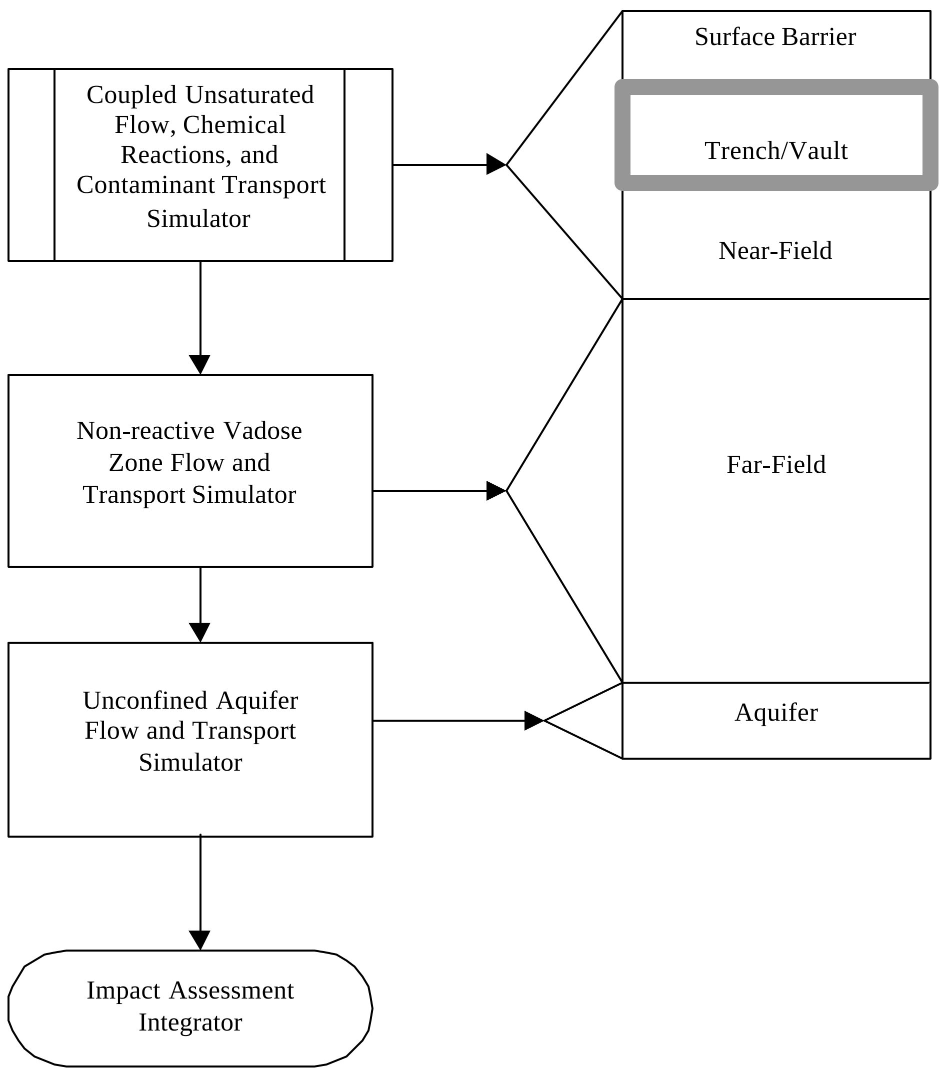

Figure 3.2. Modeling Strategy for Assessing ILAW Disposal System

A local-scale and regional-scale model of the unconfined aquifer (Wurstner et al. 1995; Cole et al. (1997) was used to evaluate the mixing of contaminated water from the vadose zone into the underlying aquifer and the subsequent lateral migration of contaminants to receptor points and/or points of groundwater discharge along the Columbia River. This model was based on the Coupled Fluid, Solute and Energy Transport (CFEST) code (Gupta et al.1987; Gupta 1996). - Mann et al. (2000) provided specific descriptions of the underlying assumptions and the implementation of the disposal facility and the vadose zone computational models and codes for the ILAW PA.

3.2 Integration of Results of Individual Model Components

According to Mann et al (2000), the computational code, INTEG (Mann 1996), calculates a specific impact (whether dose rate or concentration level) based on the inventory, vadose zone transport, aquifer transport, and dosimetry factors. The dose rate calculated depends on the type of dosimetry factor (i.e., all-pathways, drinking water). The program solves the following equation for each year under consideration.

$$\textit{Response} = \sum_I I_i(t)\, \Gamma_i(t)\, w_i\, D_i \,/\, (r\, A) \qquad (3.1)$$

where

I_i = the amount (or inventory) of radionuclide i (Ci). The time-dependent value is calculated by INTEG, based on the initial inventory and on decay and the ingrowth from other radionuclides.

Γ_i = the flux of contaminants at the bottom of the vadose zone normalized to a unit-source inventory for radionuclide i ([Ci/y]/Ci). The time-dependent value is calculated by VAM3DF.

w_i = the ratio of the concentration of radionuclide i at the well location relative to the contaminant concentration at the bottom of the vadose zone (dimensionless). This quantity was called the well intercept factor in earlier Hanford PAs. The peak value as calculated by CFEST is used.

D_i = the dose rate factor (mrem/y per Ci/m^3). The values are taken from the tables in Appendix B. D_i is unity when the response that is calculated is a concentration.

r = the recharge rate (m/y). The value at 10,000 years is used at all analysis times.

A = the area over which the contaminant flux enters the aquifer (m^2). The value used is the area of the disposal facility being modeled.

The program is modeled after GRTPA (Rittmann 1993), which served a similar function in earlier work (Rawlins et al. 1994; Mann et al. 1995). INTEG allows greater freedom in specifying data used in the integration. The code has been benchmarked against the results of GRTPA (Mann 1996). An auxiliary code was written to translate the output of VAM3DF into a readable format for INTEG.

4.0 Conceptual And Numerical Model Framework

The base-case groundwater flow and transport of contaminants from the ILAW facility was calculated with the current version of the Hanford site-wide groundwater model. This three-dimensional model, currently being used by the Hanford Groundwater Project and recommended as the proposed site-wide groundwater model in the Hanford Site groundwater model consolidation process, is based on the Coupled Fluid, Energy, and Solute Transport (CFEST-96) Code (Gupta et al. 1987; Gupta 1997). This model is fully described in Wurstner et al. (1995) and Cole et al. (1997) and was most recently used in the Hanford Site Composite Analysis (Cole et al. 1997; Kincaid et al. 1998), which is a companion analysis to the existing preliminary PA analyses of the ILAW disposal facility (Mann et al. 1997) and the solid waste burial grounds in the 200-East and 200-West areas (Wood et al. 1995, 1996). The Composite Analysis is also a companion document to the Remedial Investigation/Feasibility Study (RI/FS) (DOE 1994) that supports the Environmental Restoration Disposal Facility.

4.1 Hydrogeologic Framework

The conceptual model of the groundwater system is based on nine major hydrogeologic units identified in the left column presented in Figure 4.1. The basis for the identification of these major hydrogeologic units in the aquifer system is described in Thorne and Chamness (1992), Thorne and Newcomer (1992), and Thorne et al. (1993, 1994). Although nine hydrogeologic units were defined, only seven are found below the water table during post-Hanford conditions. Odd-numbered Ringold model units (5, 7, and 9) are predominantly coarse-grained sediments. Even-numbered Ringold model units (4, 6, and 8) are predominantly fine-grained sediments with low permeability. The Hanford formation combined with the pre-Missoula gravel deposits were designated Model Unit 1. Model units 2 and 3 correspond to the early Palouse soil and Plio-Pleistocene deposits, respectively. These units lie above the current water table. The predominantly mud facies of the upper Ringold unit identified by Lindsey (1995) was designated Model Unit 4. However, a difference in the definition of model units is that the lower, predominantly sand portion of the upper Ringold unit described in Lindsey (1995) was grouped with Model Unit 5, which also includes Ringold gravel/sand units E and C. This was done because the predominantly sand portion of the upper Ringold is expected to have hydraulic properties similar to units E and C. The lower mud unit identified by Lindsey (1995) was designated as Units 6 and 8. Where they exist, the gravel and sand units B and D, which are found within the lower Ringold, were designated as Model Unit 7. Gravels of Ringold Unit A were designated Unit 9 for the model, and the underlying basalt was designated Model Unit 10. However, the basalt was assigned a very low hydraulic conductivity and was essentially treated as an impermeable unit in the model.

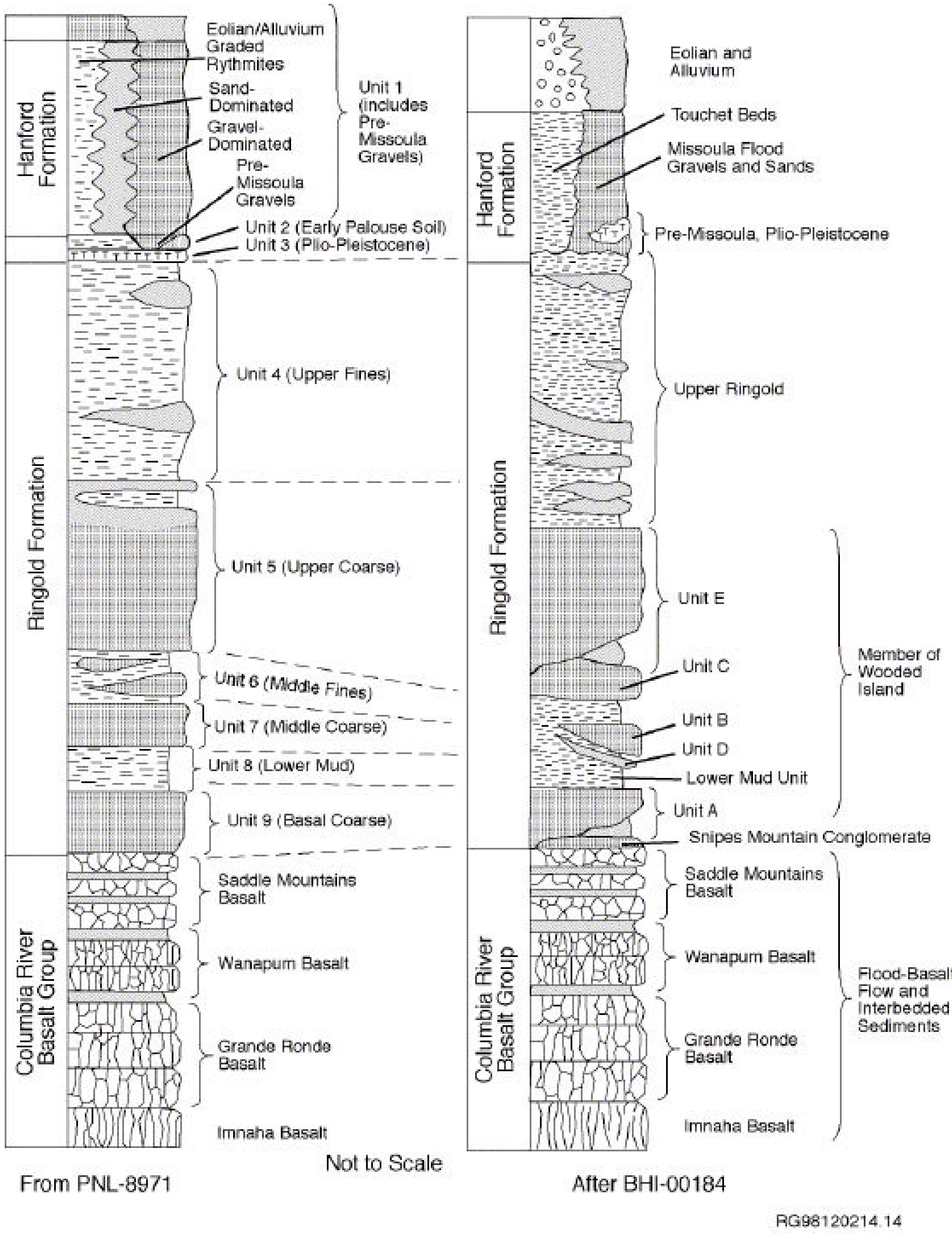

Figure 4.1. Comparison of Generalized Geology and Hydrostratigraphic Columns

The lateral extent and thickness distribution of each hydrogeologic unit were defined based on information from well drillers' logs, geophysical logs, and an understanding of the geologic environment. These interpreted areal distributions and thicknesses were then integrated into EarthVision (Dynamic Graphics, Inc., Alameda, California), a three-dimensional, visualization, software package used to construct a database of the three-dimensional hydrogeologic framework.

4.2 Recharge and Aquifer Boundaries

Both natural and artificial recharge to the aquifer were incorporated in the model. Natural recharge to the unconfined aquifer system occurs from infiltration of 1) runoff from elevated regions along the western boundary of the Hanford Site, 2) spring discharges originating from the basalt-confined aquifer system, also along the western boundary, and 3) precipitation falling across the site. Some recharge also occurs along the Yakima River in the southern portion of the site. Natural recharge from runoff and irrigation in the Cold Creek and Dry Creek Valleys up gradient of the site also provides a source of groundwater inflow. Areal recharge from precipitation on the site is highly variable, both spatially and temporally, and depends on local climate, soil type, and vegetation. A recharge distribution estimated for 1979 conditions in Cole et al. (1997) was applied in the model. The general methods used to develop these recharge estimates are described in detail in Fayer and Walters (1995).

The other source of recharge to the unconfined aquifer is wastewater disposal. Large volumes of artificial recharge from wastewater discharged to disposal facilities on the Hanford Site over the past 50 years has significantly impacted groundwater flow and contaminant transport in the unconfined aquifer system. However, the volume of artificial recharge will decrease significantly in the near future, and the water table is expected to return to more natural conditions after site closure.

The flow system is bounded by the Columbia River on the north and east and by the Yakima River and basalt ridges on the south and west. The Columbia River represents a point of regional discharge for the unconfined aquifer system. The amount of groundwater discharging to the river is a function of the local hydraulic gradient between the groundwater elevation adjacent to the river and the river-stage elevation. This hydraulic gradient is highly variable because the river stage is affected by releases from upstream dams. To approximate the long-term effect of the Columbia River on the unconfined aquifer system in the three-dimensional model, the CHARIMA river-simulation model (Walters et al. 1994) was used to generate the long-term, average river-stage elevations for the Columbia River. The river itself is represented as a constant-head boundary in the uppermost nodes of the model at the approximate locations of the river's left bank and channel midpoint. Nodes representing the thickness of the aquifer below the nodes representing mid-point of the river channel were treated as no-flow boundaries. This boundary condition is used to approximate the location of the groundwater divide that exists beneath the Columbia River where groundwater from the Hanford Site and the other side of the river discharge into the Columbia. The Yakima River was also represented as a specified-head boundary at surface nodes approximating its location. Like the

Columbia River, nodes representing the thickness of the aquifer below the Yakima River channel were treated as no-flow boundaries.

At Cold Creek and Dry Creek Valleys, the unconfined aquifer system extends westward beyond the boundary of the model. To approximate the groundwater flux entering the modeled area from these valleys, both constant-head and constant-flux boundary conditions were defined. A constant-head boundary condition was specified for Cold Creek Valley for the steady-state-model calibration runs. Once calibrated, the steady-state model was used to calculate the flux condition that was then used in the post-Hanford steady-state flow simulation. The constant-flux boundary was used because it better represents the response of the boundary to a declining water table than a constant-head boundary. Discharges from Dry Creek Valley in the model area, resulting from infiltration of precipitation and spring discharges, are approximated with a prescribed-flux boundary condition.

The basalt underlying the unconfined aquifer sediments represents a lower boundary to the unconfined aquifer system. The potential for interflow (recharge and discharge) between the basalt-confined aquifer system and the unconfined aquifer system is largely unquantified, but is postulated to be small relative to the other flow components estimated for the unconfined aquifer system. Therefore, interflow with underlying basalt units was not included in the current three-dimensional model. The basalt was defined in the model as an essentially impermeable unit underlying the sediments.

4.3 Flow and Transport Properties

To model groundwater flow, the distribution of hydraulic properties, including both horizontal and vertical hydraulic conductivity and porosity, were needed for each hydrogeologic unit defined in the model. In addition, to simulate movement of contaminant plumes, transport properties were needed, including contaminant-specific distribution coefficients, bulk density, effective porosity, and longitudinal and transverse dispersivities (D_l and D_t).

In the original model calibration procedure described in Wurstner et al. (1995), measured values of aquifer transmissivity were used in a two-dimensional model with an inverse model-calibration procedure to determine the transmissivity distribution. Hydraulic head conditions for 1979 were used in the inverse calibration because measured hydraulic heads were relatively stable at that time. Details concerning the updated calibration of the two-dimensional model are provided in Cole et al. (1997).

Hydraulic conductivities were assigned to the three-dimensional model units so that the total aquifer transmissivity from inverse calibration was preserved at every location. The vertical distribution of hydraulic conductivity at each spatial location was determined based on the transmissivity value and other information, including facies descriptions and hydraulic property values measured for similar facies. A complete description of the seven-step process used to vertically distribute the transmissivity among the model hydrogeologic units is described in

Cole et al. (1997). The resulting hydraulic conductivity distribution resulting from this redistribution of aquifer transmissivity in the upper part of the aquifer is provided in Figure 4.2.

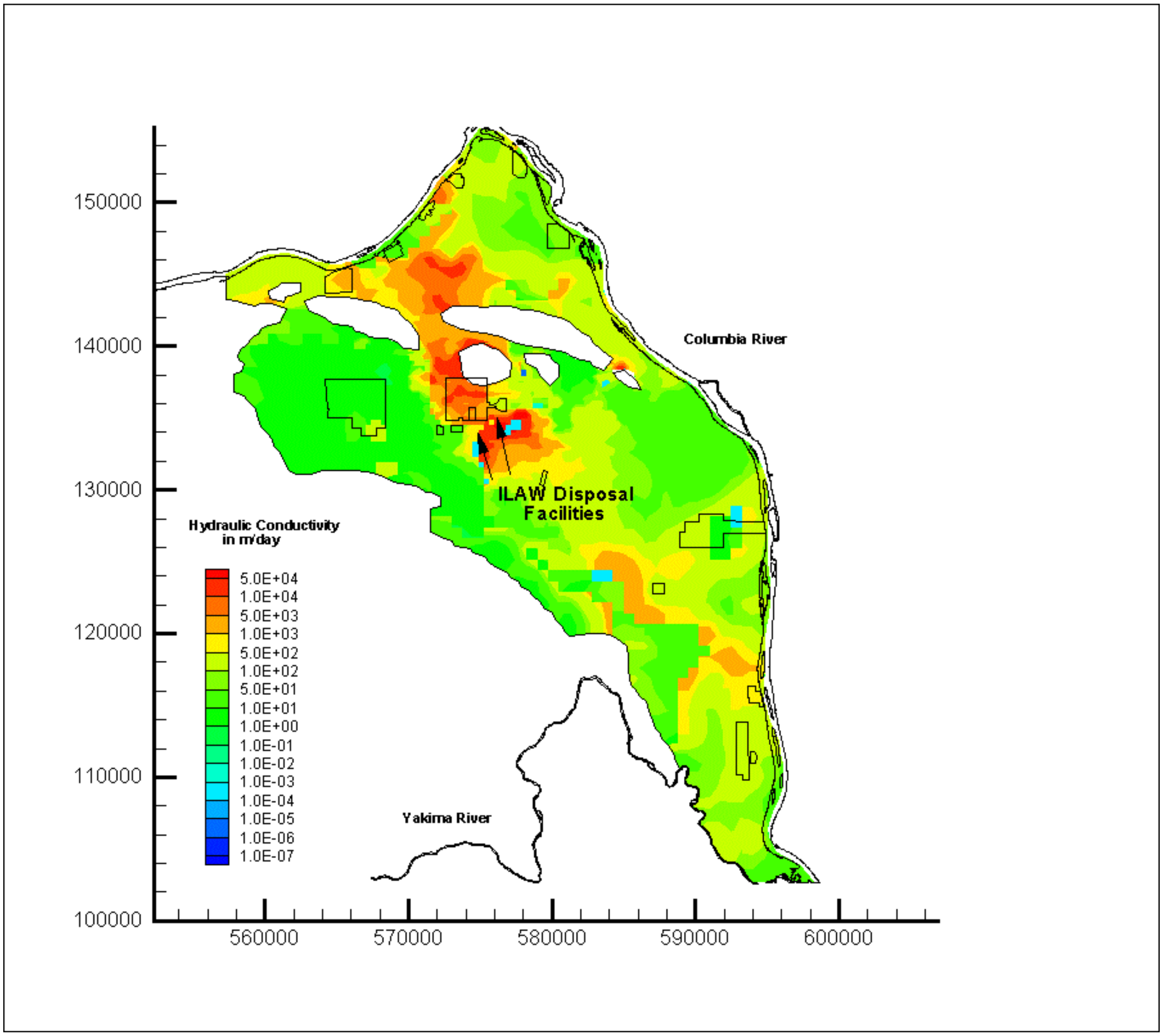

Figure 4.2. Hydraulic Conductivity Distribution Obtained from Inverse Calibration for 1979 Conditions

Information on transport properties used in past modeling studies at the Hanford Site is provided in Wurstner et al. (1995). Estimates of model parameters were developed to account for contaminant transport and dispersion in all transport simulations. Specific model parameters estimated included longtitudinal and transverse dispersivities (D_l and D_t) and aquifer porosity. This section briefly summarizes estimated transport properties.

For the regional scale analysis, a D_l of 95 m (311.7 ft) was selected to be within the range of recommended grid Peclet numbers (Pe < 4) for acceptable solutions. The 95-m (311.7 ft) estimate is about one-quarter of the grid spacing in the finest part of the model grid in the 200-Area plateau, where the smallest grid spacing is about 375 m (1230.3 ft) by 375 m (1230.3). The effective D_t was assumed to be 10 percent of the D_l. Therefore, 9.5 m (31 ft) was used in all simulations.

The effective porosity was estimated from limited measurements of porosity and specific yield obtained from multiple-well aquifer tests. These values range from 0.01 to 0.37. Laboratory measurements of porosity, which range from 0.19 to 0.41, were available for samples from a few Hanford Site wells and were also considered. The few tracer tests conducted indicate effective porosities ranging from 0.1 to 0.25. Based on the ranges of values considered, a best estimate of an effective porosity value for all simulations was assumed to be 0.25.

5.0 Groundwater Flow and Contaminant Transport Calculations

This section of the report describes the technical approach and use of the Hanford site-wide flow and transport model and the local-scale model developed in the vicinity of the existing and new ILAW disposal facility areas. These models were used to assess impacts from the transport of contaminants at hypothetical wells 100 m and 1 km down gradient of the disposal facilities and to evaluate regional flow conditions and transport from the ILAW disposal facilities to the Columbia River.

The first part of this section described the establishment of estimated Hanford post-closure flow conditions that provided the basis for all site-wide and local-scale flow and transport in the base-case calculations. The second of this section describes the development and implementation of local-scale models that were used to perform flow and transport simulations in the immediate vicinity of the disposal facility areas.

5.1. Site-Wide Flow and Transport Simulations

Site-wide flow-model simulations were used to establish future flow conditions that provided the basis for boundary conditions for local-scale models to evaluate impacts from the transport of contaminants immediately down gradient of the disposal facilities. These same flow conditions also provided the hydraulic basis for site-wide transport simulations used to evaluate concentration levels of contaminants released from the disposal facilities to the Columbia River. Following is a summary discussion of the establishment of post-Hanford steady-state flow conditions and the approach used in site-wide transport-model simulations of contaminant release from disposal facilities to the Columbia River.

5.1.1. Site-Wide Steady-State Flow Conditions

Past projections of post-Hanford water-table conditions have estimated the impact of Hanford operations ceasing and the resulting changes in artificial discharges that have been used extensively as a part of site waste-management practices. Simulated results of future transient behavior in the Hanford unconfined aquifer by Cole et al. (1997) showed an overall decline in the hydraulic head and hydraulic gradient across the entire water table over the entire Hanford Site. The results of these simulations indicate that the water table would reach steady state in 100–350 years in different areas over the Hanford Site.

Given the expected long delay of contaminants reaching the water from the low-level waste burial grounds, the hydrologic framework of all groundwater transport calculations was based on a postulated post-Hanford steady-state water table as estimated with the three-dimensional model. The predicted water table for post-Hanford conditions for these assumed steady-state conditions across the site and in the area between the ILAW new disposal facility and the Columbia River are illustrated in Figures 5.1 and 5.2. The overall flow attributes of this water-table surface are consistent with the previously simulated flow patterns described in Wurstner et al. (1995), Cole et al. (1997), and Law et al. (1996). From the ILAW new disposal facility, groundwater moves southeasterly near the site and then in an easterly and northeasterly direction before discharging into the Columbia River north of the old Hanford town site.

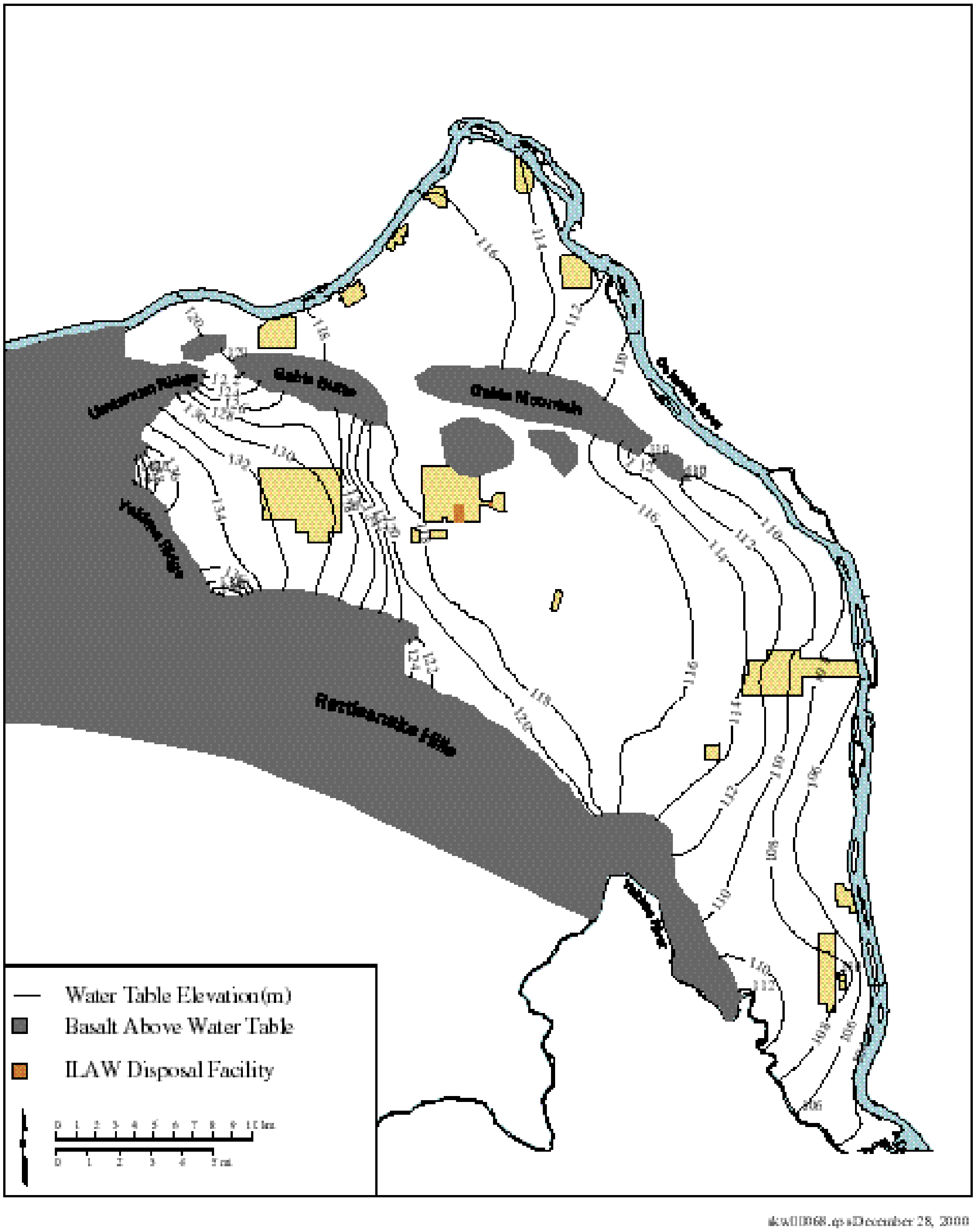

Figure 5.1. Predicted Water Table for Post-Hanford Conditions for Assumed Steady-State Conditions

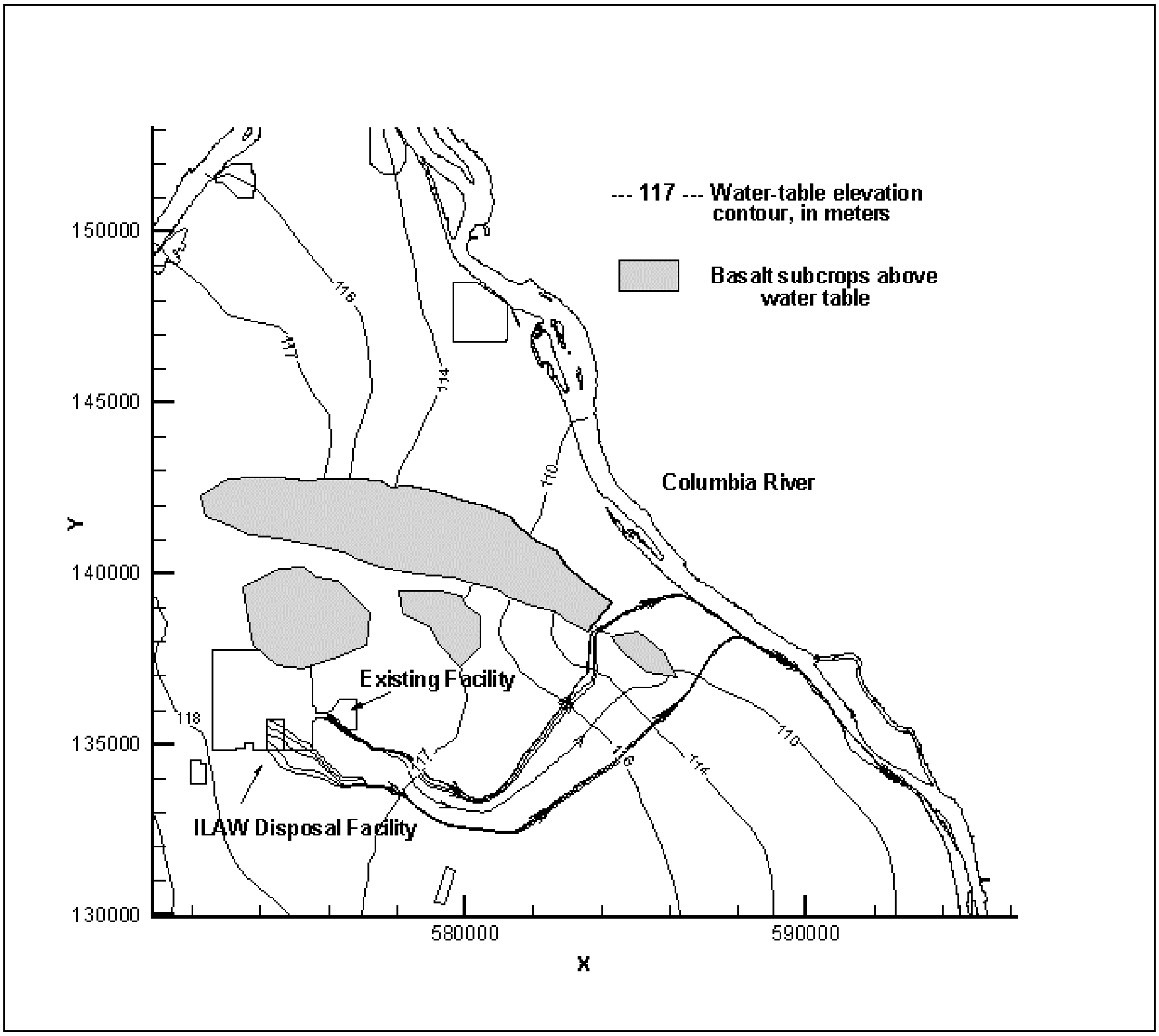

Figure 5.2. Predicted Water Table for Post-Hanford Conditions for Assumed Steady-State Conditions Between the ILAW Disposal Facility and Columbia River

5.1.2. Contaminant Transport Between Disposal Facilities and Columbia River

Flow conditions established with the site-wide model (Figures 5.1 and 5.2) provide the basis for the transport simulations of contaminants released from disposal facilities toward the Columbia River. Constant mass releases equivalent to those used in the local-scale model were introduced into the site-wide model at the approximate location of the ILAW disposal facilities. Concentration levels and WIFs were evaluated in groundwater in close proximity to the Columbia River as well as several intermediate points between the disposal areas and the river. To establish consistency of the site-wide scale calculations with those made in the local scale models, concentrations levels were evaluated and compared at approximately 1 km down gradient of the source areas in both the local-scale and site-wide models. Predicted concentration levels at 1 km in the site-wide and local-scale models are expected to be somewhat consistent with each other, but will not be the same because of inherent differences in the grid resolution used in each model. Predicted concentration levels in the site-wide model close to the source areas will in general be expected to be somewhat lower than are predicted in the local-scale models.

5.2. Local-Scale Model Development and Description

The base-case analysis for the groundwater flow and transport calculations evaluated current disposal concepts at the new ILAW disposal facility to be located in the south-central 200 East area. The approach used in this analysis was to construct local-scale models based on flow conditions calculated in the site-wide model to adequately represent flow and transport conditions near these facilities to a hypothetical well 100 m downgradient.

5.2.1. Grid Designs

Two separate local-scale models were developed to evaluate the current design concepts. One model evaluated the remote-handled trench and concrete-vault concepts at the new ILAW disposal facility. Another local-scale model was used to evaluate the concrete-vault concept at the existing ILAW disposal facility.

The grid used in the local-scale model in both areas required refinement areally and vertically. The discretized grids for the local-scale models telescope in from the grid used in regional-scale calculations.

The grid used in the new ILAW disposal facility area extends over an area of about 4,100 m (2.5 mi) west to east and 4,100 m (2.5 mi) north to south (Figure 5.3). It varies in size progressively from the outmost subdivided coarse triangular grids (regional-scale 375 by 375 m [1230 by 1230 ft] grid spaces) to the finest grid spacing (20 m by 20 m [65.6 by 65.6 ft]) in the vicinity of the ILAW disposal area. The three-dimensional model, based on this surface grid, comprises a total of 31,604 elements (9,157 surface and 22,447 subsurface elements) and 32,618 nodes.

The grid used at the existing ILAW disposal-facility area extends over an area of about 2,600 m (1.5 mi) west to east and 2600 m (1.6 mi) north to south (Figure 5.4). It varies in size progressively from the outmost subdivided coarse triangular grids (regional-scale 375 by 375 m [1230 by 1230 ft] grid spaces) to the finest grid spacing (20 m by 20 m [65.6 by 65.6 ft]) in the vicinity of the existing ILAW disposal area. This three-dimensional model comprises a total of 18,317 elements (9,157 surface and subsurface elements) and 18,914 nodes.

The vertical grid spacing for the transport (as well as the flow) model consisted of multiple transport layers that subdivided the major hydrostratigraphic units. The basic approach for this subdivision is the same approach used in Kincaid et al. (1998) to support groundwater transport calculations used in the Composite Analysis. The basic thickness of each transport layer was 8 m (26.2 ft). The transport layers were defined from the water-table surface to the basalt to account for the overall saturated thickness and to adequately represent contaminant concentrations in the three-dimensional model. At every model node, each of the major hydro-stratigraphic units below the water table was represented by at least one transport-model layer. Nonconductive (e.g., mud) units below the water table were always represented by at least two transport-model layers, regardless of their saturated thickness, to ensure that the vertical flow and transport through these units was appropriately represented.

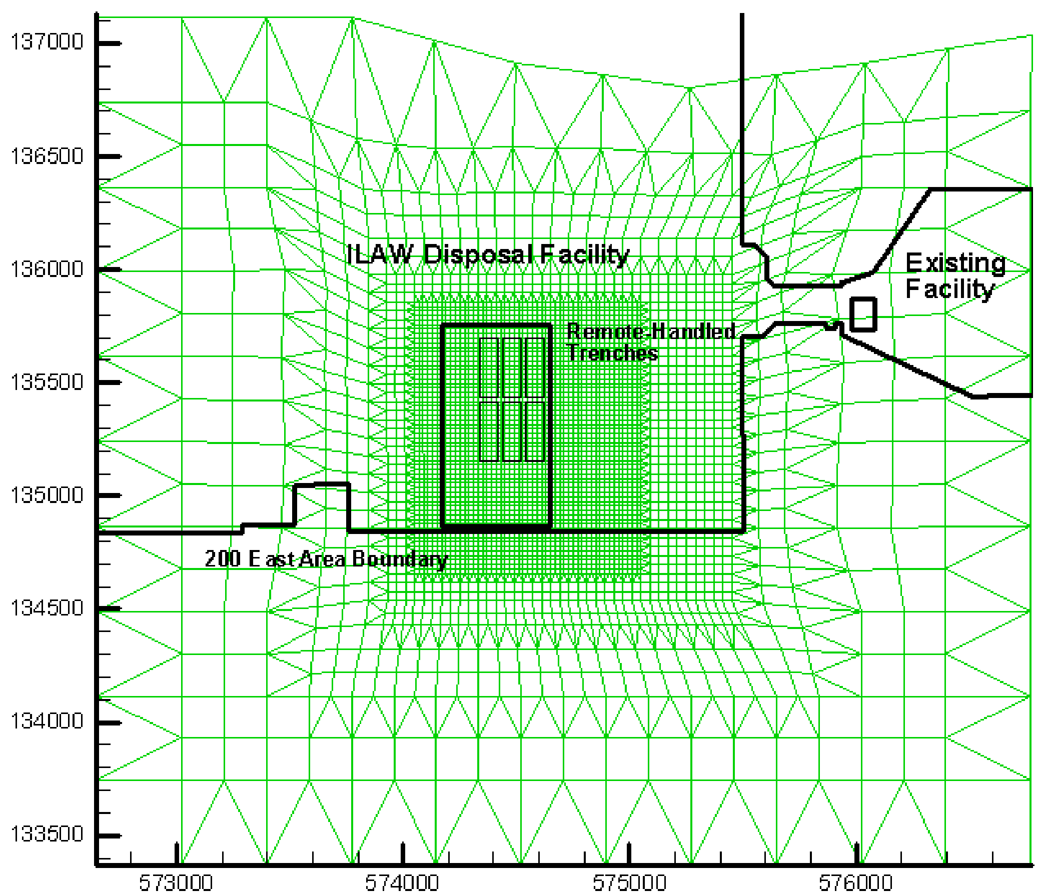

Figure 5.3. Finite Element Grid Used in the Local-Scale Model at the New ILAW Disposal Facility Area

For units with a saturated thickness <12 m (<39.4 ft), the layer thickness was set to the actual saturated thickness of the unit. Nonconductive and conductive units with saturated thickness >12 m (>39.4 ft) were divided into multiple transport-model layers in the same manner. For all units with thickness >12 m (>39.4 ft), the transport layering algorithm is as follows: create as many uniform 8-m (26.2-ft) transport layers as possible until the remaining unaccounted for saturated thickness is >12 m (>39.4 ft) but <16 m (<52.5 ft), and then create two additional transport layers set to half of the remaining saturated thickness of the hydrostratigraphic unit being layered.

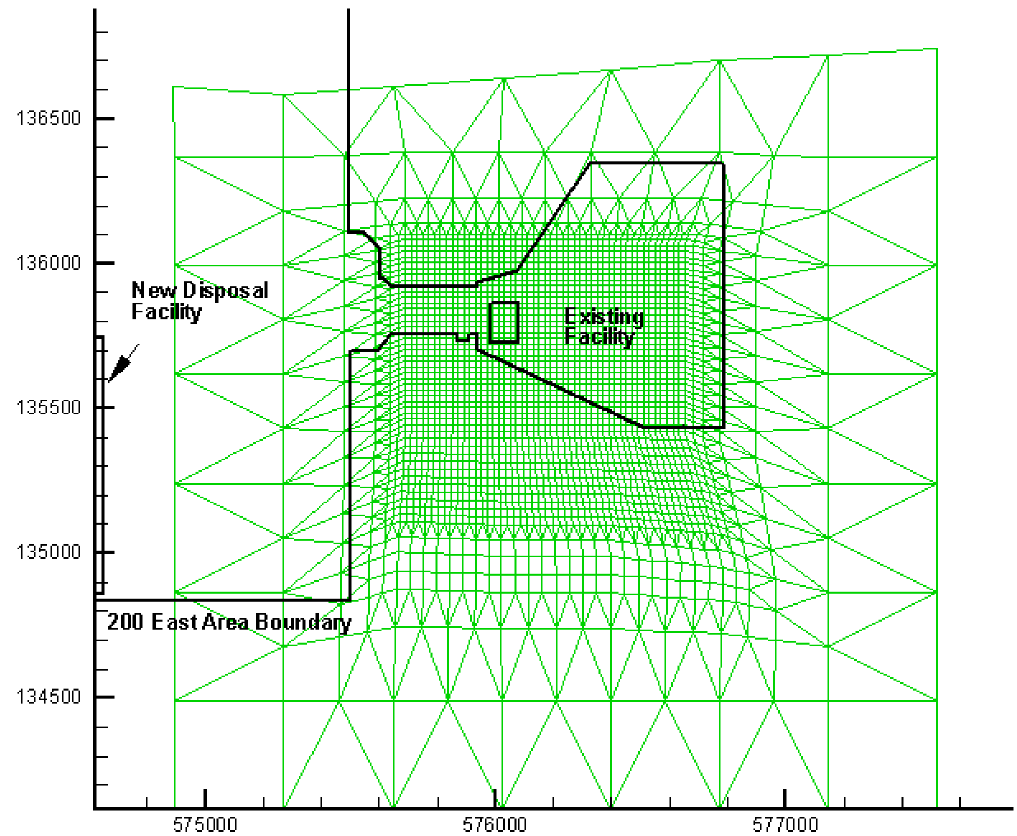

Figure 5.4. Finite Element Grid Used in the Local-Scale Model at the Existing ILAW Disposal Facility Area

At the local-scale, a total of six hydrogeologic units was found to be present, the Hanford formation (Unit 1) and several units belonging to the Ringold Formation (Units 5, 6, 7, 8, and 9). The three-dimensional distribution of these units in the local-scale model used in the new ILAW disposal area is depicted in Figure 5.5. The three-dimensional distribution of these units in the local-scale model used in the existing ILAW disposal area is depicted in Figure 5.6.

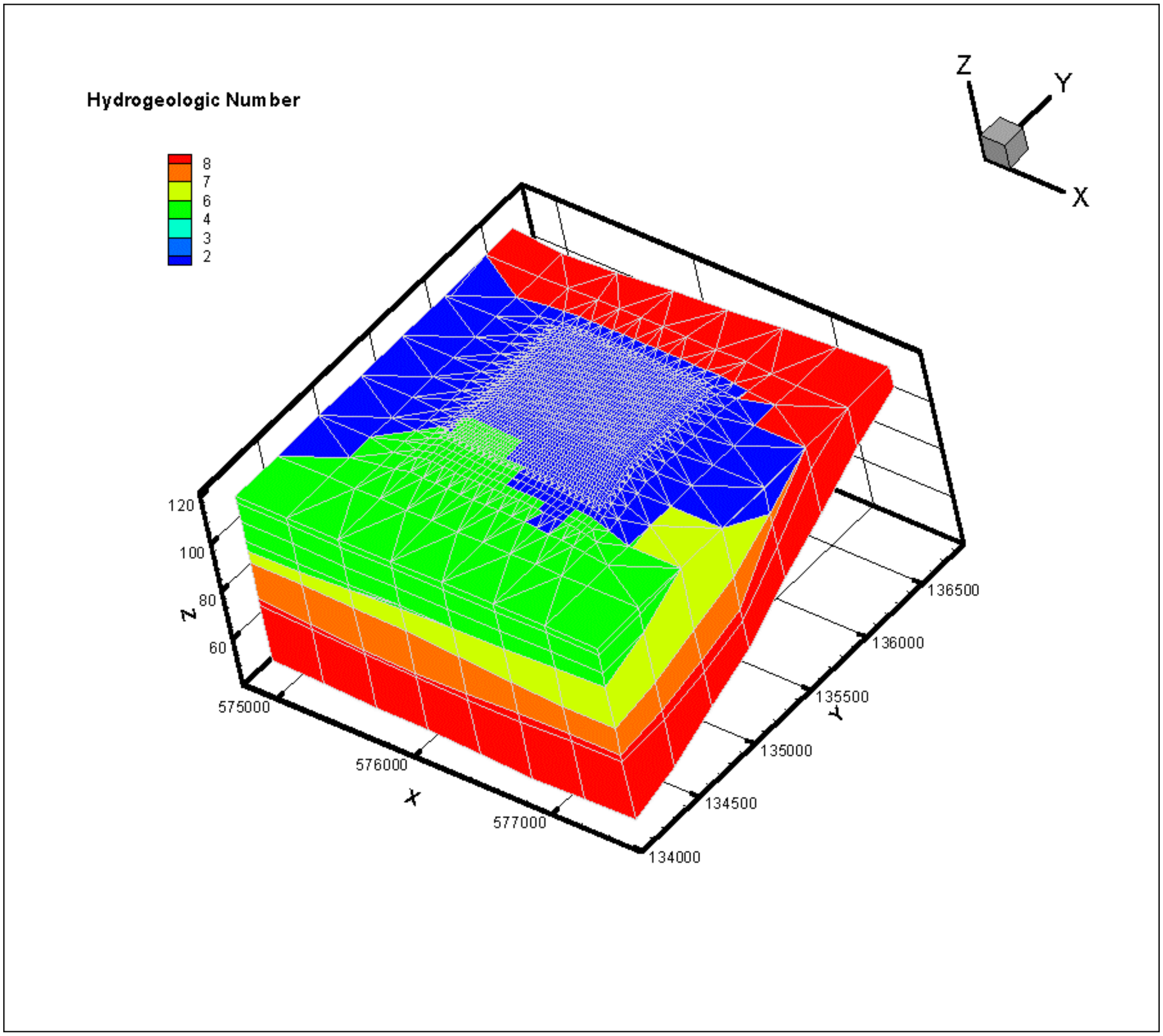

Figure 5.5. Three-Dimensional Distribution of Major Hydrogeologic Units in the New Local-Scale Model

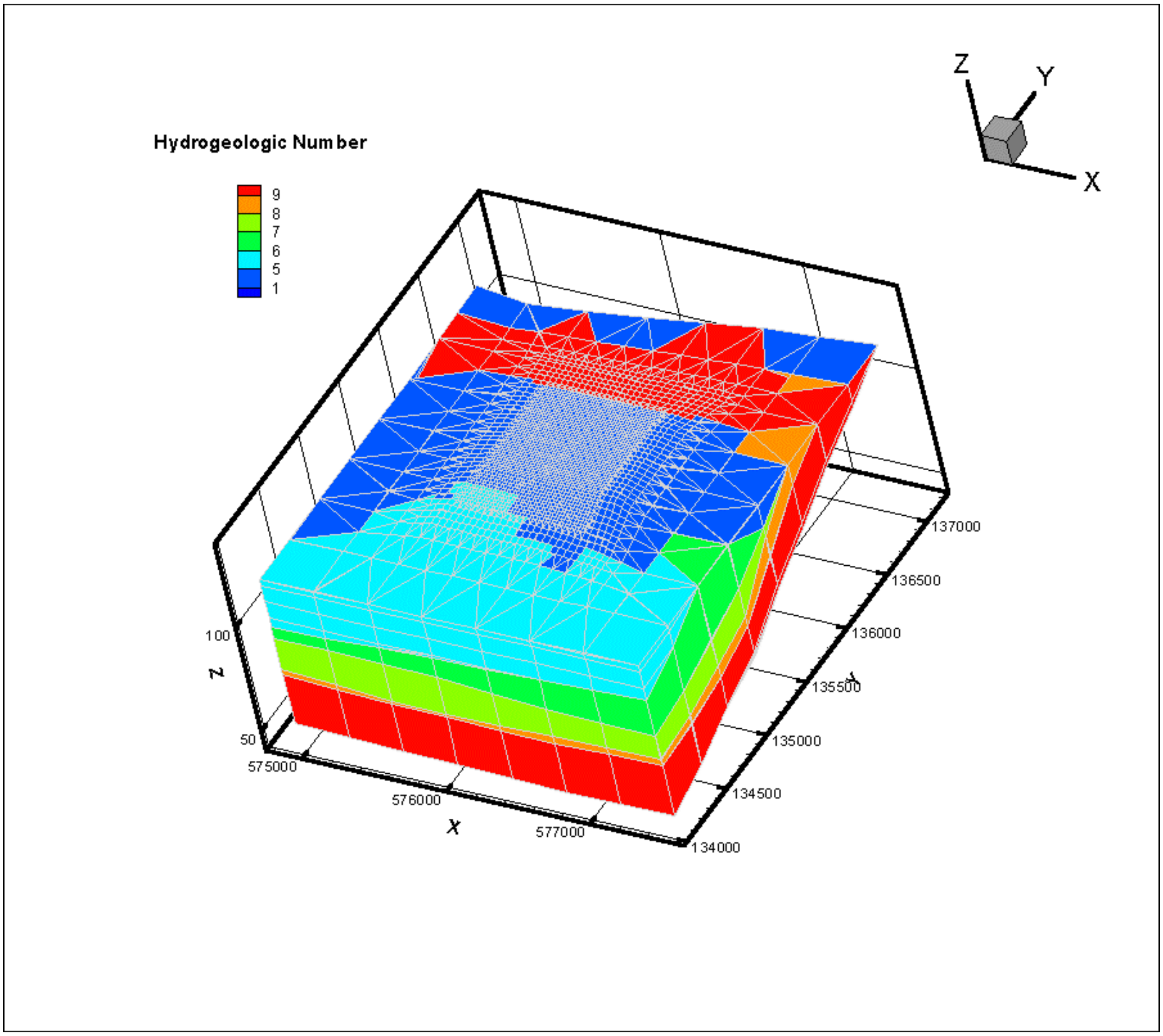

Figure 5.6. Three-Dimensional Distribution of Major Hydrogeologic Units in the Existing Local-Scale Model

5.2.2. Hydraulic Properties

The hydraulic conductivity and porosity estimates used in the local-scale model were developed based on the assumption that interpolating regional-scale estimates of hydraulic properties in the site-wide model using grid coordinates from the local-scale model can be used to represent local-scale properties in the vicinity of the ILAW disposal facility. The resulting three-dimensional distribution of these properties for the new ILAW Disposal Facility model is provided in Figure 5.7. The resulting three-dimensional distribution of these properties for the existing ILAW Disposal Facility model is provided in Figure 5.8. The estimated values generally indicate the regional high trends in hydraulic properties found in the central part of the Hanford Site. This is where the ancestral Columbia River deposited very coarse alluvial deposits in a deep channel extending to the south of the ILAW site and to the north through Gable Butte and Gable Mountain. Estimated hydraulic conductivities directly below the disposal-facility region range from several thousand to tens of thousands of m/day in the Hanford formation and several hundred m/day in the permeable parts of the Ringold Formation (Units 5, 7, and 9). Relatively low hydraulic conductivities are estimated for low-permeability units within the Ringold Formation (Units 6 and 8).

5.2.3. Transport Properties

Estimates of model parameters were developed to account for contaminant dispersion in all transport simulations. Specific model parameters examined included longitudinal and transverse dispersion coefficients (D_l and D_t) as well as estimates of effective bulk density and porosity of the aquifer materials. This section briefly summarizes estimated transport properties.

For purposes of this analysis, no adsorption was accounted for in simulating releases from the new and existing disposal facilities. All simulations were based on the release and transport of a non-sorbed, long-lived radionuclide. Iodine-129 was used as the surrogate radionuclide in all calculations.

For purposes of these calculations, a bulk density of 1.9 g/cm^3 was used for all simulations. The effective porosity was estimated from specific yields obtained from multiple-well aquifer tests. These values range from 0.01 to 0.37. Laboratory measurements of porosity, which range from 0.19 to 0.41, were available for samples from a few Hanford Site wells and were also considered. The few tracer tests conducted indicate effective porosities ranging from 0.1 to 0.25. Based on the ranges of values considered, a best estimate of an effective porosity value for all simulations was assumed to be 0.25.

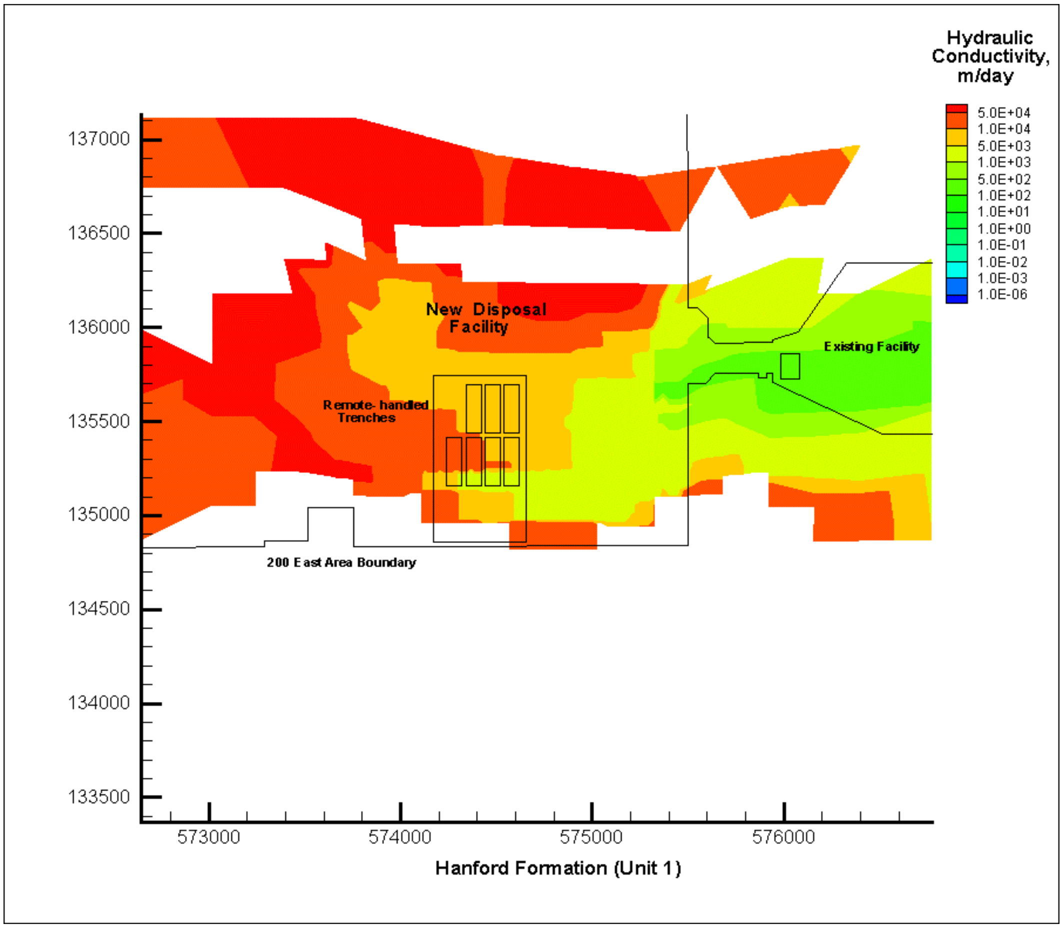

Figure 5.7. Distribution of Hydraulic Conductivities Used in the Local-Scale Model of the New ILAW Disposal Facility

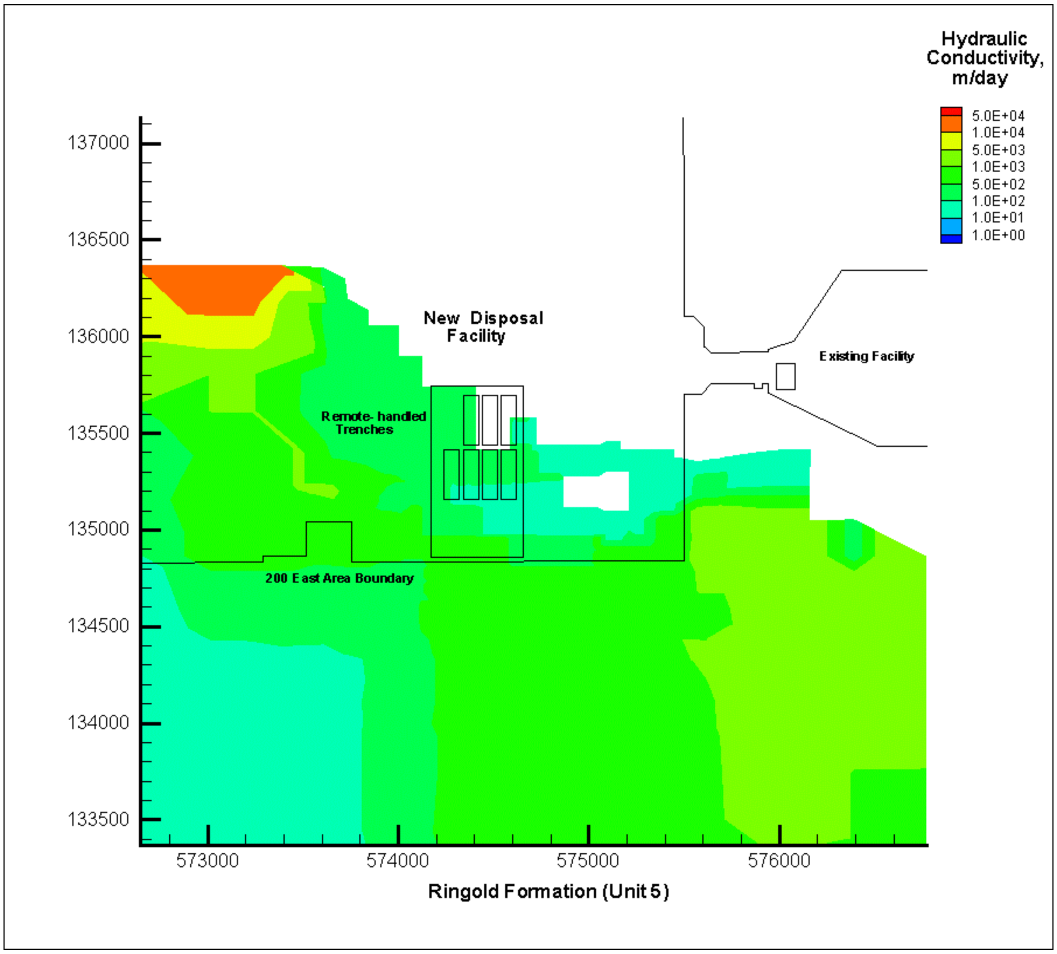

Figure 5.7 (Continued)

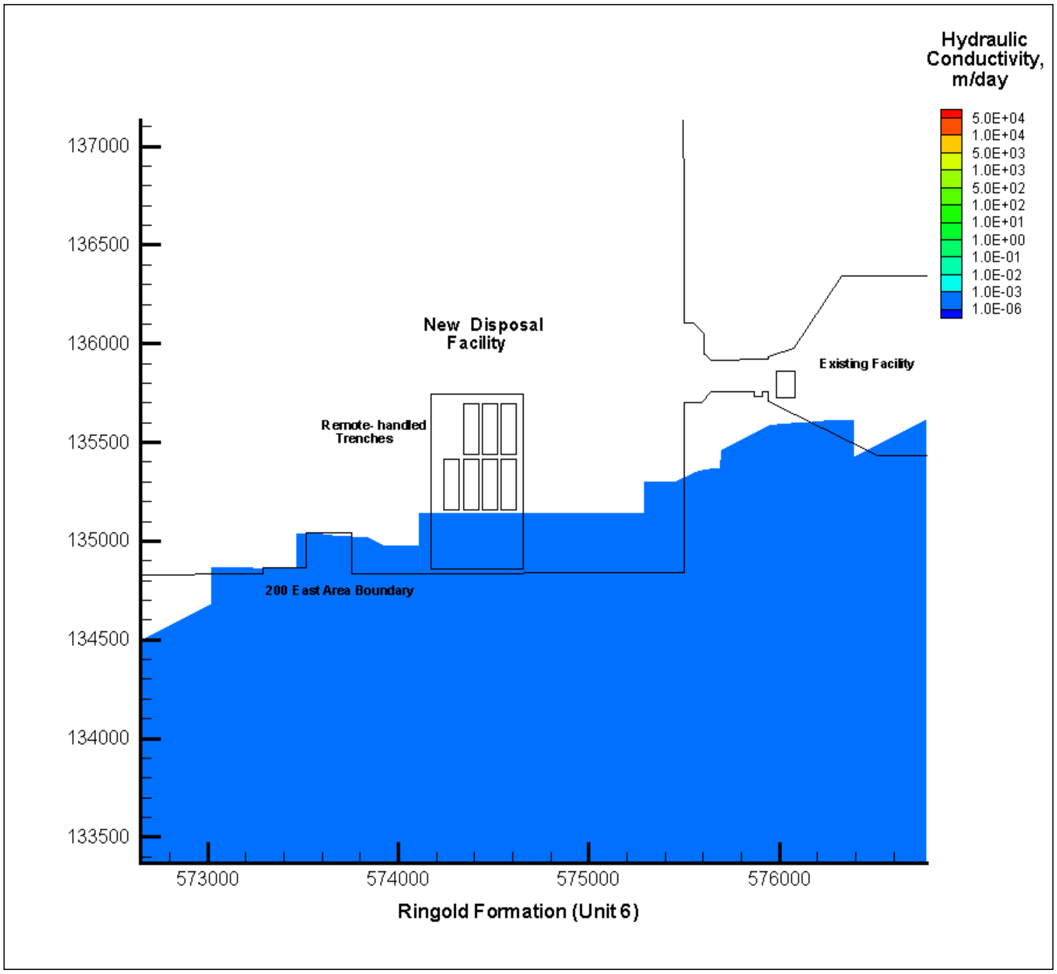

Figure 5.7 (Continued)

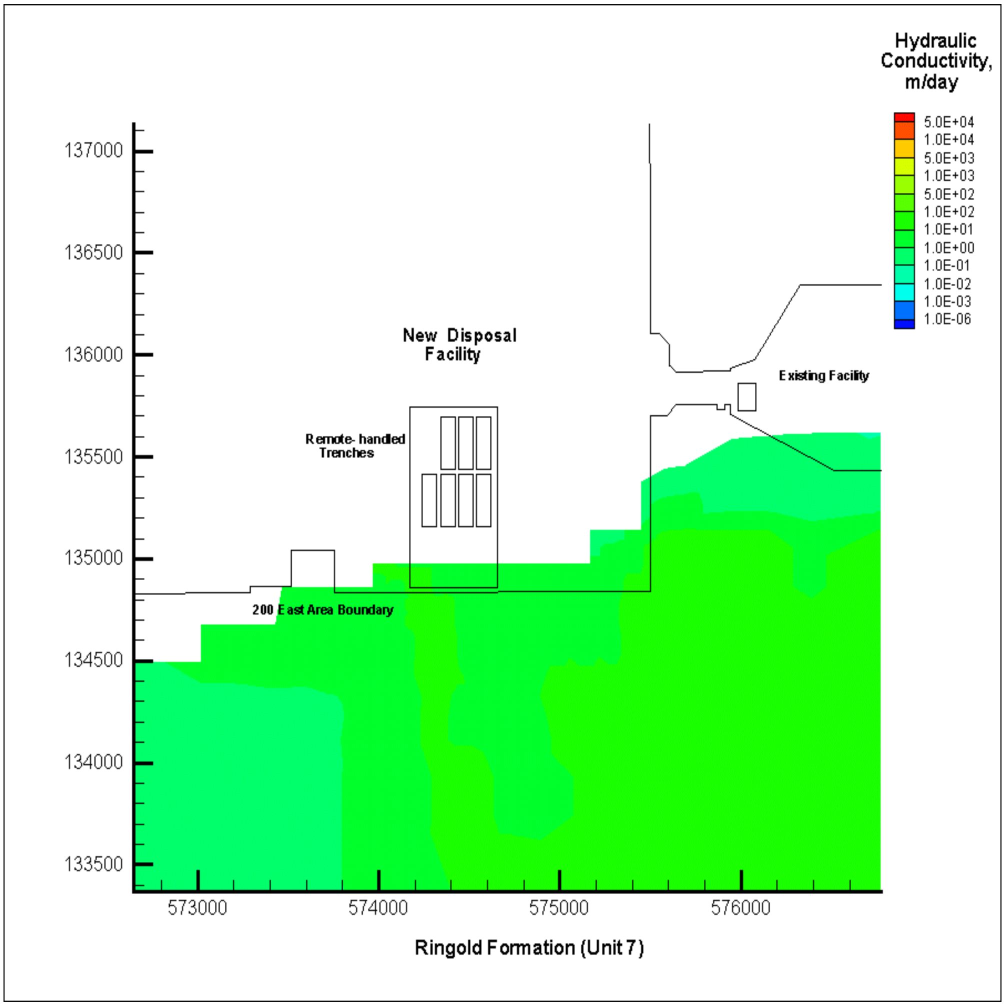

Figure 5.7 (Continued)

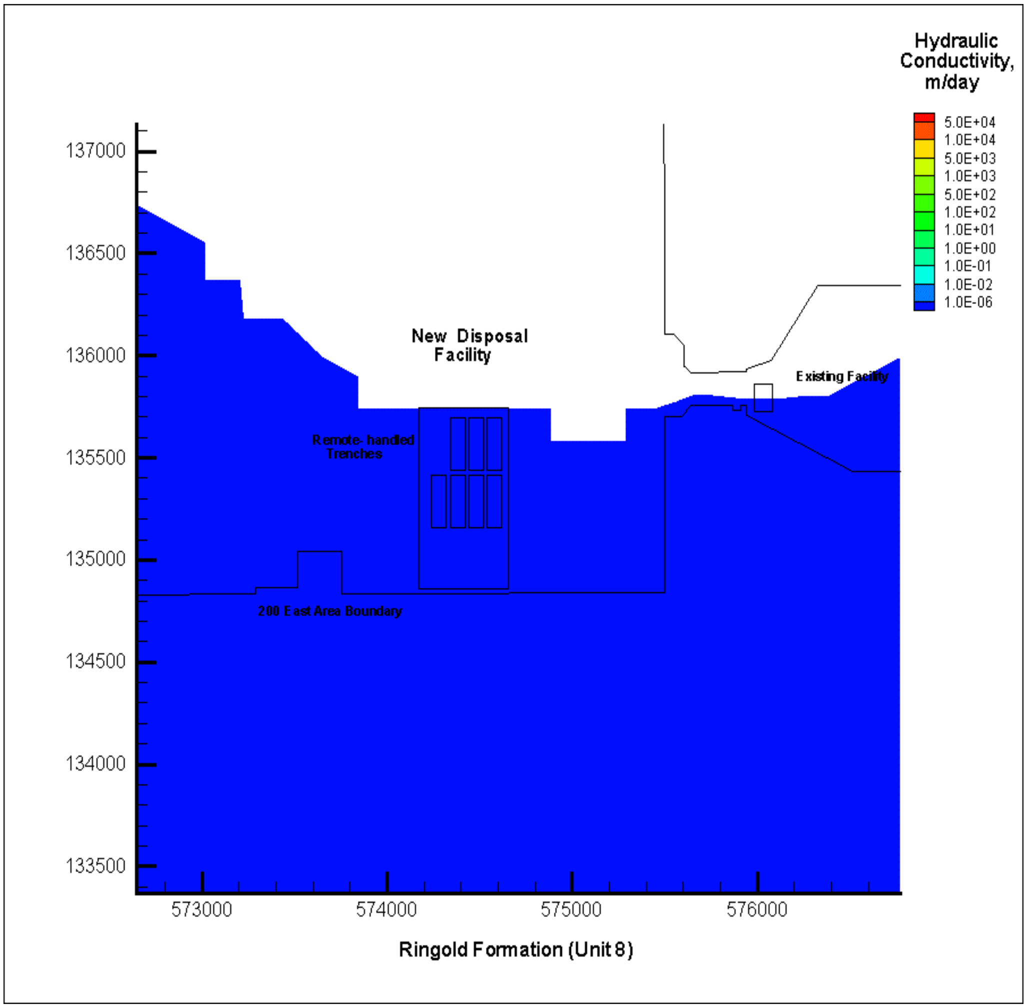

Figure 5.7 (Continued)

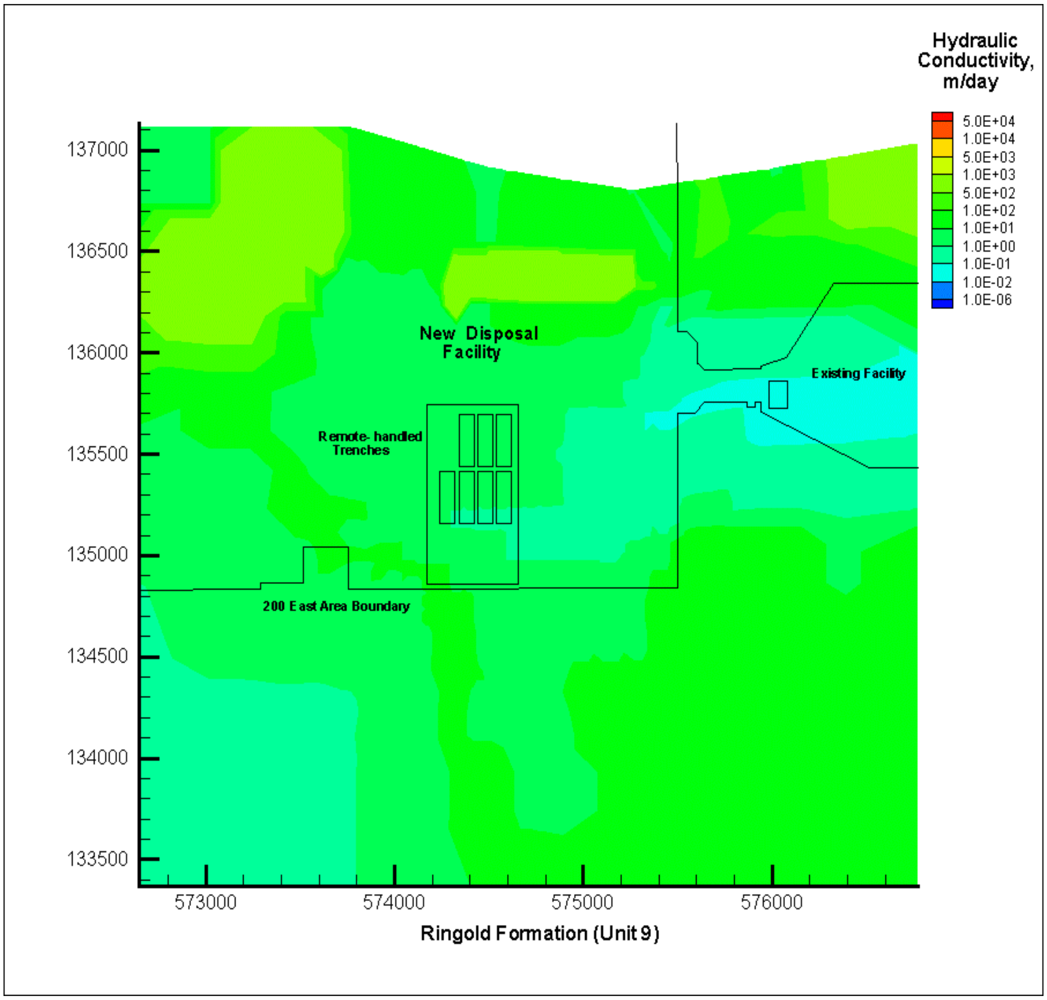

Figure 5.7 (Continued)

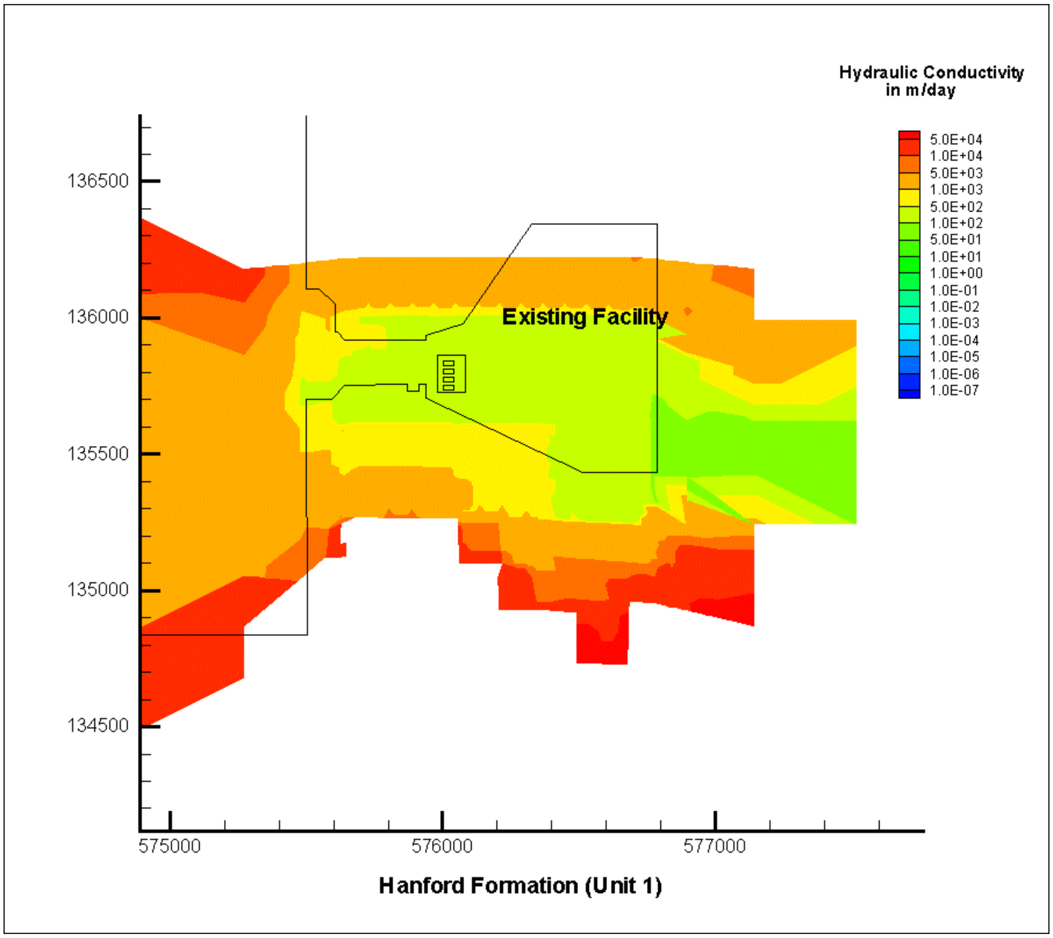

Figure 5.8. Distribution of Hydraulic Conductivities Used in the Local Scale Model of the Existing ILAW Disposal Facility Area

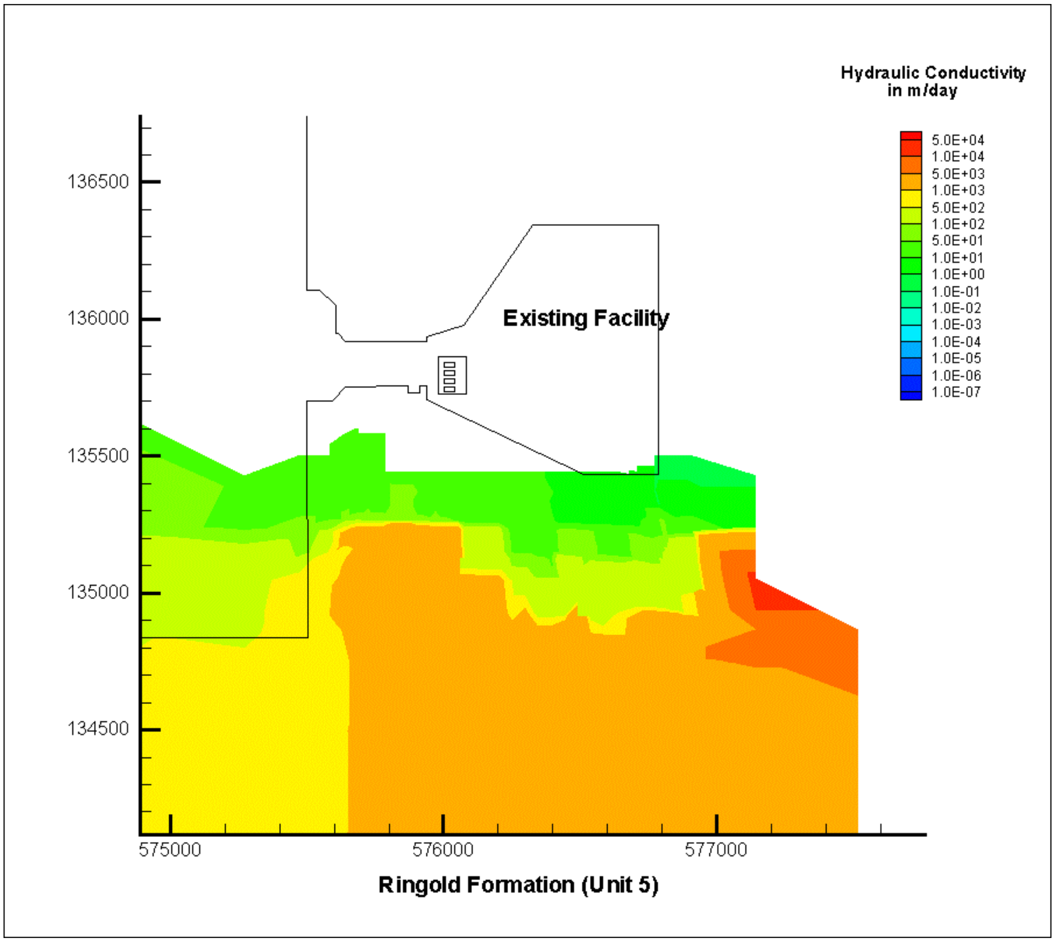

Figure 5.8 (Continued)

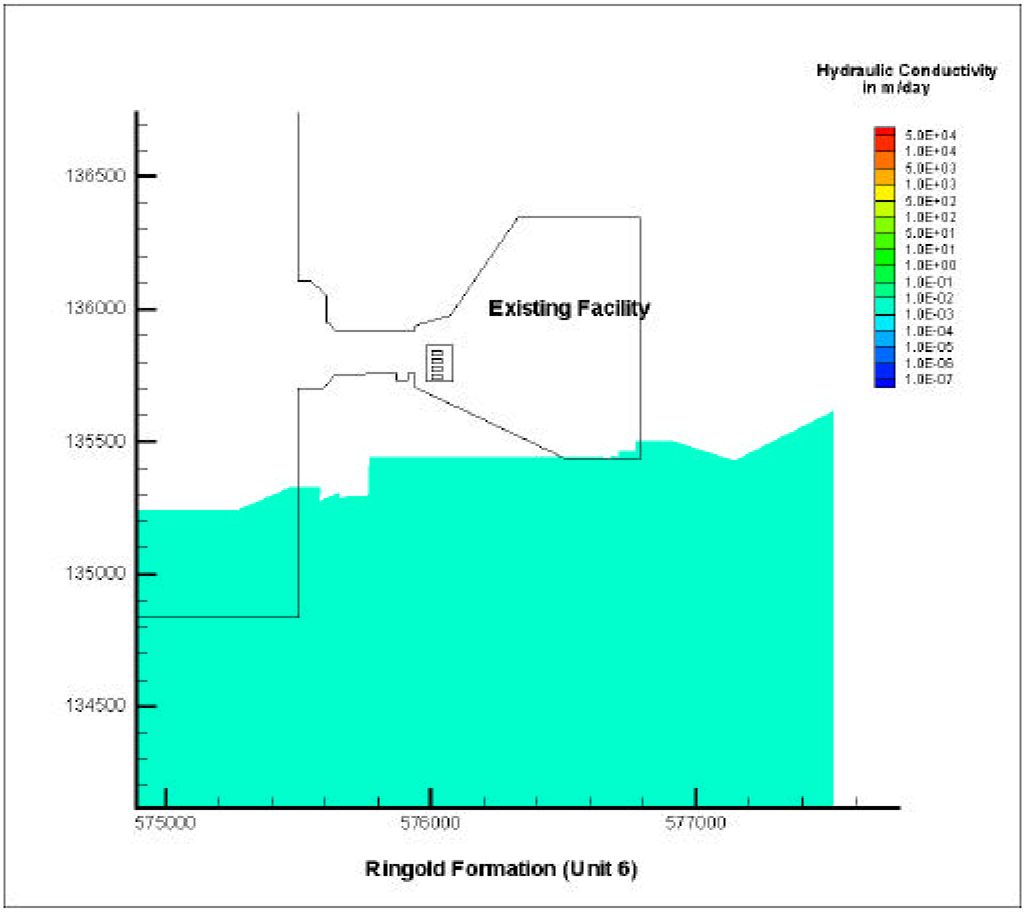

Figure 5.8 (Continued)

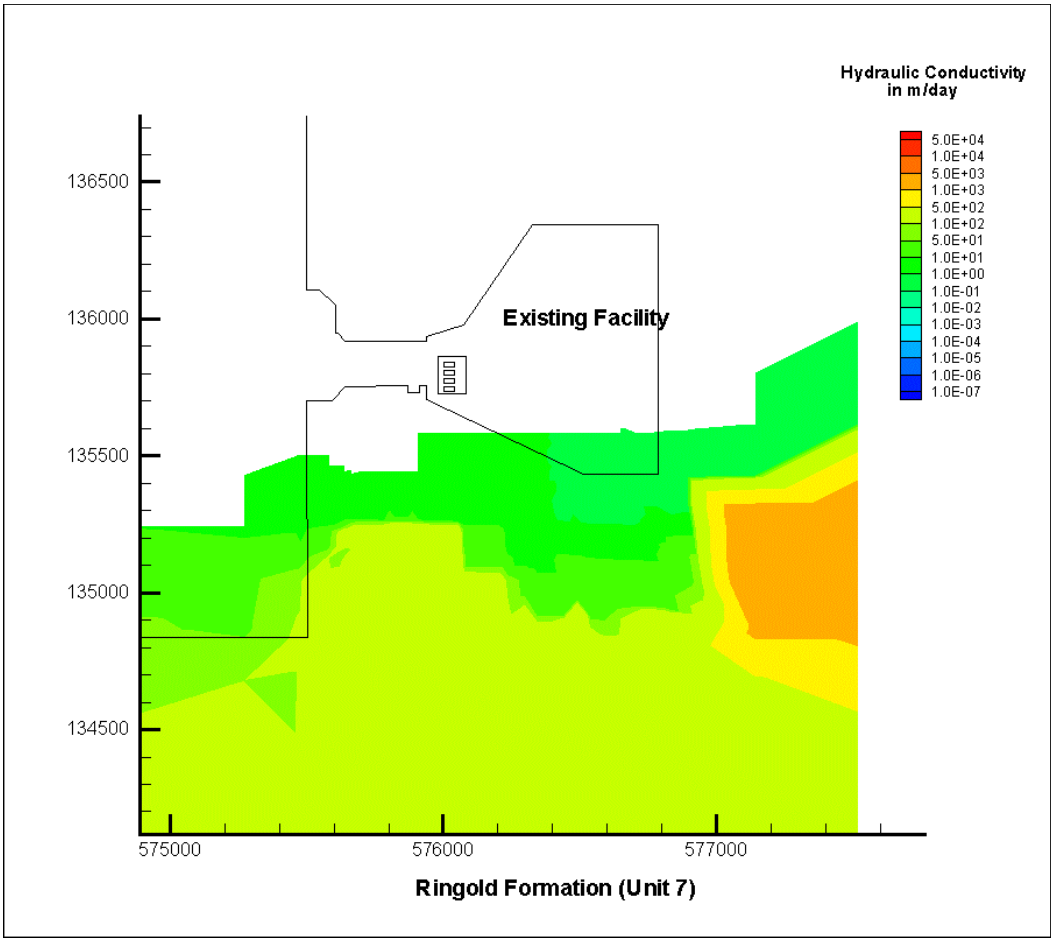

Figure 5.8 (Continued)

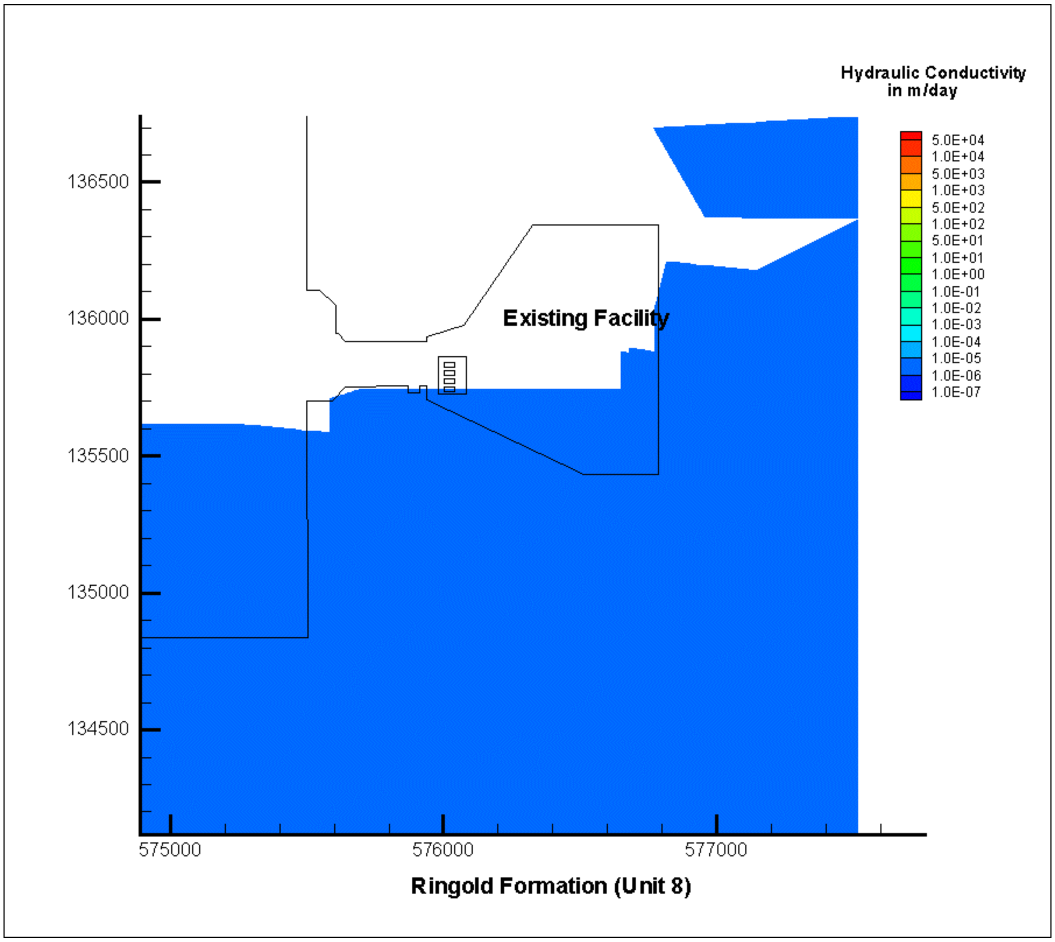

Figure 5.8 (Continued)

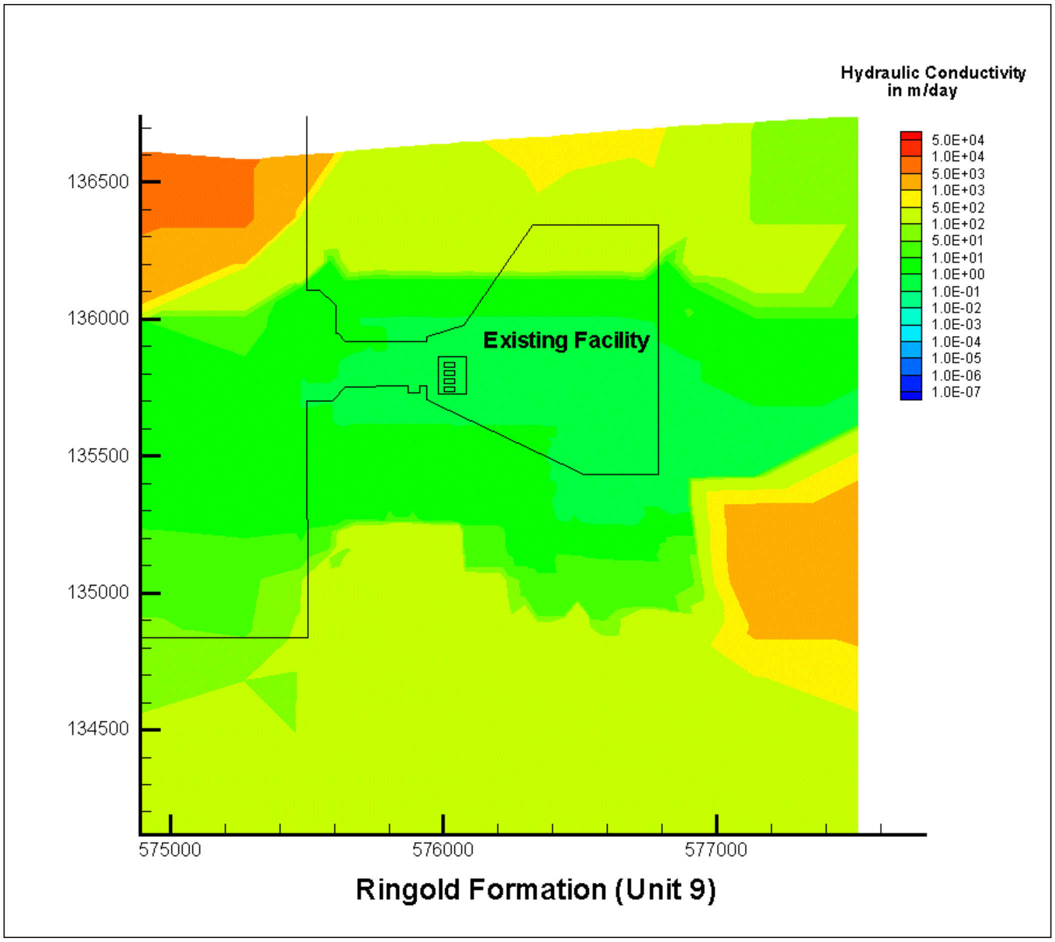

Figure 5.8 (Continued)

6.0 Results of the Groundwater Transport Analyses

This section presents the results of the groundwater transport analyses performed with the site-wide and local-scale models. The section in divided into two parts. One examines the impacts of the remote-handled-trench and concrete-vault concepts in the new ILAW disposal facility. The other evaluates the concrete-vault concept within the existing ILAW disposal facility.

6.1 New Disposal Facility

This subsection summarizes the impacts on calculated WIFs of the remote-handled trench and concrete-vault disposal concepts in the new ILAW disposal facility.

6.1.1 Remote-Handled Trench Concept

The remote-handled-trench disposal concept was evaluated in the base-case calculations. For this concept, the new ILAW disposal facility will consist of a set of six remote-handled waste trenches located in the northern part of the new ILAW disposal facility area. Each waste trench will be an underground, open-topped trench approximately 80 m (262.5 ft) wide, 260 m (853 ft) long, and 10 m (32.8 ft) deep with 3:1 side slopes. The release from these trenches in the model was approximated using the plan view area (80 m [62.5 ft] wide by 260 m [853 ft] long) of each individual trench.

The primary objective of the groundwater flow and transport calculations was to determine the WIF, defined as the ratio of the concentration at a well location in the aquifer to the concentration of infiltrating water entering the aquifer. For the purposes of these calculations, the concentration of source entering the aquifer was assumed to be 1 Ci/m^3. The rate of mass flux associated with this concentration is a function of the infiltration rate assumed for the disposal facility covered by the modified RCRA subpart C barrier. With a rate of 4.2 mm/yr assumed for the disposal facility, the resulting solute flux entering the aquifer from each of the disposal concepts is 4.2×10^{-3} $Ci/yr/m^2$. This is the product of the contaminant concentration in the infiltrating water and the infiltration rate.

Because of the uncertainty in expected infiltration rates, results developed for the 4.2 mm/yr rate for each of the cases presented were scaled to other infiltration rates that have been postulated from surface and soil conditions in the vicinity of the ILAW disposal facility by Fayer (1999). Other infiltration rates evaluated and summarized in each of the result tables included 0.1, 0.9, 1.0, and 50 mm/yr.

In all model simulations performed, the WIF was calculated at a hypothetical well located approximately 100 m (328 ft) downgradient from the boundary of the disposal along the centerline of the simulated plume. A pumping rate of 10 L (2.6 gal) per day was used at the hypothetical downgradient well location. This pumping rate would provide sufficient drinking water for a family of five at an assumed intake of 2 L (0.5 gal) per person (per day).

6.1.1.1 Simulated Results at a 100-m (328-ft) Downgradient Well

Transport model results provided for the remote-handled-trench concept were based on local-scale flow conditions (Figure 6.1). These conditions were developed based on boundary conditions provided by the steady-state simulation of Post-Hanford flow conditions performed with the site-wide model. Groundwater moves across the ILAW site in a southeasterly direction before exiting the local-scale model in the southeast corner.

The results are expressed in WIFs, which relate the contaminant concentration in groundwater to the vadose zone contaminant flux. WIFs were calculated at a distance of 100 m (328 ft) downgradient from the facility and at an approximate distance of 1,000 m (3280 ft) downgradient of the disposal-facility boundaries. The WIFs for 4.2 mm/yr and other assumed infiltration rates at this location are summarized in Table 6.1.

Simulated concentration histories at 100 m (328 ft) downgradient of the disposal facilities containing six trenches are presented in Figures 6.2 through 6.4. Figure 6.2 shows the distribution of contaminant concentration in the uppermost element of the local-scale model. Figure 6.3 shows concentration profiles in a cross section from the source area through the 100-m (328 ft) well to the edge of the local-scale model region. Figure 6.4 shows concentration histories at the 100-m (328 ft) and 1000-m (3280 ft) wells for a period of 100 yr after the source is introduced into the aquifer. In this six-trench calculation, the concentration profile reaches steady state within about 10 yr with a maximum value of 1.1×10^{-3} Ci/m^3 at the 100-m well and 7.8×10^{-4} Ci/m^3 at the 1-km well. At an assumed recharge rate of 4.2 mm/yr, the calculated WIF would be 1.1×10^{-3} at the 100-m well and 7.8×10^{-4} at the 1-km well.

Table 6.1. Well Intercept Factors at the 100-m (328-ft) and 1000-m (3280-ft) Wells for the Remote-Handled-Trench Disposal Concept Using Different Infiltration Rates – New Disposal Facility

	Infiltration Rates (mm/yr)				
Well Locations	**0.1**	**0.9**	**1.0**	**4.2**	**50**
100 m	2.5E-05	2.3E-04	2.5E-04	1.1E-03	1.3E-02
1000 m	1.9E-05	1.7E-04	1.9E-04	7.8E-04	9.3E-03

6.1.1.2 Well-Intercept Factor at Distant Downgradient Wells

Steady-state flow conditions established with the site-wide model as presented in Section 5 (Figures 5.1 and 5.2) provide the basis for transport calculations of source releases from the remote-handled-trench concept between the disposal site area and the Columbia River. Simulated transport results at several locations downgradient of the disposal facilities containing multiple remote-handled trenches are presented in Figures 6.5 and 6.6. Figure 6.5 shows the distribution of contaminant concentration in the uppermost element of the site-wide scale model. Figure 6.6 shows concentration histories at the several well locations for a period of 400 yr after the source is introduced into the aquifer. In this six-trench calculation, the concentration profile reaches steady state within about 30 to 50 yr, with a maximum value of 5.4 x 10^{-4} Ci/m^3 at the 1000-m (3280-ft) well location. Steady state is reached within 400+ yr, with a maximum value of 9.8 x 10^{-5} Ci/m^3 at the well located near the Columbia River. As expected, the associated WIF at the 1000-m (3280-ft) well location is somewhat less than with those calculated at a similar distance in the local-scale model, but is generally consistent with local-scale concentration levels, given the large differences in model resolution. At an assumed recharge rate of 4.2 mm/yr, the calculated WIFs would range from 5.4 x 10^{-4} at 1000 m (3280 ft) downgradient to 9.8x10^{-5} at a hypothetical well near the Columbia River. The WIF factors for 4.2 mm/yr and other assumed infiltration rates at all locations examined are summarized in Table 6.2.

Table 6.2. Well Intercept Factors at Several Downgradient Well Locations for the Remote-Handled-Trench Disposal Concept Using Different Infiltration Rates – New Disposal Facility

	Infiltration Rates (mm/yr)				
Well Locations*	**0.1**	**0.9**	**1.0**	**4.2**	**50**
1.0 km	1.3E-05	1.2E-04	1.3E-04	5.4E-04	6.4E-03
3.1 km	9.0E-06	8.1E-05	9.0E-05	3.8E-04	4.5E-03
5.0 km	7.9E-06	7.1E-05	7.9E-05	3.3E-04	3.9E-03
7.6 km	6.7E-06	6.0E-05	6.7E-05	2.8E-04	3.3E-03
9.3 km	5.8E-06	5.2E-05	5.8E-05	2.4E-04	2.9E-03
11.1 km	4.5E-06	4.0E-05	4.5E-05	1.9E-04	2.2E-03
14.8 km (river well)	2.3E-06	2.1E-05	2.3E-05	9.8E-05	1.2E-03

* Well locations are shown in Figure 6.5.

6.1.2 Concrete Vault Concept

For this concrete-vault concept, the new ILAW disposal facility will consist of a set of seven concrete vaults located in the northern part of the ILAW disposal facility area. As described in Chapter 2, each vault is built above a RCRA-compliant leak detection and collection system. It consists of a cast-in-place reinforced concrete basin approximately 209.5 m (687 ft) long and 24.7 m (81 ft) wide with walls 1.07 m (3.5 ft) high. The release from these vaults in the model was approximated using the plan view area (approximately 25 m [82 ft] wide by 210 m [689 ft] long) of each individual vault. The same assumption used for mass release and the hypothetical downgradient wells used for the remote-handled concept described in the previous section were used for the concrete-vault concept.

6.1.2.1 Simulated Results at the 100-m (328-ft) Downgradient Well

Local-scale flow conditions, illustrated in Figure 6.1, also provide the basis for transport-model results developed for the concrete-vault concept. This concept was based on releases from seven individual concrete vaults distributed in the new disposal-facility area. The WIFs were calculated at a distance of 100 m (328 ft) downgradient from the facility and at an approximate distance of 1,000 m (3280 ft) downgradient of the disposal-facility boundaries. The WIF factors for 4.2 mm/yr and other assumed infiltration rates at this location are summarized in Table 6.3.

Simulated concentration histories at 100 m (328 ft) downgradient of the disposal facilities containing seven vaults are presented in Figures 6.7 through 6.9. Figure 6.7 shows the distribution of contaminant concentration in the uppermost element of the local-scale model. Figure 6.8 shows concentration profiles in a cross section from the source area through the 100 m (328 ft) well to the edge of the local-scale model region. Figure 6.9 shows concentration histories at the 100 m (328 ft) well for a period of 100 yr after the source is introduced into the aquifer. In the concrete vault calculation, the concentration profile at the 100-m (328-ft) well reaches steady state within about 10 yr, with a maximum value of 2.8 x 10^{-4} Ci/m^3. At 1000 m (3280 ft), the concentration profile reaches a steady-state maximum value of 2.2 x 10^{-4} Ci/m^3. At an assumed recharge rate of 4.2 mm/yr, the calculated WIF at the 100 m (328 ft) well would be 2.8 x 10^{-4} Ci/m^3. The WIF factors for 4.2 mm/yr and other assumed infiltration rates at 100 and 1000 m (328 and 3280 ft), respectively, are summarized in Table 6.3

Table 6.3. Well Intercept Factors at the 100-m (328-ft) and 1000-m (3280-ft) Well Locations for the Concrete-Vault Disposal Concept Using Different Infiltration Rates

	Infiltration Rates (mm/yr)				
Well Locations	**0.1**	**0.9**	**1.0**	**4.2**	**50**
100 m	6.7E-06	6.1E-05	6.7E-05	2.8E-04	3.4E-03
1000 m	5.4E-06	4.8E-05	5.4E-05	2.2E-04	2.7E-03

Differences between the WIFs calculated for this case compared to the remote-handled-trench case are directly attributable to assumptions used for source-release areas in both cases. The remote-handled-trench calculations were based on an assumed release area of 124,800 m^2, reflecting the footprint of the six-trench configuration. The concrete-vault calculations were based on the assumption of a 36,750 m^2 release area, reflecting the footprint of the seven-concrete-vault configuration. The ratio of the WIFs between the two cases at 100 m are on the order of 3.9, which is reflective, though slightly higher, than the ratio of the release areas (3.4).

6.1.2.2 Well-Intercept Factor at Distant Downgradient Wells

Simulated concentration histories at several locations downgradient of the disposal facilities containing the seven concrete vaults were also developed using the regional flow field described previously and illustrated in Figure 6.5. In this seven-concrete-vault calculation, the concentration profile reaches steady state at the 1000-m well location within about 30 to 50 yr, with a maximum value of 1.6 x 10^{-4} Ci/m^3, assuming a recharge of 4.2 mm/yr. Steady state is reached within 400+ yr at the well located near the Columbia River with a maximum value of 3.9 x 10^{-4} Ci/m^3. As expected, the associated WIF at the 1000-m well location is less but similar to those calculated at a similar distance in the local-scale model. At an assumed recharge rate of 4.2 mm/yr, the calculated WIFs would range from 2.1 x 10^{-4} at 1000 m downgradient and 4.1 x 10^{-5} at a hypothetical well near the Columbia River. The WIF factors for 4.2 mm/yr and other assumed infiltration rates at all locations examined are summarized in Table 6.4.

Table 6.4. Well Intercept Factors at Several Downgradient Well Locations for the Concrete-Vault Disposal Concept Using Different Infiltration Rates

	Infiltration Rates (mm/yr)				
Well Locations*	**0.1**	**0.9**	**1.0**	**4.2**	**50**
1.0 km	3.8E-06	3.5E-05	3.8E-05	1.6E-04	1.9E-03
3.1 km	2.7E-06	2.4E-05	2.7E-05	1.1E-04	1.4E-03
5.0 km	2.4E-06	2.1E-05	2.4E-05	1.0E-04	1.2E-03
7.6 km	2.1E-06	1.9E-05	2.1E-05	8.6E-05	1.0E-03
9.3 km	1.8E-06	1.6E-05	1.8E-05	7.6E-05	9.0E-04
11.1 km	1.5E-06	1.3E-05	1.5E-05	6.1E-05	7.3E-04
14.8 km (river well)	9.2E-07	8.3E-06	9.2E-06	3.9E-05	4.6E-04

* Well locations are shown in Figure 6.10.

6.2 Existing Disposal Facility

This subsection summarizes the impacts on calculated WIFs of the concrete-vault concept in the existing ILAW disposal facility.

6.2.1 Concrete-Vault Concept

For this concrete vault concept, the existing ILAW disposal facility will contain a set of four concrete vaults as described in Section 2.2.2. Each vault at the existing disposal facility would be built above a RCRA-compliant leak-detection and collection system and would consist of a cast-in-place reinforced concrete basin. Each vault would be approximately 37.6 m (687.0 ft) long and 15.4 m (81 ft) wide with a roof clearance of 10.4 m (3.5 ft) high. The release from these vaults in the model was approximated using the plan view area (approximately 16 m [52.5 ft] wide by 40 m [131 ft] long) of each individual vault. The same assumption used for mass release and the hypothetical downgradient wells used for the concrete vault concept described in the previous section were used for the concrete-vault concept considered here.

6.2.1.1 Simulated Results at the 100-m (328-ft) Downgradient Well

Local-scale flow conditions, illustrated in Figure 6.10, provide the basis for transport-model results developed for the concrete-vault concept at the existing disposal facility. As in the other cases, concentration levels and WIFs were calculated at a distance of 100 m (328 ft) downgradient from the facility and approximately 1,000 m (3281 ft) downgradient of the disposal-facility boundaries.

Simulated concentration histories at 100 m (328 ft) downgradient of the disposal facilities containing four vaults are presented in Figures 6.11 through 6.13. Figure 6.11 shows the distribution of contaminant concentration in the uppermost element of the local-scale model. Figure 6.12 shows concentration profiles in a cross section from the source area through the 100-m (328-ft) well to the edge of the local-scale model region. Figure 6.13 shows concentration histories at the 100-m (328-ft) well for a period of 100 yr after the source is introduced into the aquifer. In the concrete vault calculation, the concentration profile at the 100-m (328-ft) well reaches steady state within about 10 yr, with a maximum value of 4.6×10^{-4} Ci/m^3. At 1000 m (3281 ft), the concentration profile reaches a steady-state maximum value of 5.7×10^{-5} Ci/m^3. At an assumed recharge rate of 4.2 mm/yr, the calculated WIF at the 100-m (328-ft) well would be 4.6×10^{-4} Ci/m^3. The WIF factors for 4.2 mm/yr and other assumed infiltration rates at 100 and 1000 m (328 and 3281 ft) respectively, are summarized in Table 6.5

Table 6.5. Well Intercept Factors at the 100-m (328-ft) and 1000-m (3281-ft) Well Locations for the Concrete-Vault Disposal Concept Using Different Infiltration Rates – Existing Disposal

	Infiltration Rates (mm/yr)				
Well Locations	**0.1**	**0.9**	**1.0**	**4.2**	**50**
100 m	1.1E-05	9.7E-05	1.1E-04	4.5E-04	5.4E-03
1000 m	1.4E-06	1.2E-05	1.4E-05	5.7E-05	6.8E-04

The large differences between the WIFs calculated for this case compared to those calculated for the remote-handled-trench case are attributable to assumptions used for source release areas and the lower estimated values for hydraulic properties used for hydrogeologic units in the existing grout facility model. The remote-handled-trench calculations were based on an assumed release area of 124,800 m^2, reflecting the footprint of the assumed six-trench configuration. The concrete-vault calculations were based on the assumed 2,560 m^2 release area, reflecting the footprint of the smaller four-concrete-vault configuration. The ratio of the WIFs between the two cases at 100 m are on the order of 2.4, which is much lower than expected, given that the ratio of the release area is on the order of 50. The higher-than-expected WIF in this case is affected by the lower hydraulic conducitivities used in this lowcal scale model. Hydraulic conductivities used for the Hanford Formation beneath the existing grout facilities, which are on the order of 200 to 300 m/day, are about a factor of 25 to 50 times lower than those used beneath the new ILAW disposal-facility area, which vary from about 6,500 to 14,500 m/day). In general, the lower hydraulic conductivities used in the existing grout-facility model contribute to lower pore water velocities and lower horizontal flow beneath the existing grout facility; they create an overall increase in the calculated WIF. The general increase in the WIF for this case reflects differences in the release area and the estimated hydraulic properties.

6.2.1.2 Well-Intercept Factor at Distant Downgradient Wells

Simulated transport results at several locations downgradient of the existing disposal facility containing four concrete vaults were also developed using the regional flow field described previously and illustrated in Figure 5.2. In this four-concrete-vault calculation, the concentration profile reaches steady state at the 1000 m (3281 ft) well location within about 30 to 50 yr, with a maximum value of 3.0 x 10^{-5} Ci/m^3, assuming a recharge of 4.2 mm/yr. Steady state is reached within 400+ yr at the well located near the Columbia River, with a maximum value of 5.2 x 10^{-6} Ci/m^3. The associated WIF at the 1000-m (3281-ft) well location is similar to those calculated at a similar distance in the local-scale model. At an assumed recharge rate of 4.2 mm/yr, the calculated WIFs would range from 3.0 x 10^{-5} at 1000 m (3281 ft) downgradient and 5.2 x 10^{-6} at a hypothetical well near the Columbia River. The WIF factors for 4.2 mm/yr and other assumed infiltration rates at all locations examined are summarized in Table 6.6.

Table 6.6. Well Intercept Factors at Several Downgradient Well Locations for the Concrete-Vault Disposal Concept Using Different Infiltration Rates – Existing Disposal Facility

	Infiltration Rates (mm/yr)				
Well Locations*	**0.1**	**0.9**	**1.0**	**4.2**	**50**
1.0 km	7.1E-07	6.4E-06	7.1E-06	3.0E-05	3.6E-04
3.1 km	3.5E-07	3.1E-06	3.5E-06	1.5E-05	1.7E-04
5.0 km	2.3E-07	2.0E-06	2.3E-06	9.5E-06	1.1E-04
7.6 km	2.0E-07	1.8E-06	2.0E-06	8.3E-06	9.9E-05
9.3 km	1.9E-07	1.7E-06	1.9E-06	7.8E-06	9.3E-05
11.1 km	1.5E-07	1.4E-06	1.5E-06	6.4E-06	7.6E-05
14.8 km (river well)	1.2E-07	1.1E-06	1.2E-06	5.2E-06	6.2E-05

* Well locations are shown in Figure 6.14

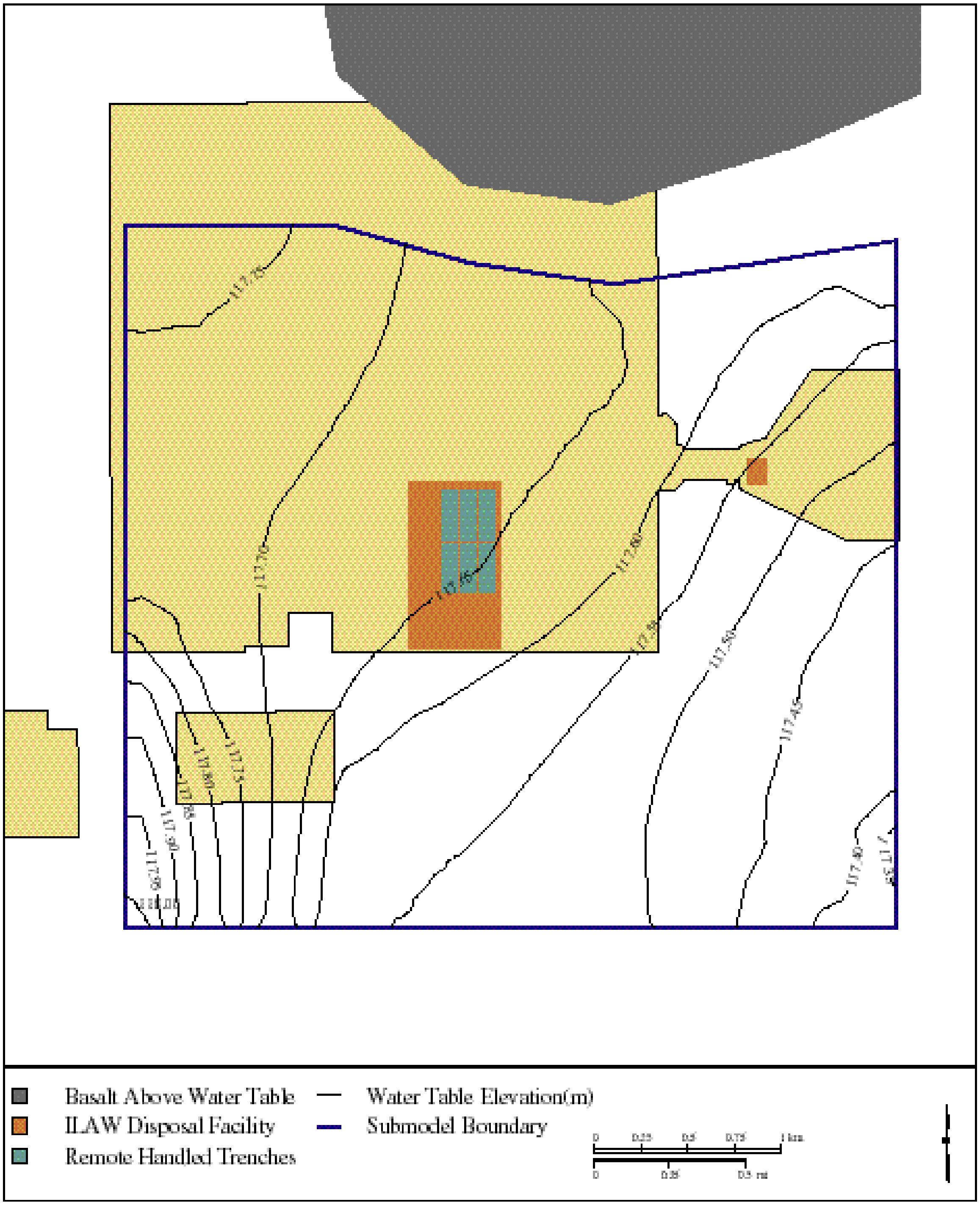

skw00072.qxd December 28, 2000

Figure 6.1. Distribution of Hydraulic Head in Unconfined Aquifer in Local-Scale Model – New Disposal Facility Area

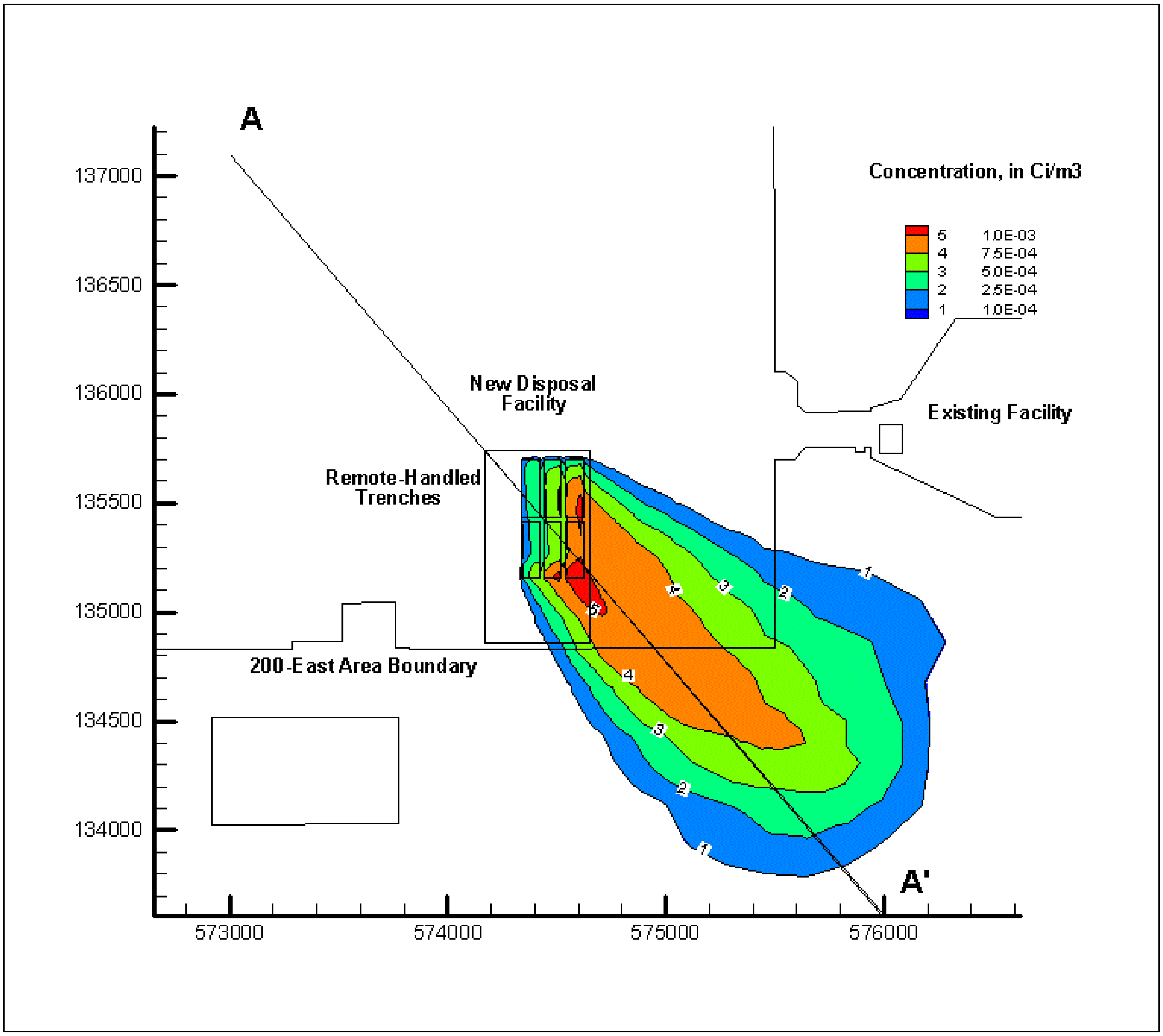

Figure 6.2. Areal Distribution of Contaminant Plume Resulting From Simulation of the Remote-Handled Trench Concept – New Disposal Facility Area

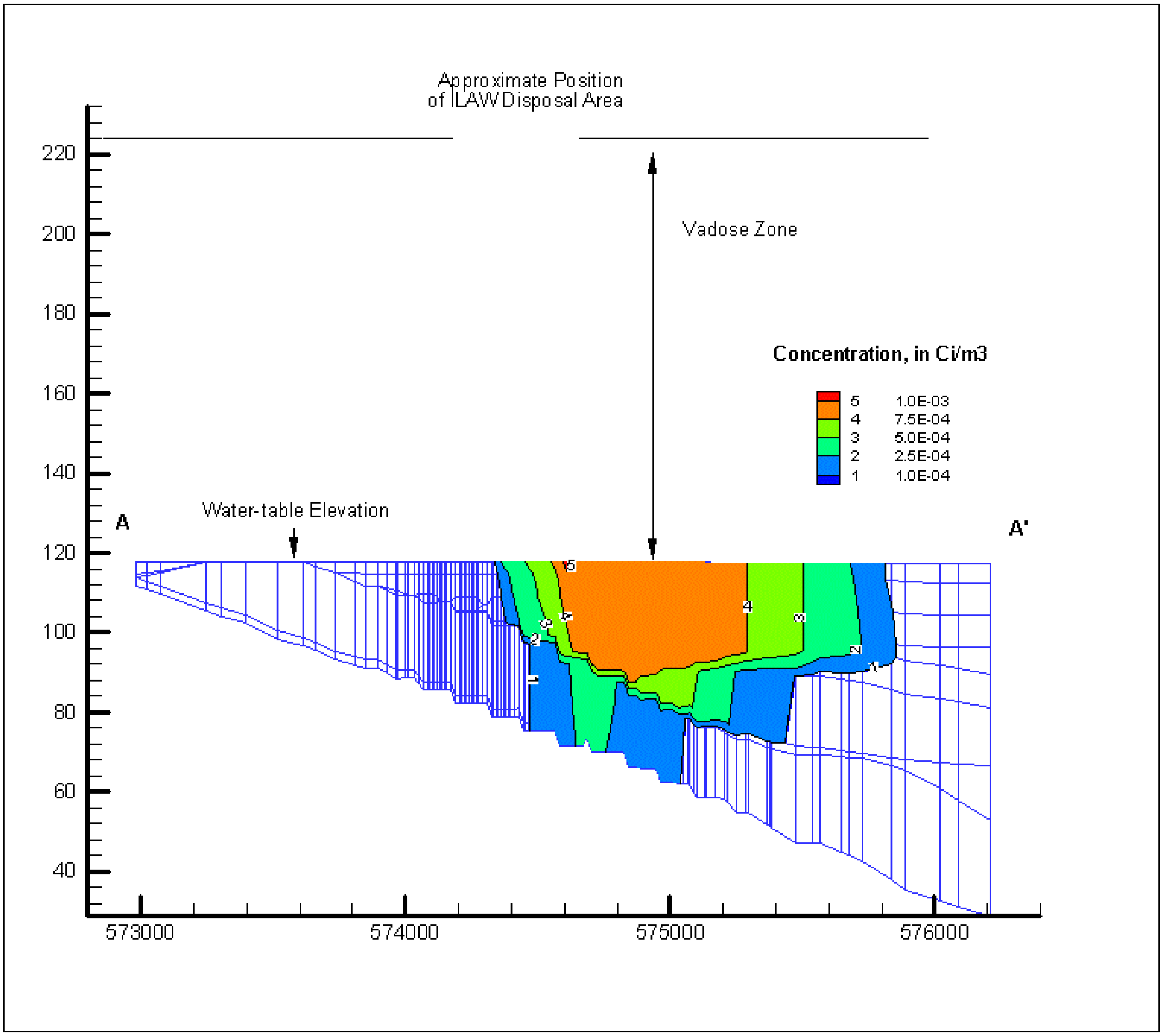

Figure 6.3. Vertical Distribution of a Contaminant Plume Resulting from Simulation of the Remote-Handled Trench Concept (Along the Approximate Centerline of the Plume) – New Disposal Facility Area

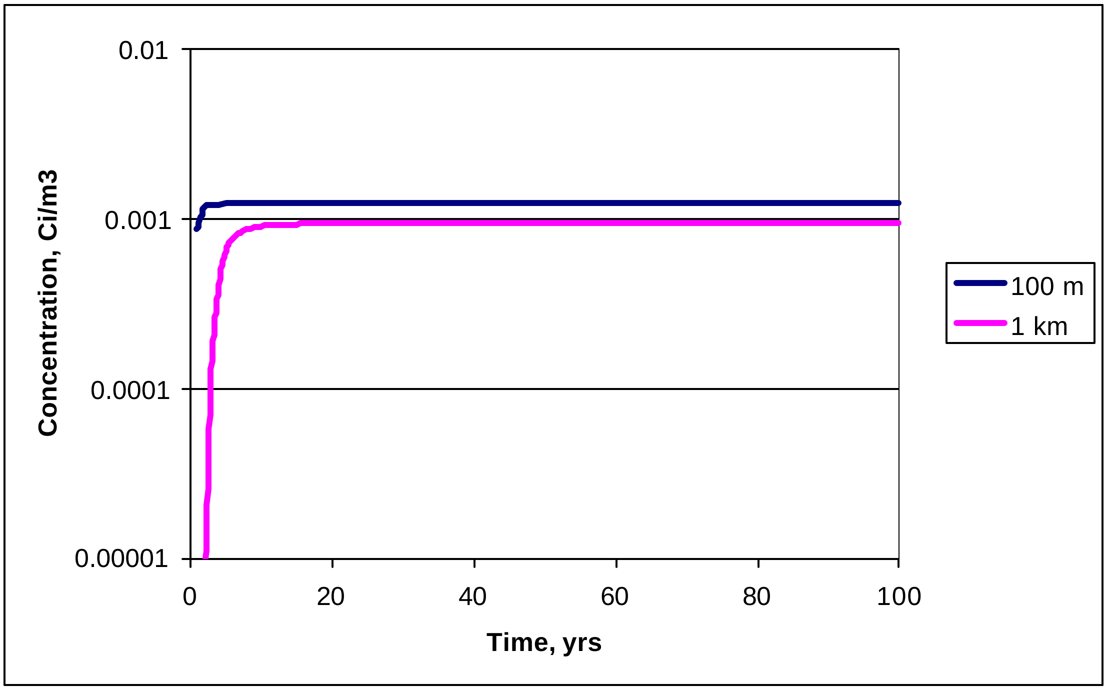

Figure 6.4. Concentration History at 100-m (328-ft) and 1000-m (328-ft) Wells, Local Scale Model – New Disposal Facility Area

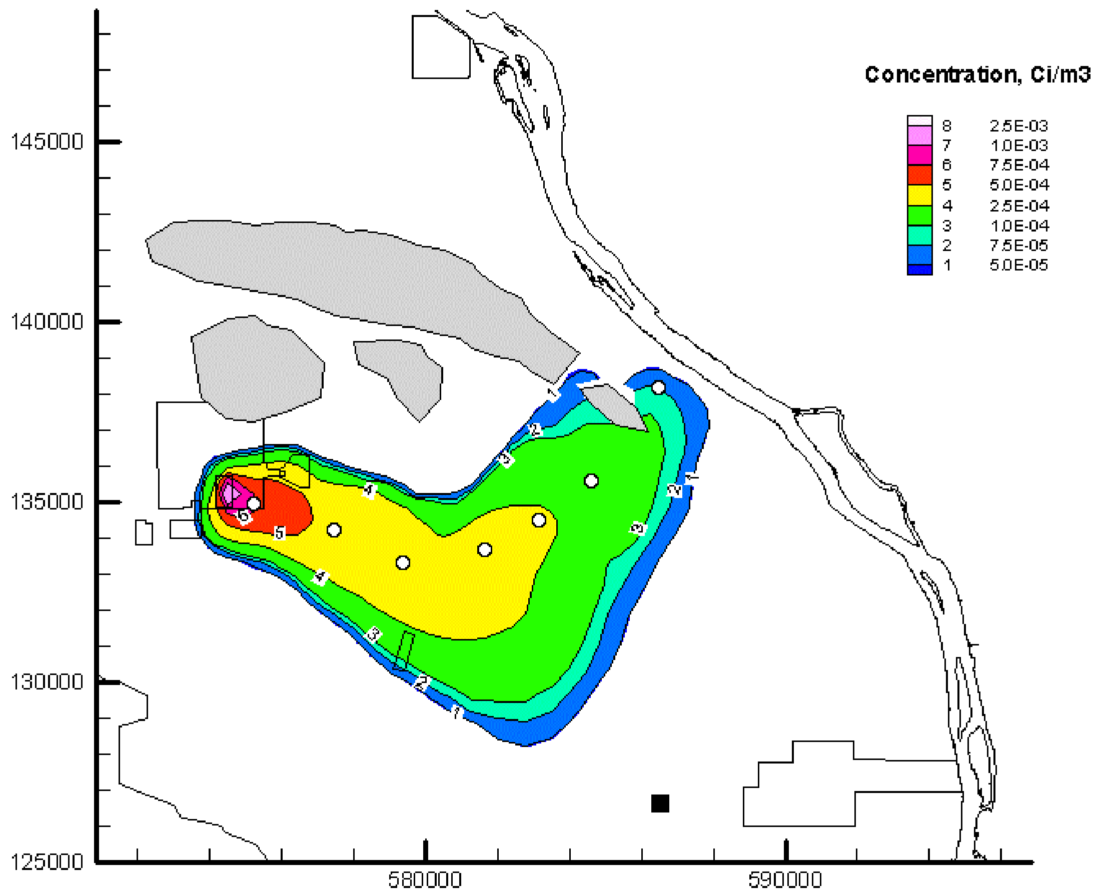

Figure 6.5. Areal Distribution of Contaminant Plume between the ILAW New Facility and the Columbia River, Remote Trench Concept – New Disposal Facility Area

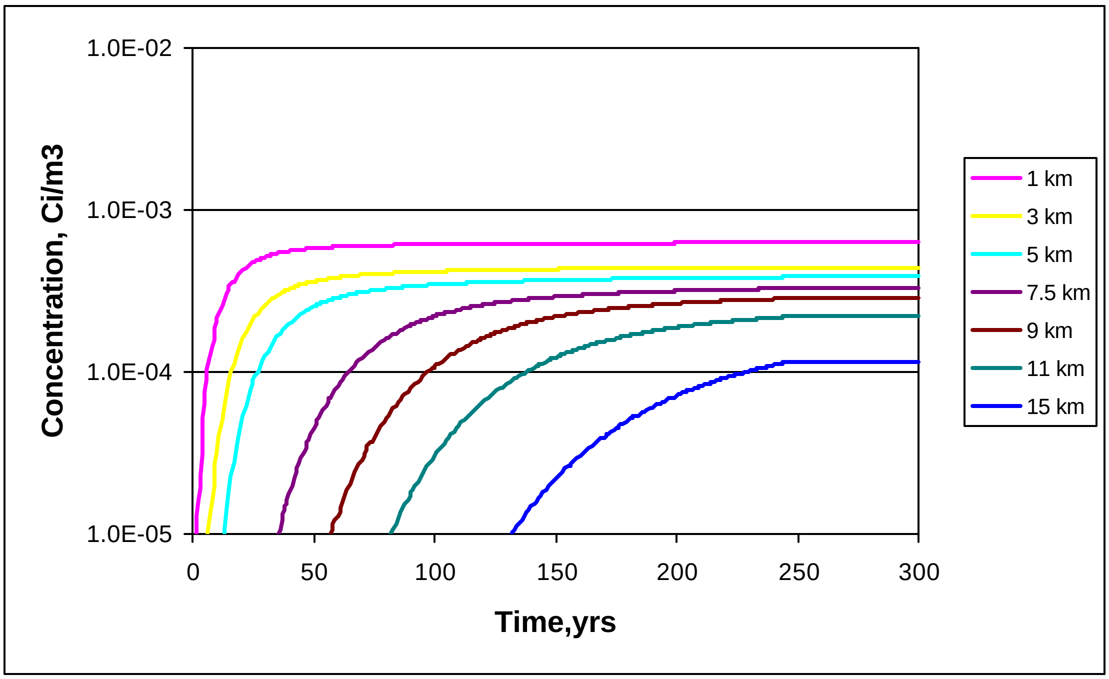

Figure 6.6. Concentration History at Selected Well Locations, Site-Wide Model – New Disposal Facility Area

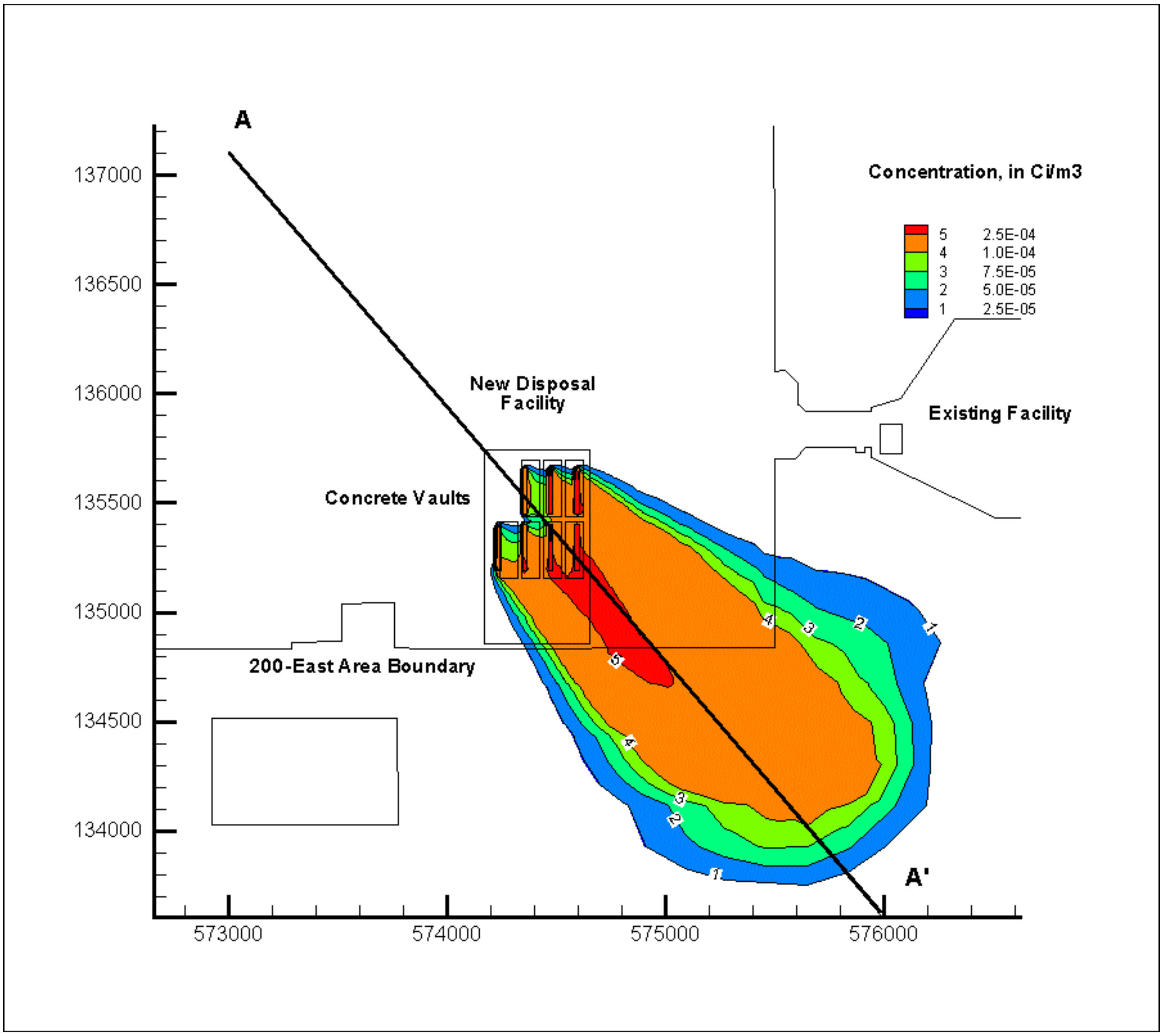

Figure 6.7. Areal Distribution of Contaminant Plume Resulting from Simulation of the Concrete Vault Concept – New Disposal Facility Area

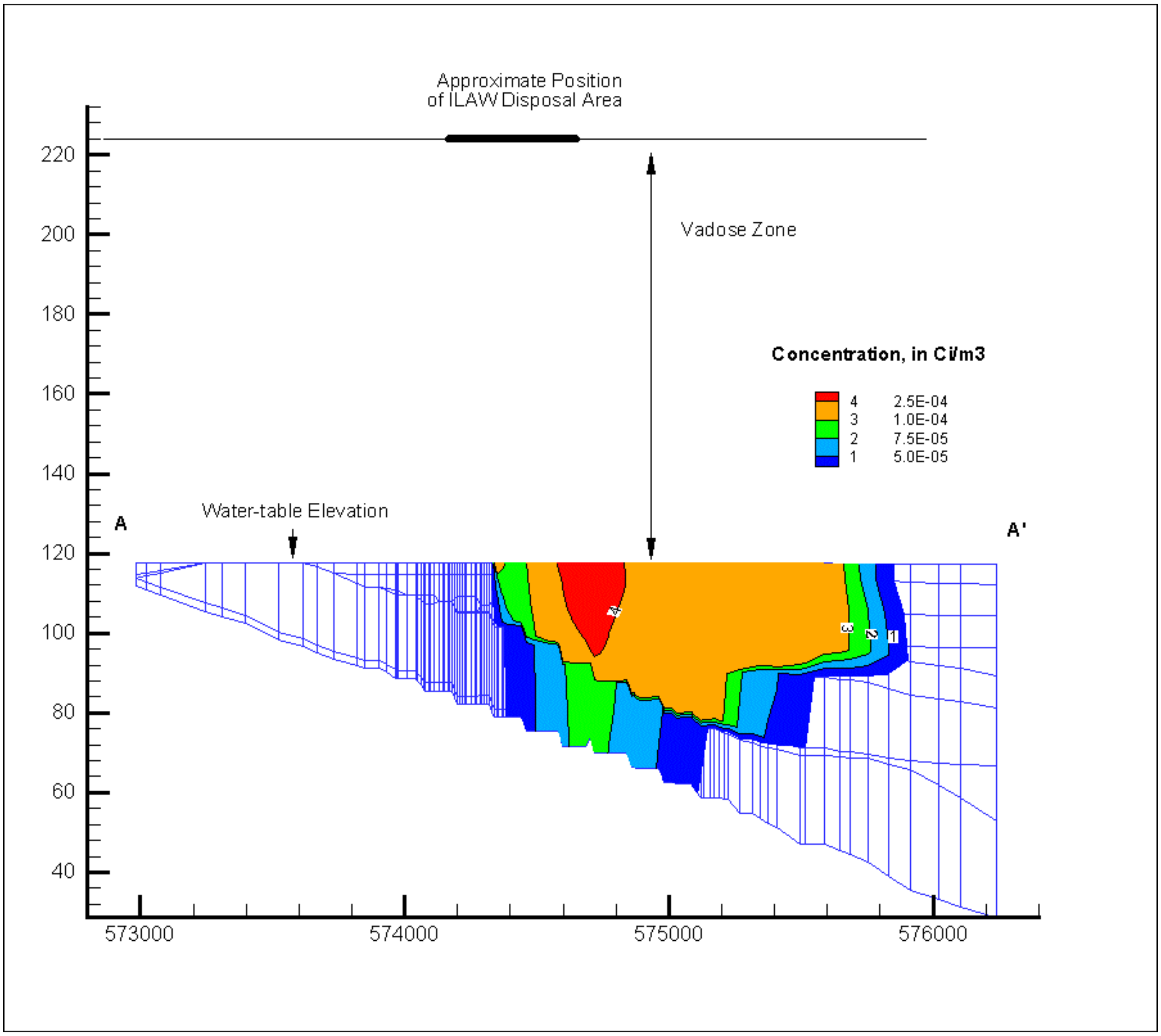

Figure 6.8. Vertical Distribution of a Contaminant Plume Resulting from Simulation of the Concrete Vault Concept (Along the Approximate Centerline of the Plume) – New Disposal Facility Area

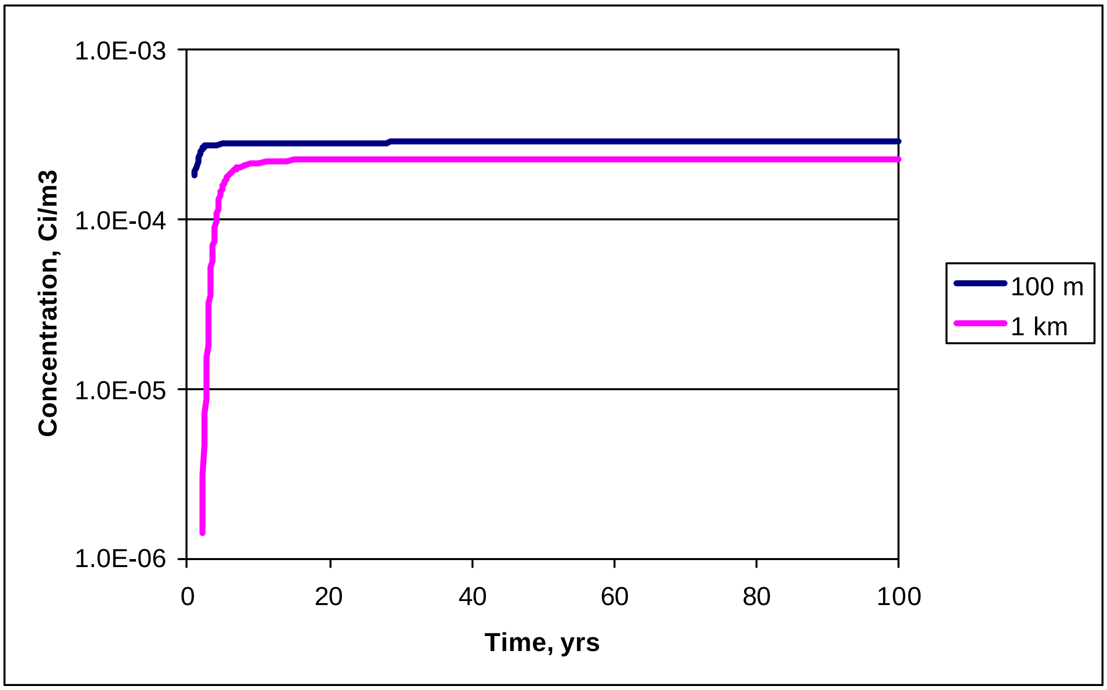

Figure 6.9. Concentration History at 100-m (328-ft) and 1000-m (3281-ft) Wells, Local Scale Model, Concrete Vault Concept – New Disposal Facility Area

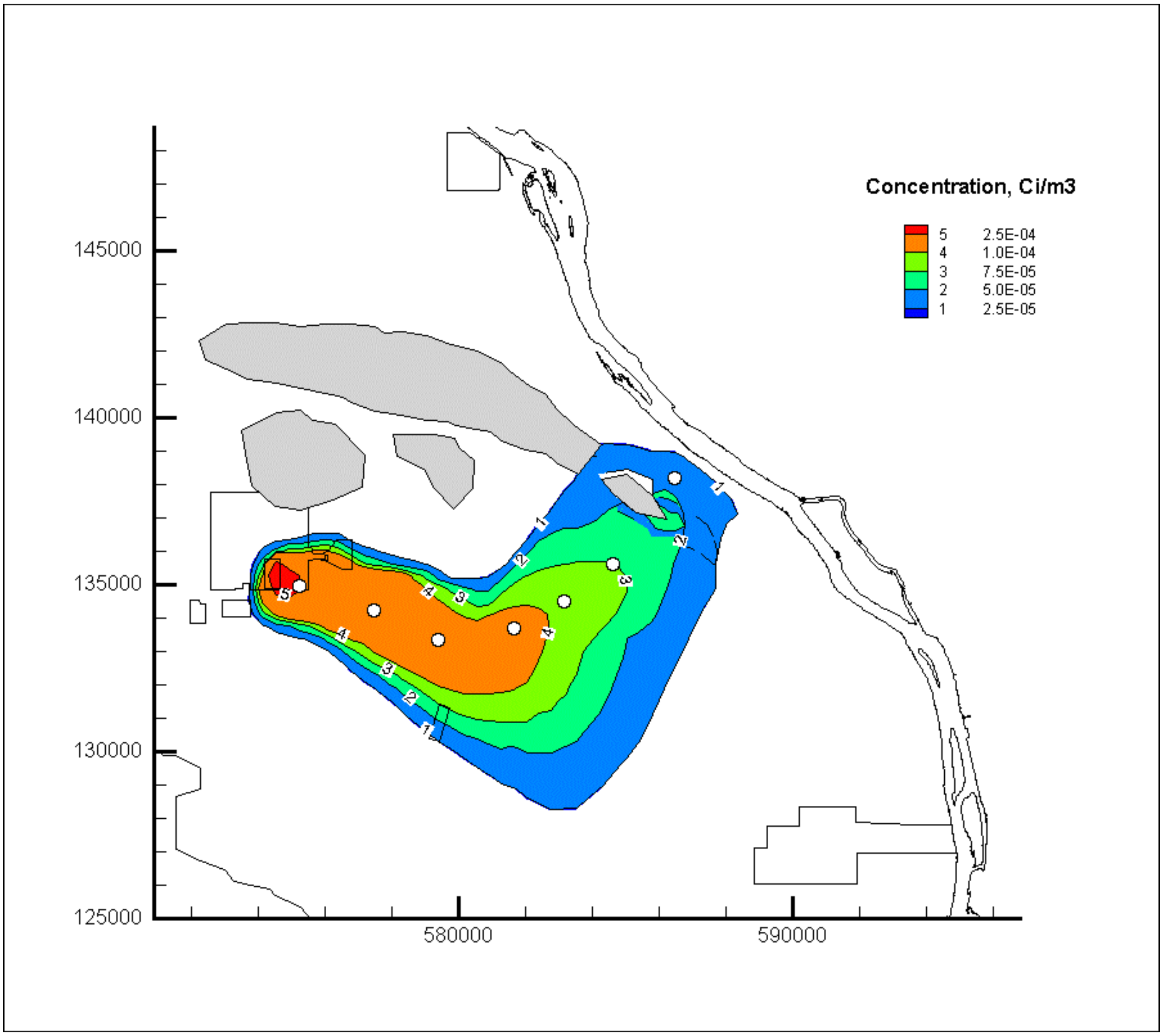

Figure 6.10. Areal Distribution of Contaminant Plume Between ILAW New Facility and Columbia River, Concrete Vault Concept – New Disposal Facility Area

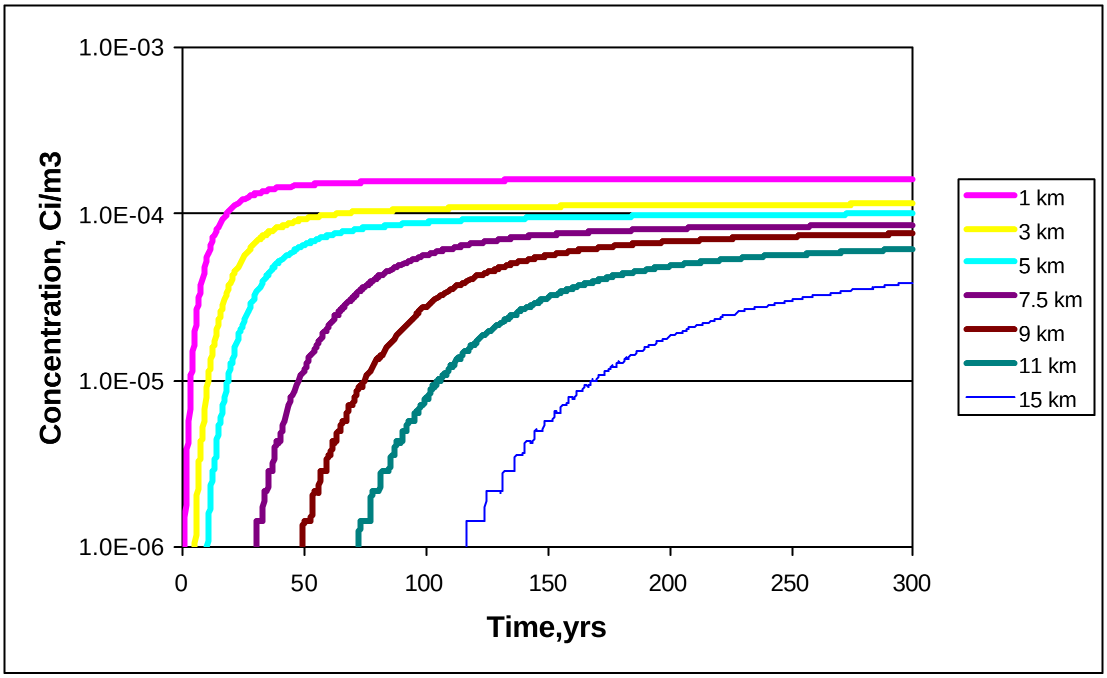

Figure 6.11. Concentration History at Selected Well Locations, Site-Wide Model, Concrete Vault Concept – New Disposal Facility Area

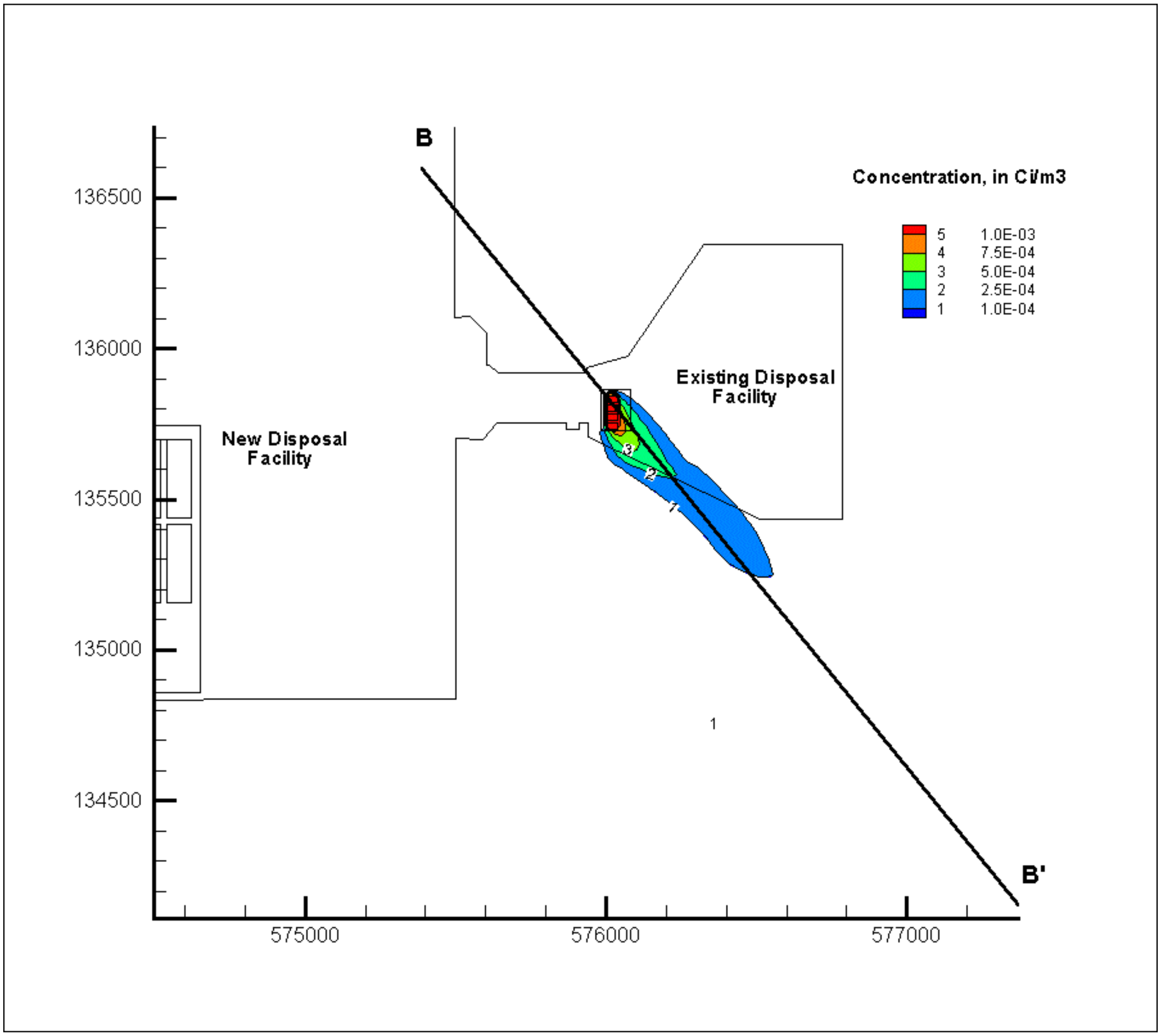

Figure 6.12. Areal Distribution of Contaminant Plume Resulting from Simulation of the Concrete Vault Concept – Existing Disposal Facility Area

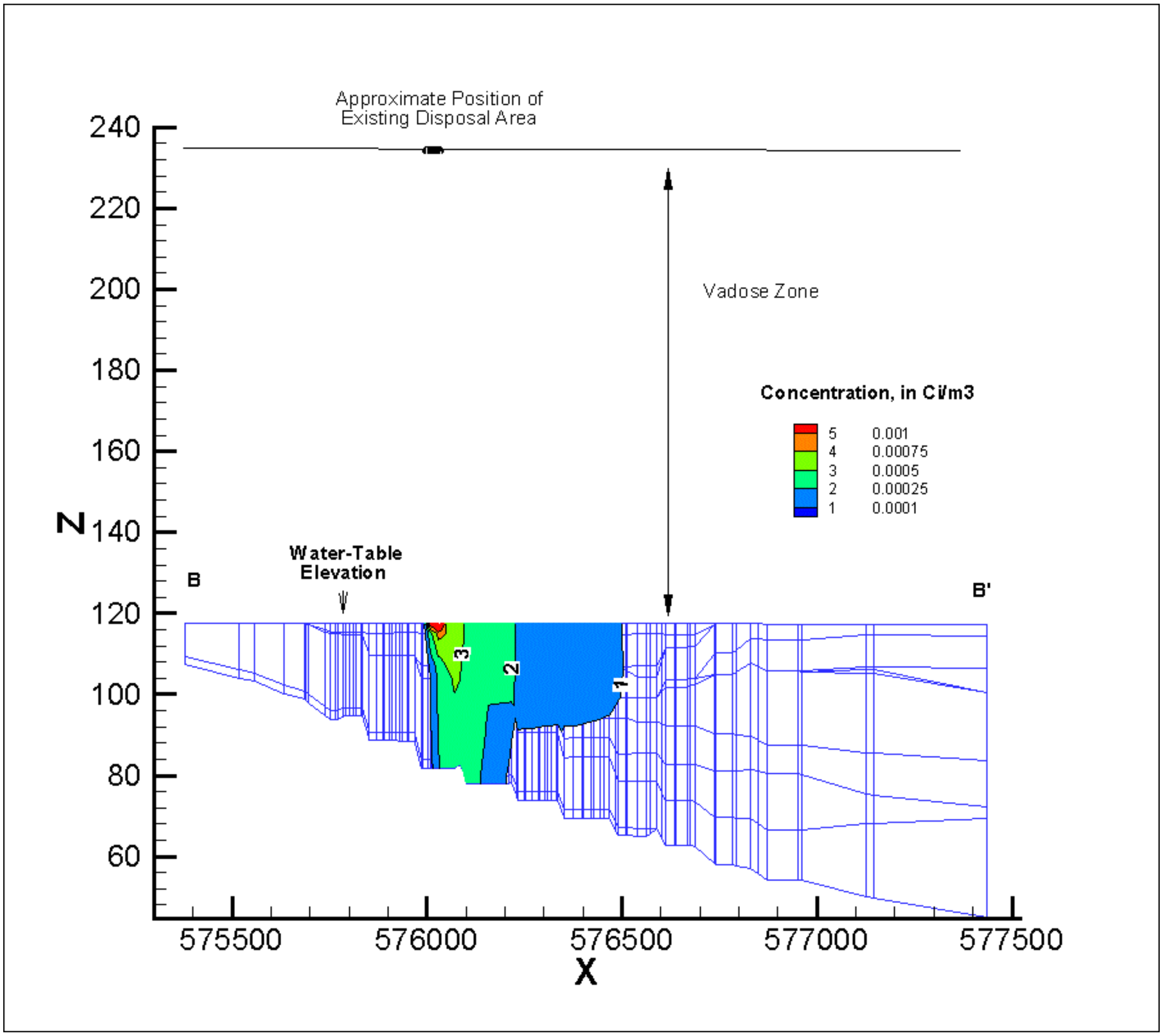

Figure 6.13. Vertical Distribution of a Contaminant Plume Resulting from Simulation of the Concrete-Vault Concept (Along the Approximate Centerline of the Plume) – Existing Disposal Facility Area

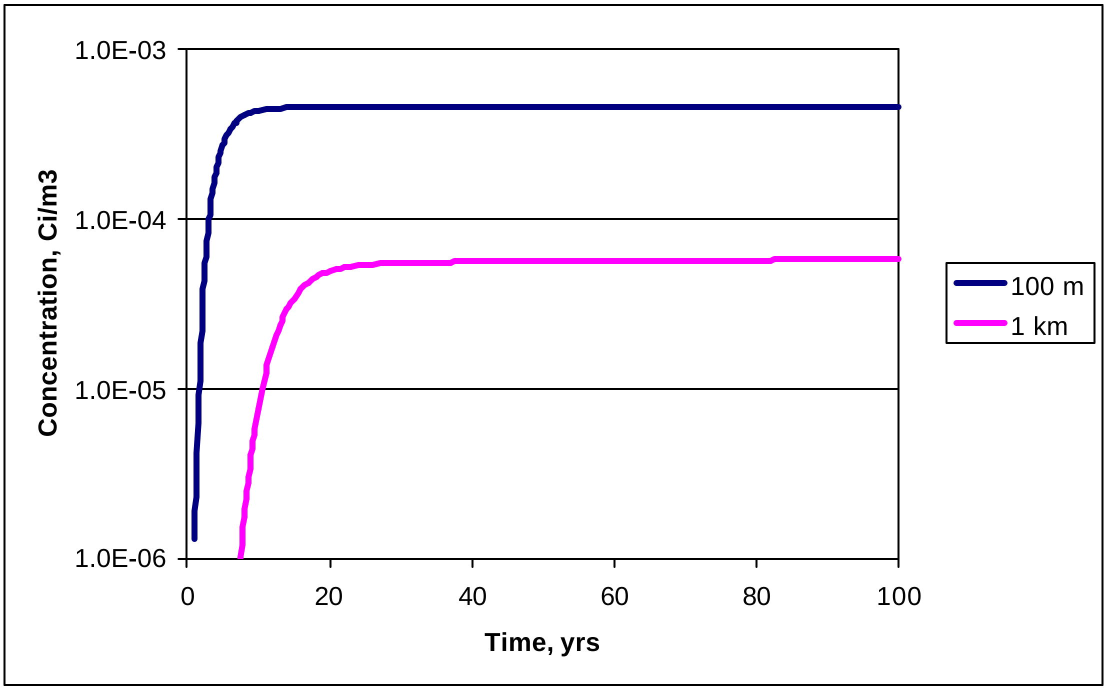

Figure 6.14. Concentration History at 100-m (328-ft) and 1000-m (3281-ft) Wells, Local Scale Model – Existing Disposal Facility Area

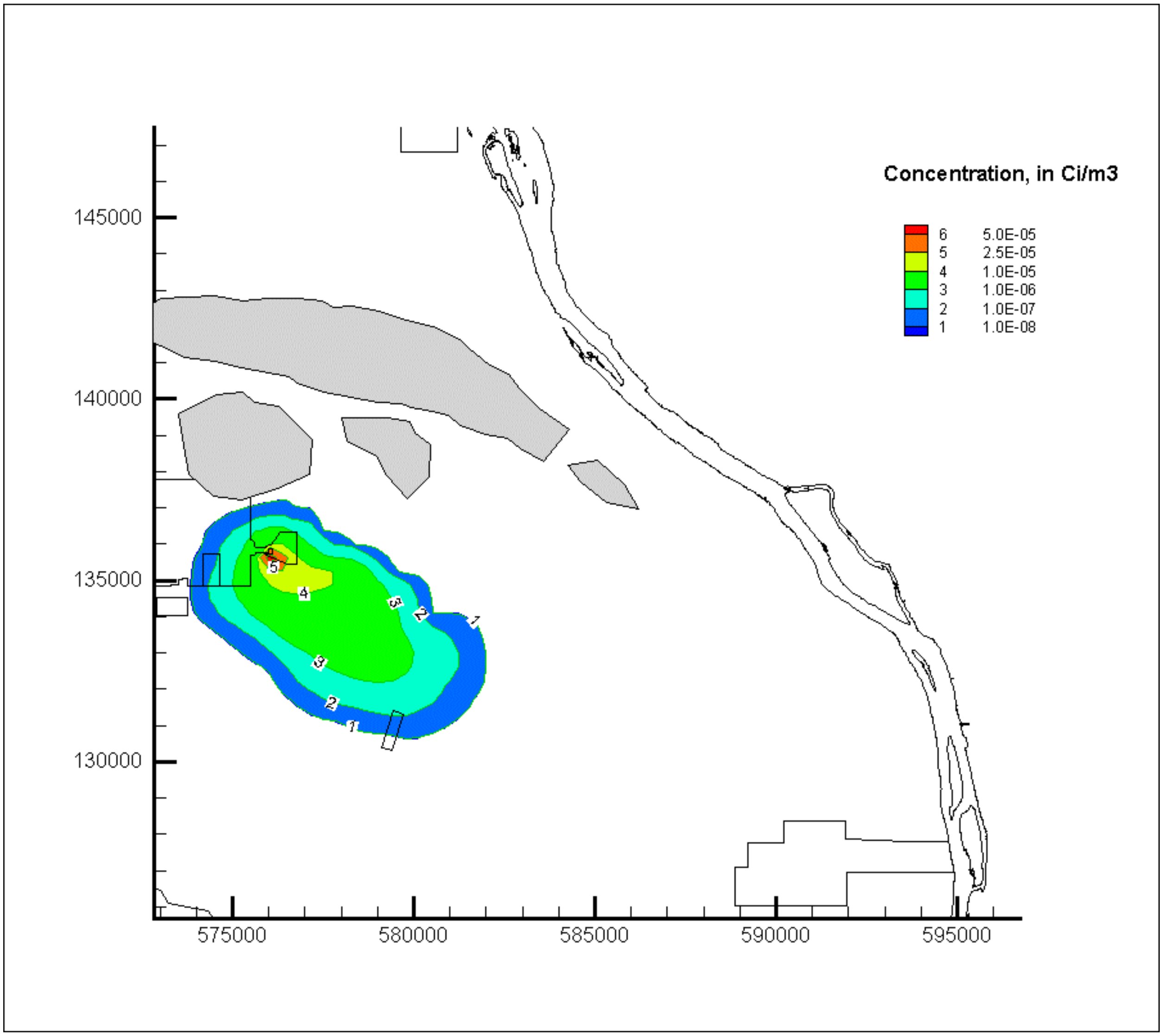

Figure 6.15. Areal Distribution of Contaminant Plume Between ILAW New Facility and Columbia River, Concrete Vault Concept - Existing Disposal Facility

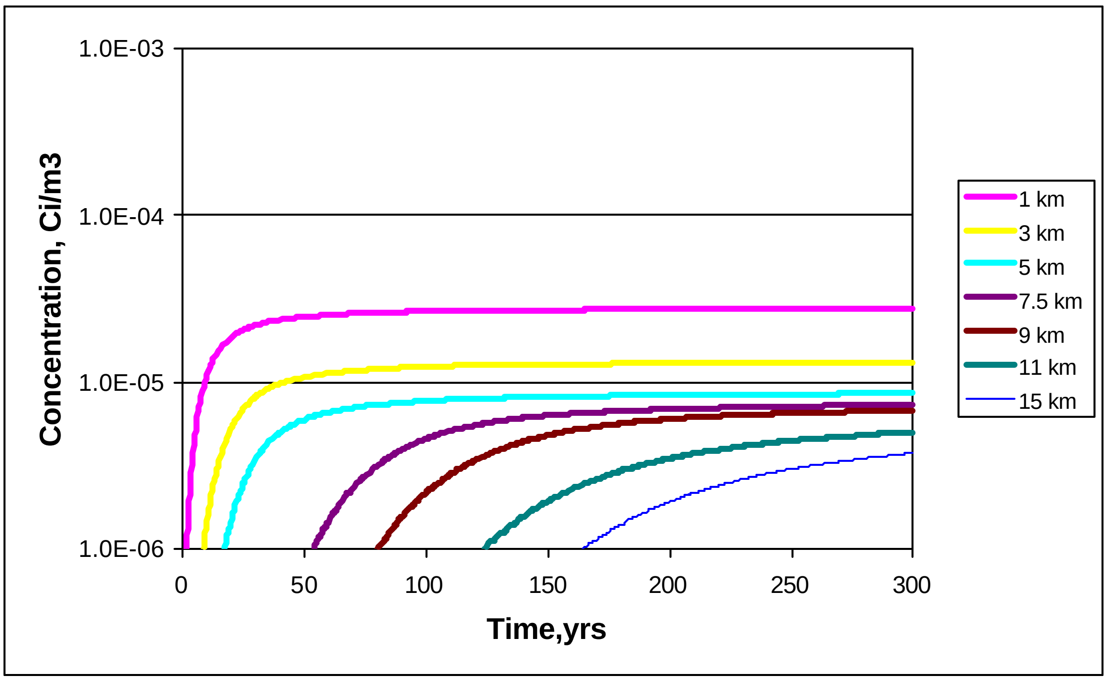

Figure 6.16. Concentration History at Selected Well Locations, Site-Wide Model – Existing Disposal Facility Area

7.0 Results of Sensitivity Analyses

This section of the report describes and presents results from several sensitivity analyses that were performed to evaluate the effect of key factors and assumptions used in the base-case analyses discussed in the previous section. The sensitivity cases evaluated the effect of the following changes:

- Disposal site location
- Disposal site orientation
- Increasing pumping rates at the hypothetical 100-m (328-ft) well downgradient of the facility
- Decreasing hydraulic conductivities in the hydrogeologic unit at the water table beneath the site
- Increasing the effective source-release area
- Raising and lowering the water-table position by:
  - increasing regional estimates of natural recharge
  - decreasing regional estimates of natural recharge
  - reducing in regional boundary fluxes upgradient of the disposal site

Following are results associated with each one of the sensitivity cases.

7.1 Disposal Site Location (Case 1)

This sensitivity study examined the effect of locating the seven disposal-facility remote-handled trenches evaluated in the base case at the southern end of the ILAW disposal-facility area. One of the key factors in the calculated WIF for base-case analysis was the assumed hydrogeologic unit and corresponding hydraulic conductivity found at the water table directly below the facility. With the disposal trenches located in the northern part of the ILAW disposal facility area, the disposal facility is largely underlain by relatively high-permeability sediments associated with the Hanford Formation. Moving the disposal trenches to the southern end of the facility area will position the disposal facility closer to the water-table contact between the Hanford Formation and the lower permeability sediments associated with the Ringold Formation. The change in postulated hydraulic properties at the water table will result in a different velocity distribution beneath the facility that could affect calculated WIFs.

Model-simulation results of the contaminant plume and the trench configuration used for this case are provided in Figure 7.1. Tabular results of the calculated WIFs at 100 m (328 ft) and 1 km (0.62 mi) downgradient of the source area are provided in Table 7.1. The direction of plume movement in this case is very similar to the base case, but calculated WIFs are a factor of 80 percent higher than in the base case. This result is consistent with the postulation that with a thinner distribution of Hanford formation sediments in the south end of the facility, the overall distribution of groundwater velocities would be lower and the resulting WIF would be higher than the base case.

Table 7.1. Well Intercept Factors at the 100-m (328-ft) and 1000-m (3281-ft) Wells for the Remote-Handled Trench Disposal Concept with All Trenches Situated in the South End of the New Disposal Facility (Case 1)

	Infiltration Rates (mm/yr)				
Well Locations	**0.1**	**0.9**	**1.0**	**4.2**	**50.0**
BaseCase					
100 m	2.5E-05	2.3E-04	2.5E-04	1.1E-03	1.3E-02
1000 m	1.9E-05	1.7E-04	1.9E-04	7.8E-04	9.3E-03
Case 1					
100 m	4.8E-05	4.3E-04	4.8E-04	2.0E-03	2.4E-02
1000 m	2.7E-05	2.4E-04	2.7E-04	1.1E-03	1.4E-02

7.2 Disposal Site Orientation (Case 2)

This sensitivity case examines the effect on the WIF of rotating the orientation of the seven remote-handled trenches evaluated in the base case by 90 degrees. Conceptually, flow across the facility is predominantly in a northwest to southeast direction. The change in orientation would put the longest dimension of the individual remote-handled trenches in an orientation closer to perpendicular to the dominant direction of flow. This would conceivably decrease the overall width of the disposal facility and increase the magnitude of the WIF.

Model simulation results of the contaminant plume and the trench configuration used for this case are provided in Figure 7.2. Tabular results of calculated WIFs at 100 m (328 ft) and 1 km (0.62 mi) downgradient of the source area are provided in Table 7.2. While changing the trench configuration did have some effect on the calculated WIFs, the resulting WIF at the 100-m (328-ft) well was only a factor of 15 percent higher than the 100-m (328-ft) well WIFs calculated for the base case. The calculated WIF at 1 km (0.62 mi) was increased by a factor of about 4 percent over the 1 km (0.62 mi) WIF in the basecase.

Table 7.2. Well Intercept Factors at 100-m (328-ft) and 1000-m (3281-ft) Wells for the Remote-Handled Trench Disposal Concept with a 90-Degree Change in Trench Orientation (Case 2)

	Infiltration Rates (mm/yr)				
Well Locations	**0.1**	**0.9**	**1.0**	**4.2**	**50. 0**
BaseCase					
100 m	2.5E-05	2.3E-04	2.5E-04	1.1E-03	1.3E-02
1000 m	1.9E-05	1.7E-04	1.9E-04	7.8E-04	9.3E-03
Case 2					
100 m	3.1E-05	2.8E-04	3.1E-04	1.3E-03	1.5E-02
1000 m	1.9E-05	1.7E-04	1.9E-04	8.1E-04	9.7E-03

7.3 Pumping at a 100-m (328-ft) Well (Case 3)

This sensitivity study examines the effect of varying the assumed pumping rate at the 100-m (328-ft) well downgradient of the facility on the calculated WIF and the behavior of the contaminant plume. Conceptually, increased pumping would reduce the calculated WIFs and contaminant levels at downstream wells as the capture zone caused by the increased pumping at the well reaches out beyond the contaminated water zone. This sensitivity case examined four pumping rates: 30 L (8 gal)/day, 100 L (26.4 gal)/day, 300 L (79 gal)/day, and 1000 L (264 gal)/day.

Results of these sensitivity cases showed that pumping in the ranges of rates investigated would have little effect on the calculated WIFs. The effect of these relatively low pumping rates is consistent with the fact that water pumped at the 100-m (328-ft) well location is largely derived from the Hanford Formation. Given the magnitude of the estimated permeabilities of the Hanford Formation at the location of the 100-m (328 ft) well (about 4,400 m/day), the hydraulic effect of the pumping would be minimal and would not significantly alter the local flow field and the overall plume movement (Figure 7.3). Calculated WIFs for these cases are virtually identical as those calculated at the 100-m (328 ft) well and 1 km (0.62 mi) in the base case (Table 7.3).

7.4 Reduction in Hydraulic Properties of the Hydrogeologic Unit at Water Table (Case 4)

The estimated hydraulic properties and interpretations of the distribution of major hydrogeologic units used in the site-wide model and local-scale models are based on interpretations of limited measurements and well log information. Uncertainties in estimates of hydraulic properties and boundaries of the major units are associated with these interpretations. In this sensitivity study, the effect of the position and the associated hydraulic-property differences between the Hanford formation and the underlying Ringold Formation (Unit 5) is investigated. Directly beneath the disposal-facility area, the estimated hydraulic properties of the Hanford formation are relatively higher compared to the Ringold Formation (Unit 5) where they range from 2500 to 30,000 m/day (27,340 to 32,808 yd/day). In contrast, the hydraulic conductivity of the Ringold Formation (Unit 5) ranges from 40 to 350 m/day (44 to 383 yd/day). For purposes of this sensitivity study, the permeability of the Hanford Formation where it exists beneath the disposal facility was lowered to hydraulic-conductivity levels of the underlying Ringold Formation. The resulting distribution of hydraulic conductivity for Unit 1 is provided in Figure 7.4. Conceptually, this change effectively reduces simulated velocities and flow rates in the hydrogeologic unit at the water table and would result in an increase in the calculated WIFs.

Table 7.3. Well Intercept Factors at the 100-m (328-ft) and 1000-m (3281-ft) Wells for the Remote-Handled Trench Disposal Concept Using Increased Pumping Rates at the 100-m (328-ft) Downgradient Well (Case 3)

	Infiltration Rates (mm/yr)				
Well Locations	**0.1**	**0.9**	**1.0**	**4.2**	**50. 0**
BaseCase					
100 m	2.5E-05	2.3E-04	2.5E-04	1.1E-03	1.3E-02
1000 m	1.9E-05	1.7E-04	1.9E-04	7.8E-04	9.3E-03
Case 3					
a) 30 lpd					
100 m	2.5E-05	2.3E-04	2.5E-04	1.1E-03	1.3E-02
1 km	1.9E-05	1.7E-04	1.9E-04	7.8E-04	9.3E-03
b) 100 lpd					
100 m	2.5E-05	2.3E-04	2.5E-04	1.1E-03	1.3E-02
1 km	1.9E-05	1.7E-04	1.9E-04	7.8E-04	9.3E-03
c) 300 lpd					
100 m	2.5E-05	2.3E-04	2.5E-04	1.1E-03	1.3E-02
1 km	1.9E-05	1.7E-04	1.9E-04	7.8E-04	9.3E-03
d) 1000 lpd					
100 m	2.5E-05	2.3E-04	2.5E-04	1.1E-03	1.3E-02
1 km	1.9E-05	1.7E-04	1.9E-04	7.8E-04	9.3E-03

The reduction in hydraulic properties changed the primary direction of groundwater beneath the facility to a more easterly direction as shown in Figure 7.5. Calculated WIFs for this case are calculated at the 100-m (328 ft) well and 1 km (0.62 mi) in the base case (Table 7.4). These results indicate that a reduction in the hydraulic conductivity of the underlying Hanford Formation to those in the Ringold Formation (Unit 5) below Hanford would increase calculated WIFs by about an order of magnitude at the 100-m (328-ft) well (1.25×10^{-2} versus 1.25×10^{-3} for the 4.2 mm/yr infiltration rate). The resulting WIF for the 4.2 infiltration rate at 1-km (0.62-mi) location (4.0×10^{-3}) was calculated to be a factor of 5 higher than at the same location in the base case (9.7×10^{-4}). The predicted distribution of contaminant concentrations from the seven trenches' release is provided in Figure 7.6.

Table 7.4. Well Intercept Factors at the 100-m (328-ft) and 1000-m (3281-ft) Wells for the Remote-Handled Trench Disposal Concept Using a Reduction in the Hydraulic Conductivity of the Hanford Formation (Case 4)

	Infiltration Rates (mm/yr)				
Well Locations	**0.1**	**0.9**	**1.0**	**4.2**	**50. 0**
BaseCase					
100 m	2.5E-05	2.3E-04	2.5E-04	1.1E-03	1.3E-02
1000 m	1.9E-05	1.7E-04	1.9E-04	7.8E-04	9.3E-03
Case 4					
100 m	3.0E-04	2.7E-03	3.0E-03	1.3E-02	1.5E-01
1000 m	9.6E-05	8.7E-04	9.6E-04	4.0E-03	4.8E-02

7.5 Increasing Surface Area of Release (Cases 5 and 6)

This sensitivity analysis examines the effect of increasing the effective surface area of release at the water table beyond the basic footprint of the either the remote-handled trenches or the concrete vault. After transport through the vadose zone, contaminants originating from the individual disposal trenches or vaults will disperse in a pattern that will be much larger than the original footprint of the individual trench configuration. In this sensitivity case, two subcases were evaluated. Case 5 evaluated a source-release area for the remote-handled trench concept reflective of not only the individual remote-handled trench areas but the intervening inter-trench areas. Case 6 evaluated a source-release area for the concrete-vault concept reflective of not only the individual remote-handled trench areas but the intervening inter-trench areas.

Model-simulation results of the contaminant plume and the trench configuration used for Case 5 are provided in Figure 7.5. Tabular results of the calculated WIFs at 100 m (328 ft) and 1 km (0.62 mi) downgradient of the source area are provided in Table 7.5. Calculations for this case showed that the assumed 21 percent increase in the source-release area resulted in about a 21 percent increase in the WIFs over the base-case values at both the 100-m and 1-km wells. This result is consistent with the additional contaminant mass introduced at the water-table for this case. This result combined with previous results for remote-handled trench basecase and the concrete vault releases suggest a linear relationship between source-release area and calculated WIFs over the range of assumed release area.

Model-simulation results of the contaminant plume and the trench configuration used for Case 6 are provided in Figure 7.6. Tabular results of the calculated WIFs at 100 m (328 ft) and 1 km (0.62 mi) downgradient of the source area are provided in Table 7.6. Calculations for this case also showed a result consistent with those for case 5. The assumed increase in the source-release area (580 percent) resulted in about a 580 percent increase in the WIFs over the base-case values at both the 100-m and 1-km wells. This result is consistent with the previous conclusion of a linear relationship between source-release area and calculated WIFs over the range of assumed release areas.

Table 7.5. Well Intercept Factors at the 100-m (328-ft) and 1000-m (3281-ft) Wells for the Remote-Handled Trench Disposal Concept Using an Increase in Surface Area of Release (Case 5)

	Infiltration Rates (mm/yr)				
Well Locations	**0.1**	**0.9**	**1.0**	**4.2**	**50. 0**
Base Case					
100 m	2.5E-05	2.3E-04	2.5E-04	1.1E-03	1.3E-02
1000 m	1.9E-05	1.7E-04	1.9E-04	7.8E-04	9.3E-03
Case 5					
100 m	3.0E-05	2.7E-04	3.0E-04	1.3E-03	1.5E-02
1000 m	2.3E-05	2.1E-04	2.3E-04	9.8E-04	1.2E-02

Table 7.6. Well Intercept Factors at the 100-m (328-ft) and 1000-m (3281-ft) Wells for the Concrete-Vault Disposal Concept Using an Increase in Surface Area of Release (Case 6)

	Infiltration Rates (mm/yr)				
Well Locations	**0.1**	**0.9**	**1.0**	**4.2**	**50. 0**
BaseCase					
100 m	6.7E-06	6.1E-05	6.7E-05	2.8E-04	3.4E-03
1000 m	5.4E-06	4.8E-05	5.4E-05	2.2E-04	2.7E-03
Case 6					
100 m	3.9E-05	3.5E-04	3.9E-04	1.6E-03	1.9E-02
1000 m	3.0E-05	2.7E-04	3.0E-04	1.3E-03	1.5E-02

7.6 Changes in the Position of the Water Table

Results of previous work by Lu (1996) and the results of this study have shown that the characteristics of the hydrogeologic unit and the estimated water table are an important consideration and will have an influence on the calculated WIFs downgradient of the ILAW facility. The actual position of the water-table in the far future is indeed uncertain, and a series of sensitivity studies were done to examine the effect of factors that could affect the position of the water-table position beneath the ILAW facility. The two main factors that could have an influence include the estimated levels of regional natural recharge and inflow onto the Hanford Site from upgradient off-site sources. Following is a summary of these sensitivity studies that investigated these two factors.

7.6.1 Increase in Regional Areal Recharge (Case 7)

This sensitivity case examines the effect of increasing regional natural recharge on the regional and local water-table conditions. In this case, the recharge was increased by a factor of 3 in the site-wide model, and the resulting predicted water table was used to evaluate the effect of these changes in the local-scale flow and transport model.

The simulated change in natural recharge in the site-wide model (shown in Figure 7.9) raised the regional water table and significantly changed the overall predicted regional flow path for the ILAW facility from southeast and east toward the Columbia River to a predominant flow path north through the gap between Gable Butte and Gable Mountain to the Columbia River. The discharge area to the Columbia River for these conditions is eventually in the vicinity of 100-N Area.

Locally, water-table conditions were raised by about 3 m (50 ft) in the vicinity of the new disposal facility (Figure 7.10), resulting in an increased saturation of the Hanford Formation beneath the ILAW facility. Results for these conditions, summarized in Table 7.7, indicate about a 25 to 30 percent reduction in the calculated WIF over the base case WIF at the 100-m (328 ft) well location (9.8×10^{-4} versus 1.25×10^{-3}) for the 4.2 infiltration rate case. At the 1-km (0.62 mi) location, the resultant WIF (8×10^{-4}) 18 to 20 percent than the WIF at the same location in the base case (9.8×10^{-4}) for the same assumed infiltration rate. The predicted distribution of contaminant concentrations from the seven-trenches release is provided in Figure 7.11.

Table 7.7. Well Intercept Factors at the 100-m (328-ft) and 1000-m (3281-ft) Wells for the Remote-Handled Trench Disposal Concept Using an Increase (Factor of 3) in Regional Natural Recharge Rates (Case 7)

	Infiltration Rates (mm/yr)				
Well Locations	**0.1**	**0.9**	**1.0**	**4.2**	**50. 0**
BaseCase					
100 m	2.5E-05	2.3E-04	2.5E-04	1.1E-03	1.3E-02
1000 m	1.9E-05	1.7E-04	1.9E-04	7.8E-04	9.3E-03
Case 7					
100 m	2.3E-05	2.1E-04	2.3E-04	9.7E-04	1.2E-02
1000 m	8.0E-06	7.2E-05	8.0E-05	3.4E-04	4.0E-03

7.6.2 Decrease in Regional Areal Recharge (Case 8)

This sensitivity case examines the effect of reducing regional natural recharge on the regional and local water-table conditions. In this case, the recharge was reduced by a factor of 3.

Results of the simulated change in natural recharge in the site-wide model (shown in Figure 7.12) lowered the regional water table, but did not significantly change the overall predicted regional flow path for the ILAW facility from southeast and east toward the Columbia River. The discharge area into the Columbia River for these conditions is, as in the base case, in the vicinity of the old Hanford Town Site.

Locally, water-table conditions were changed slightly from the base-conditions and were lowered by about 1.2 m (4 ft) in the vicinity of the new disposal facility (Figure 7.13), resulting in a slight decrease in saturation of the Hanford Formation beneath the ILAW facility. Although the water table dropped for this case, the overall hydraulic gradient in the vicinity of the disposal facility is over a factor of 2.4 higher than was calculated using the basecase areal recharge (1.6e-4 m/m versus 6.6e-5 m/m). The resulting effect was an overall reduction in the calculated WIF and an increase in dilution for this case. Results for these simulated conditions, summarized in Table 7.8, indicate about a 50-percent reduction in the calculated WIF over the base case WIF at the 100-m (328 ft) well location (7.9 x 10-4 versus 1.25 x10^{-3}) for the 4.2 infiltration rate case. At the 1 km (0.62 mi) location, the resultant WIF (6 x 10^{-4}) was 55 percent lower than the WIF at the same location in the base case (9.8 x 10^{-4}) for the same assumed infiltration rate. The predicted distribution of contaminant concentrations from the seven-trenches release is provided in Figure 7.14.

Table 7.8. Well Intercept Factors at the 100-m (328-ft) and 1000-m (3281-ft) Wells for the Remote-Handled Trench Disposal Concept Using A Decrease (Factor of 3) in Regional Natural Recharge Rates (Case 8)

	Infiltration Rates (mm/yr)				
Well Locations	**0.1**	**0.9**	**1.0**	**4.2**	**50. 0**
BaseCase					
100 m	2.5E-05	2.3E-04	2.5E-04	1.1E-03	1.3E-02
1000 m	1.9E-05	1.7E-04	1.9E-04	7.8E-04	9.3E-03
Case 8					
100 m	1.7E-05	1.5E-04	1.7E-04	7.1E-04	8.5E-03
1000 m	1.3E-05	1.2E-04	1.3E-04	5.4E-04	6.4E-03

7.6.3 Decrease in Regional Upgradient Boundary Fluxes (Case 9)

This sensitivity case examines the effect of reducing regional boundary fluxes on the regional and local water table conditions at the Cold Creek and Dry Creek entrances to the Hanford Site as well as recharge to the unconfined aquifer from springs emanating along the base of Rattlesnake Hills. In this case, the simulated boundary fluxes were reduced by a factor of 2.

Results of the simulated change in natural recharge in the site-wide model (shown in Figure 7.15) lowered the regional water table, but did not significantly change the overall predicted regional flow path for the ILAW facility from southeast and east toward the Columbia River. The discharge area into the Columbia River for these conditions is, as in the base case, in the vicinity of the old Hanford Town Site.

Locally, water-table conditions were changed slightly from the base conditions and were lowered by about 0.5 m (1.6 ft) in the vicinity of the new disposal facility (Figure 7.16), resulting in a slight decrease in saturation of the Hanford Formation and slight changes to flow conditions beneath the ILAW facility. As in the previous case, although the water table dropped for this case, the overall hydraulic gradient in the vicinity of the disposal facility is over a factor of 2.4 higher than was calculated using the base case areal recharge (1.6e-4 m/m versus 6.6e-5 m/m). The resulting effect was a small increase in the calculated WIF and an increase in dilution for this case. Results for these simulated conditions, summarized in Table 7.9, indicate about a 50-percent reduction in the calculated WIF over the base case WIF at the 100-m (328 ft) well location (1.0×10^{-3} versus 1.25×10^{-3}) for the 4.2 infiltration rate case. At the 1 km (0.62 mi) location, the resultant WIF (7.8×10^{-4}) was 25 percent lower than the WIF at the same location in the base case (9.8×10^{-4}) for the same assumed infiltration rate. The distribution of predicted contaminant concentration, for this case is illustrated in Figure 7.17.

Table 7.9. Well Intercept Factors at the 100-m (328-ft) and 1000-m (3281-ft) Wells for the Remote-Handled Trench Disposal Concept Using a Decrease (Factor of 2) in Regional Boundary Fluxes (Case 9)

	Infiltration Rates (mm/yr)				
Well Locations	**0.1**	**0.9**	**1.0**	**4.2**	**50.0**
BaseCase					
100 m	2.5E-05	2.3E-04	2.5E-04	1.1E-03	1.3E-02
1000 m	1.9E-05	1.7E-04	1.9E-04	7.8E-04	9.3E-03
Case 9					
100 m	2.1E-05	1.9E-04	2.1E-04	8.8E-04	1.1E-02
1000 m	1.6E-05	1.5E-04	1.6E-04	6.8E-04	8.1E-03

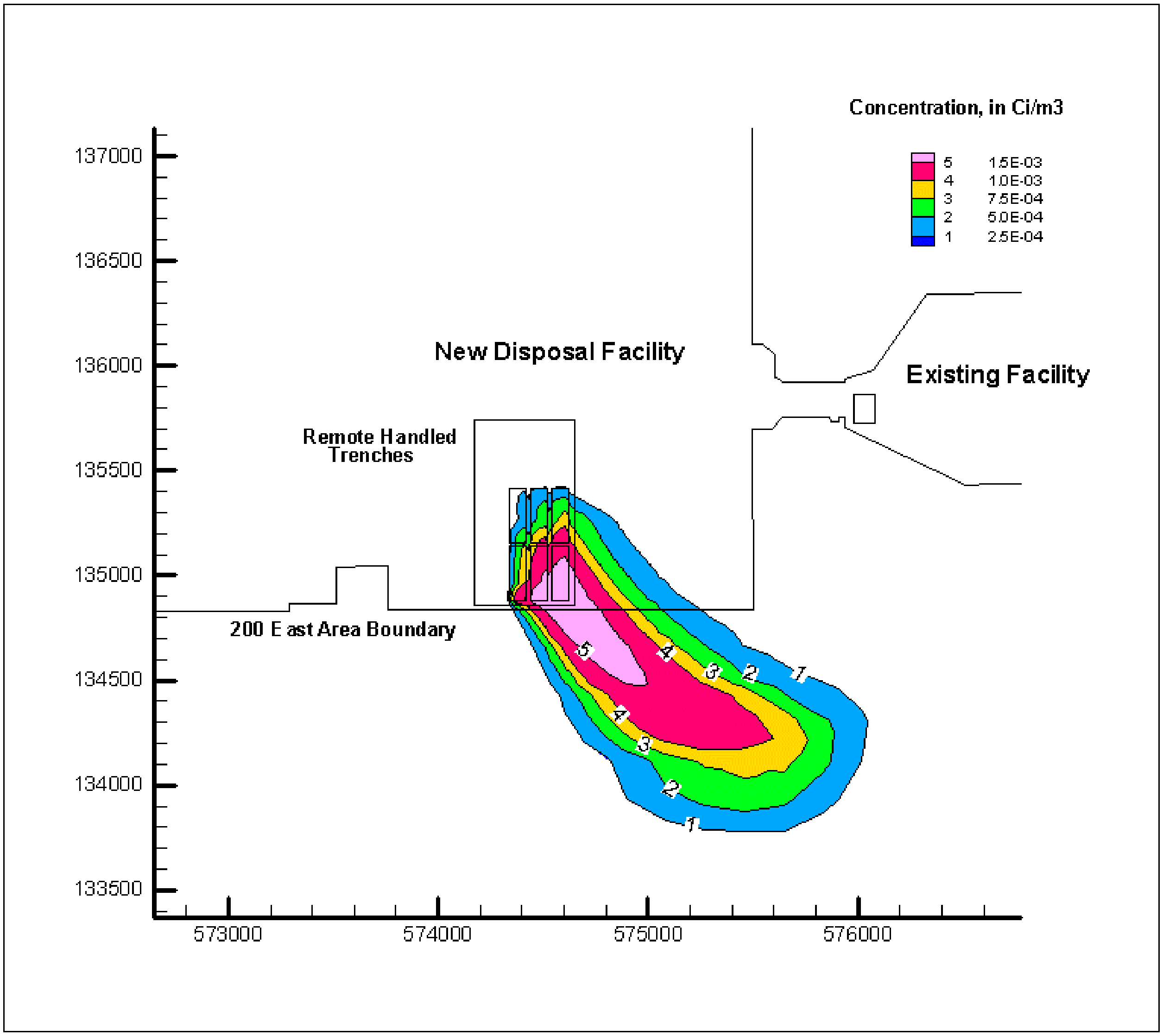

Figure 7.1. Areal Distribution of Contaminant Plume Resulting from the Remote-Handled Trench Concept – Sensitivity to Placing Disposal Trenches at South End of Disposal Facility Area

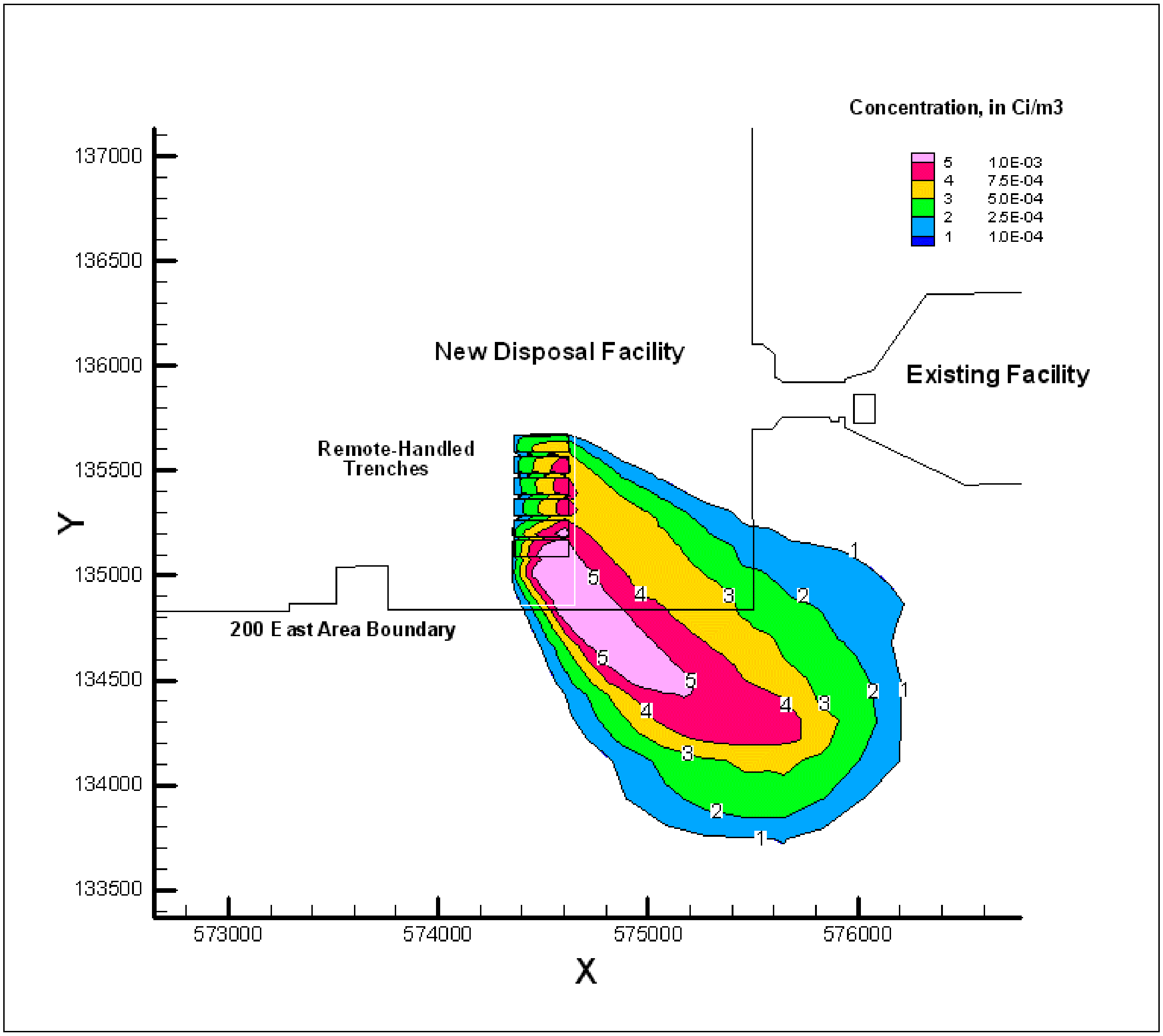

Figure 7.2. Areal Distribution of Contaminant Plume Resulting from the Remote-Handled Trench Concept – Sensitivity to Rotation of Remote Handled Trenched by 90 degrees

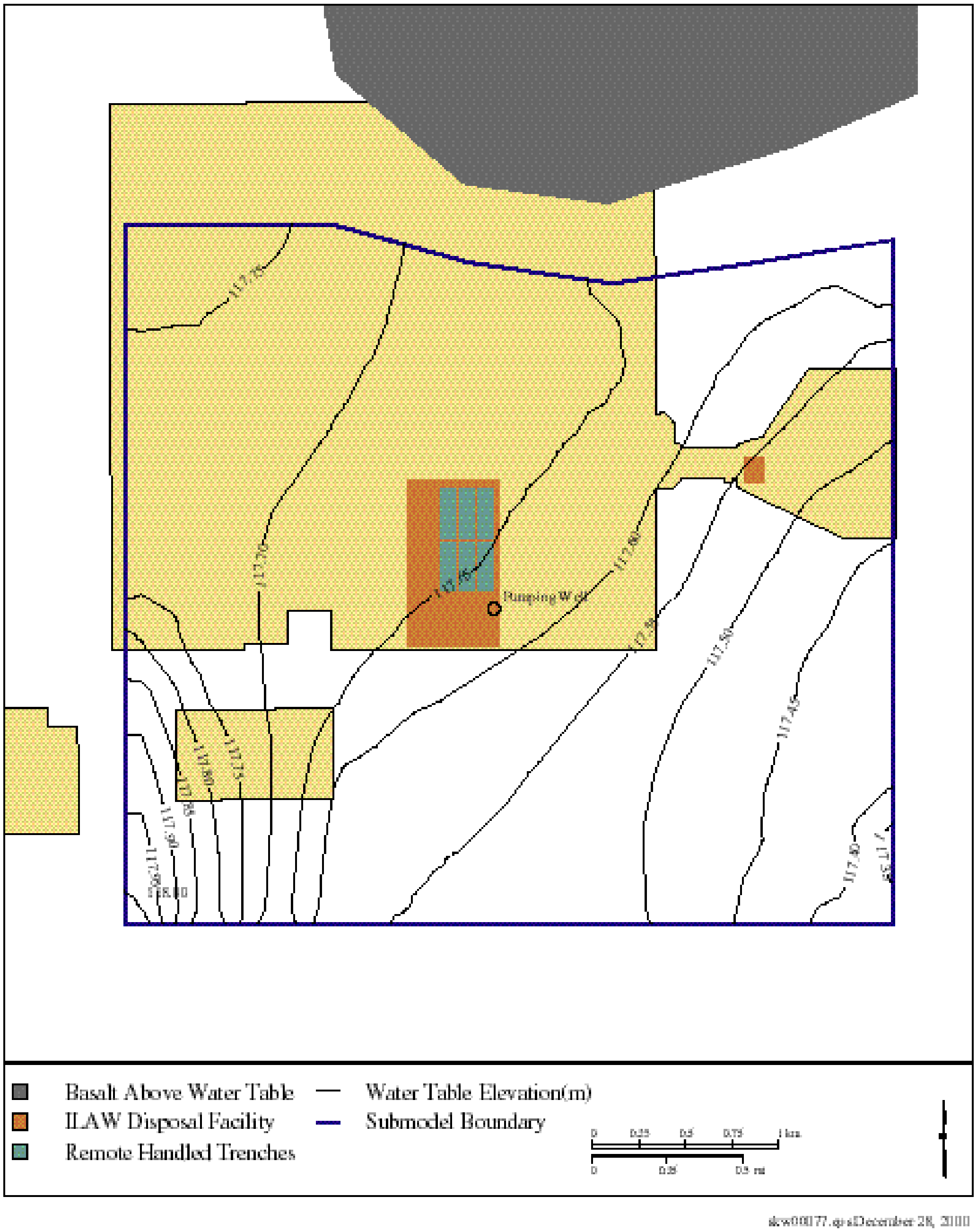

A) 30 1/Day

Figure 7.3. Local-Scale Model Head Distribution Resulting from the Remote-Handled Trench Concept – Sensitivity to Increased Pumping at 100-m (328-ft) Well: A) 30 l/Day, B) 100 l/Day, C) 300 l/Day, and D) 1000 l/Day

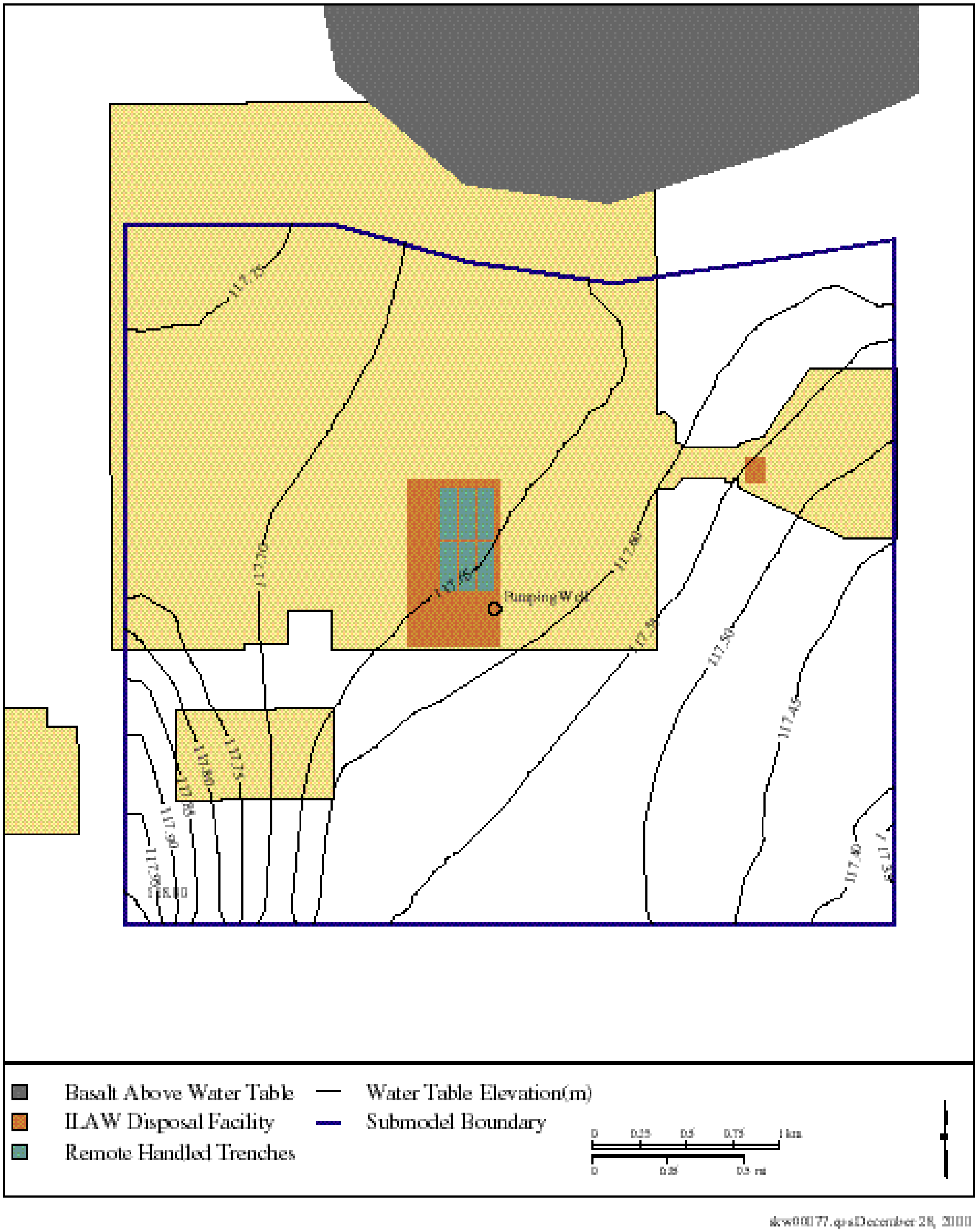
117.75
117.70
117.65
117.60
117.55
117.50
117.45
117.40
117.35
117.80
117.85
117.90
117.95
118.00
Pumping Well
Basalt Above Water Table
ILAW Disposal Facility
Remote Handled Trenches
Water Table Elevation(m)
Submodel Boundary
skw00177.apr December 28, 2000

B) 100 1/Day

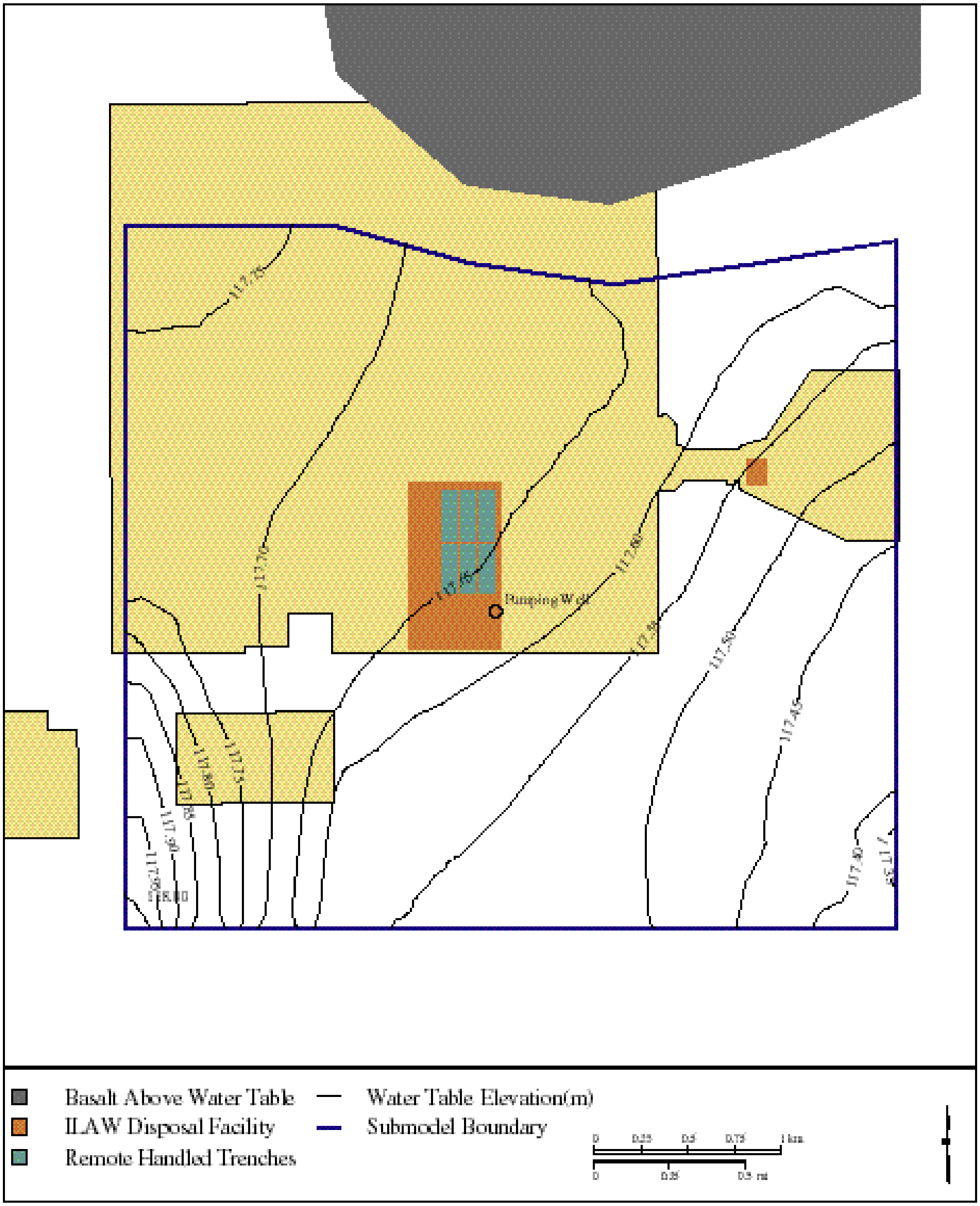

skw00177.eps December 28, 2000

C) 300 1/Day

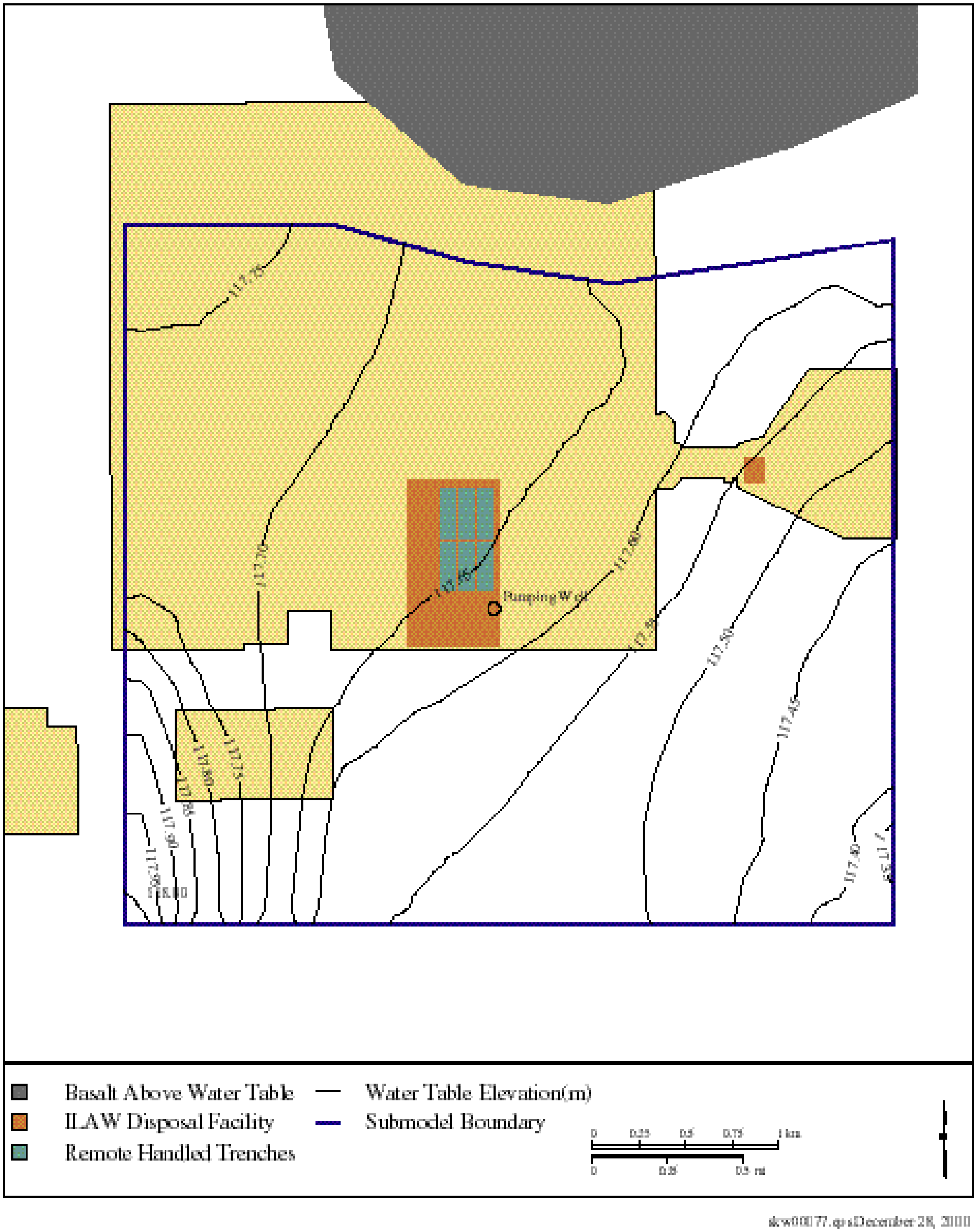
Pumping Well
Basalt Above Water Table
ILAW Disposal Facility
Remote Handled Trenches
Water Table Elevation(m)
Submodel Boundary
skw00177.eps December 28, 2000

D) 1000 l/Day

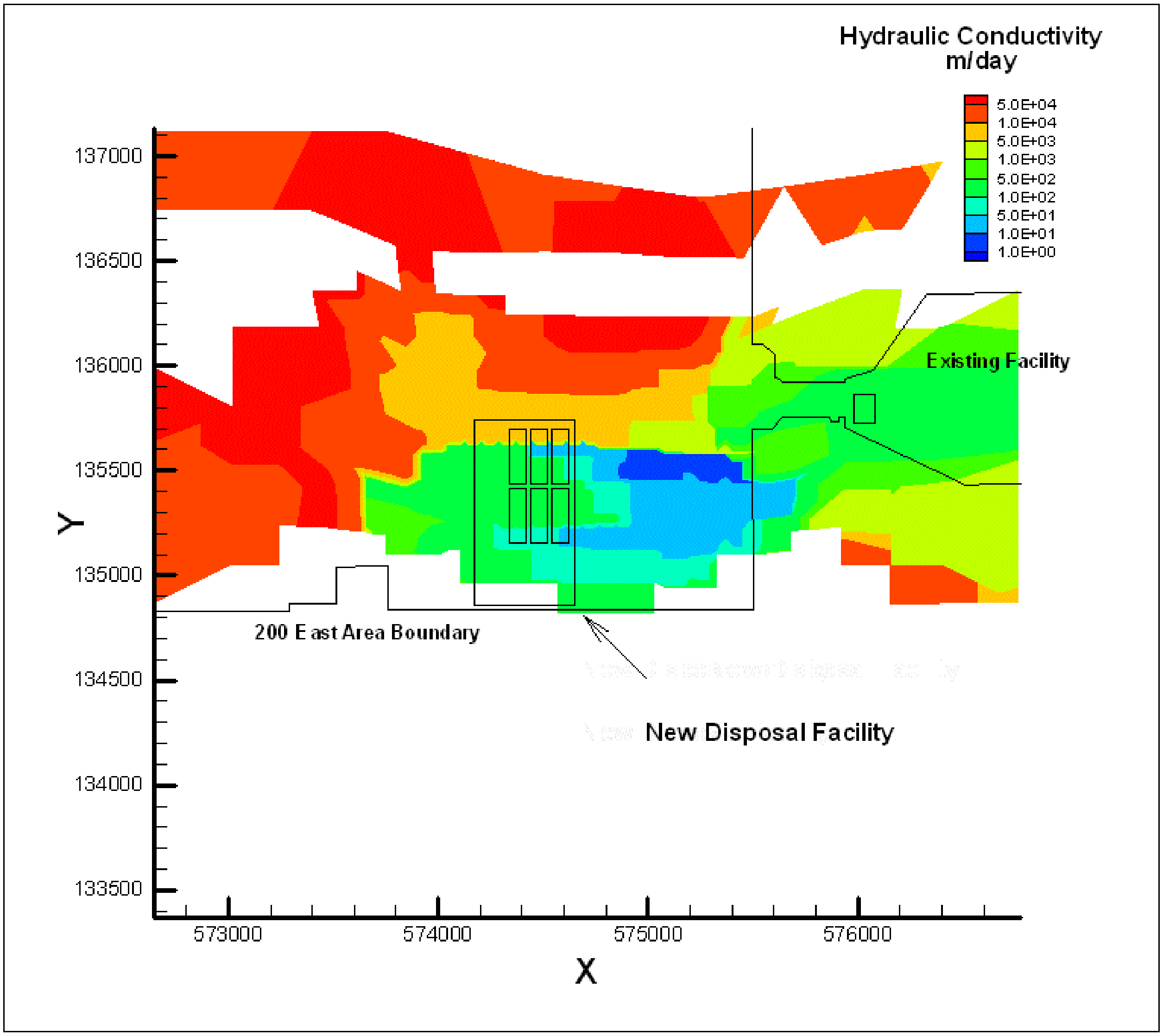

Figure 7.4. Distribution of Hydraulic Conductivity Used in Decreased Hydraulic Conductivity Sensitivity Case

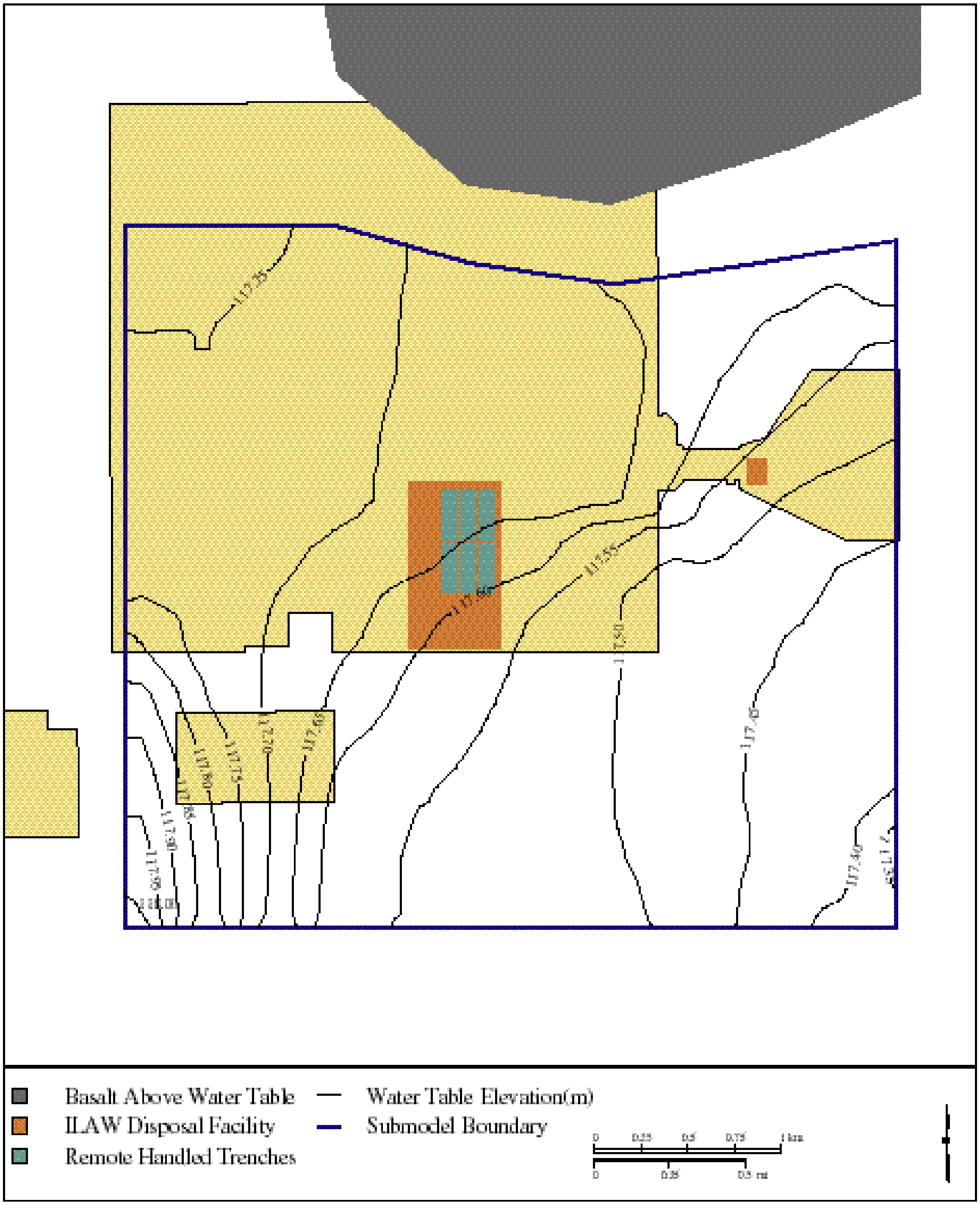

Figure 7.5. Local-Scale Head Distribution Resulting from Decreased Hydraulic Conductivity of Hanford Formation

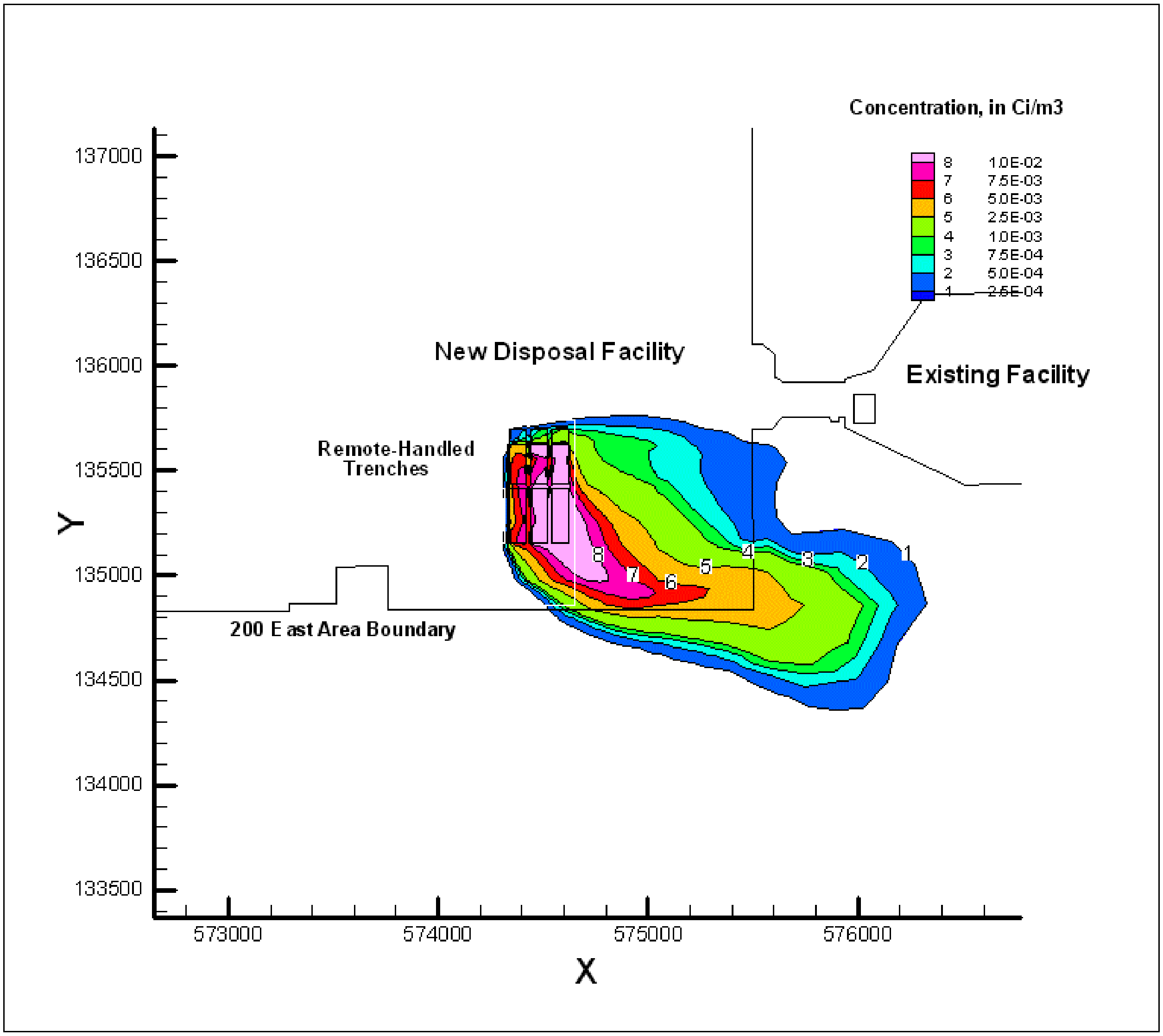

Figure 7.6. Areal Distribution of Contaminant Plume Resulting from the Remote-Handled Trench Concept – Sensitivity to Decreased Hydraulic Conductivity of Hanford Formation

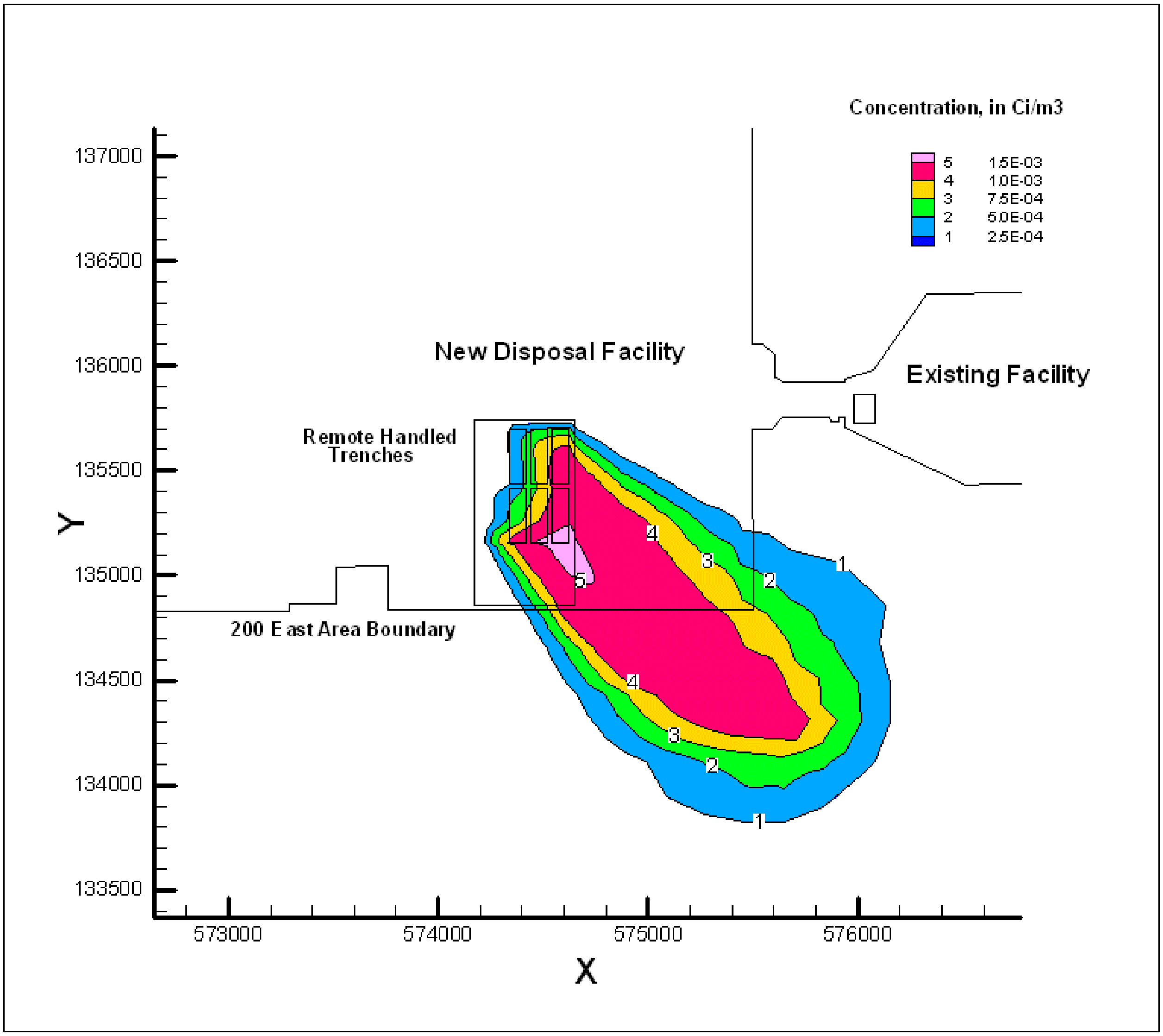

Figure 7.7. Areal Distribution of Contaminant Plume Resulting from the Remote-Handled Trench Concept – Sensitivity to Increase in Source-Release Area (Case 5)

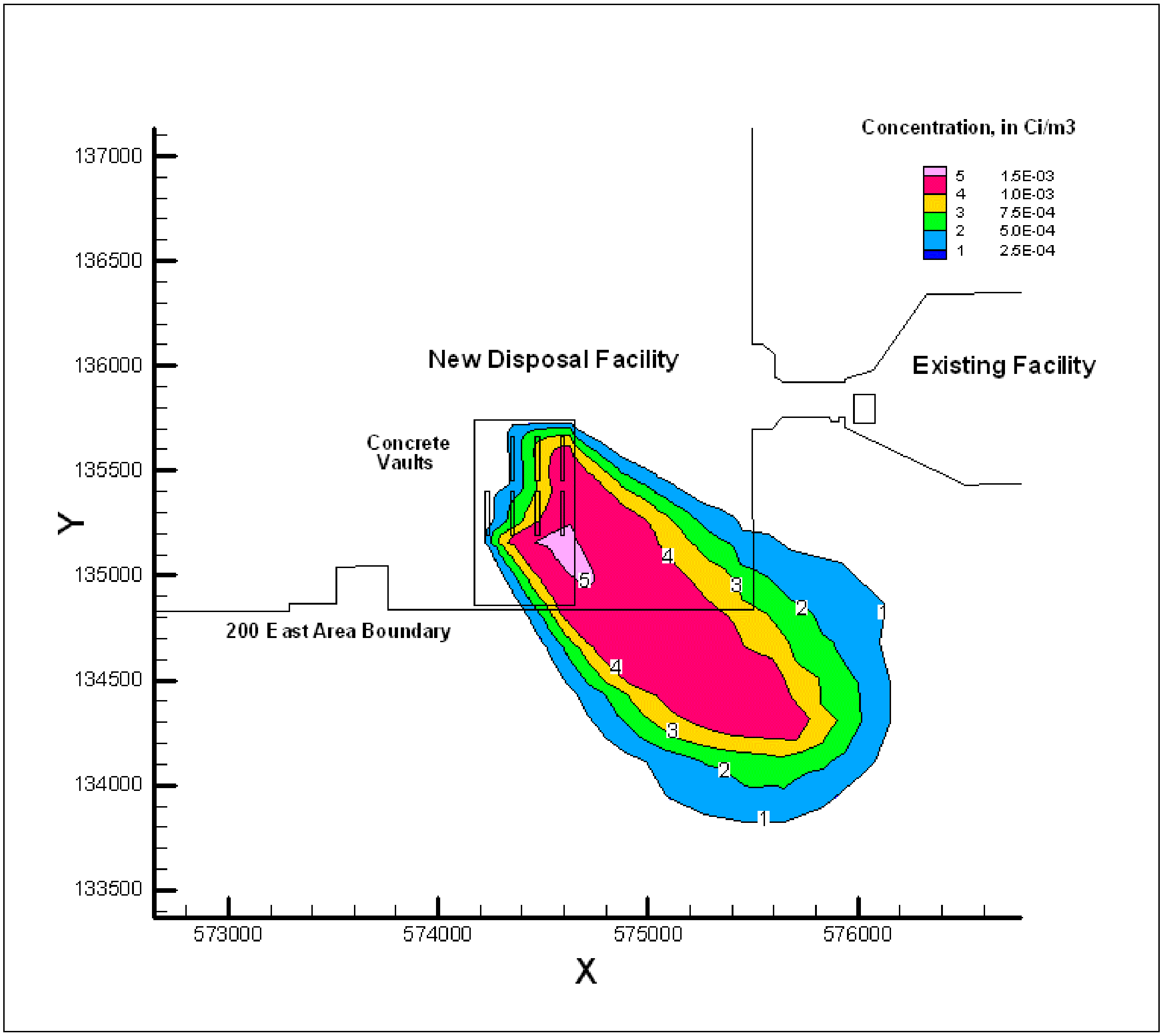

Figure 7.8. Areal Distribution of Contaminant Plume Resulting from the Concrete-Vault Concept – Sensitivity to Increase in Source-release Area (Case 6)

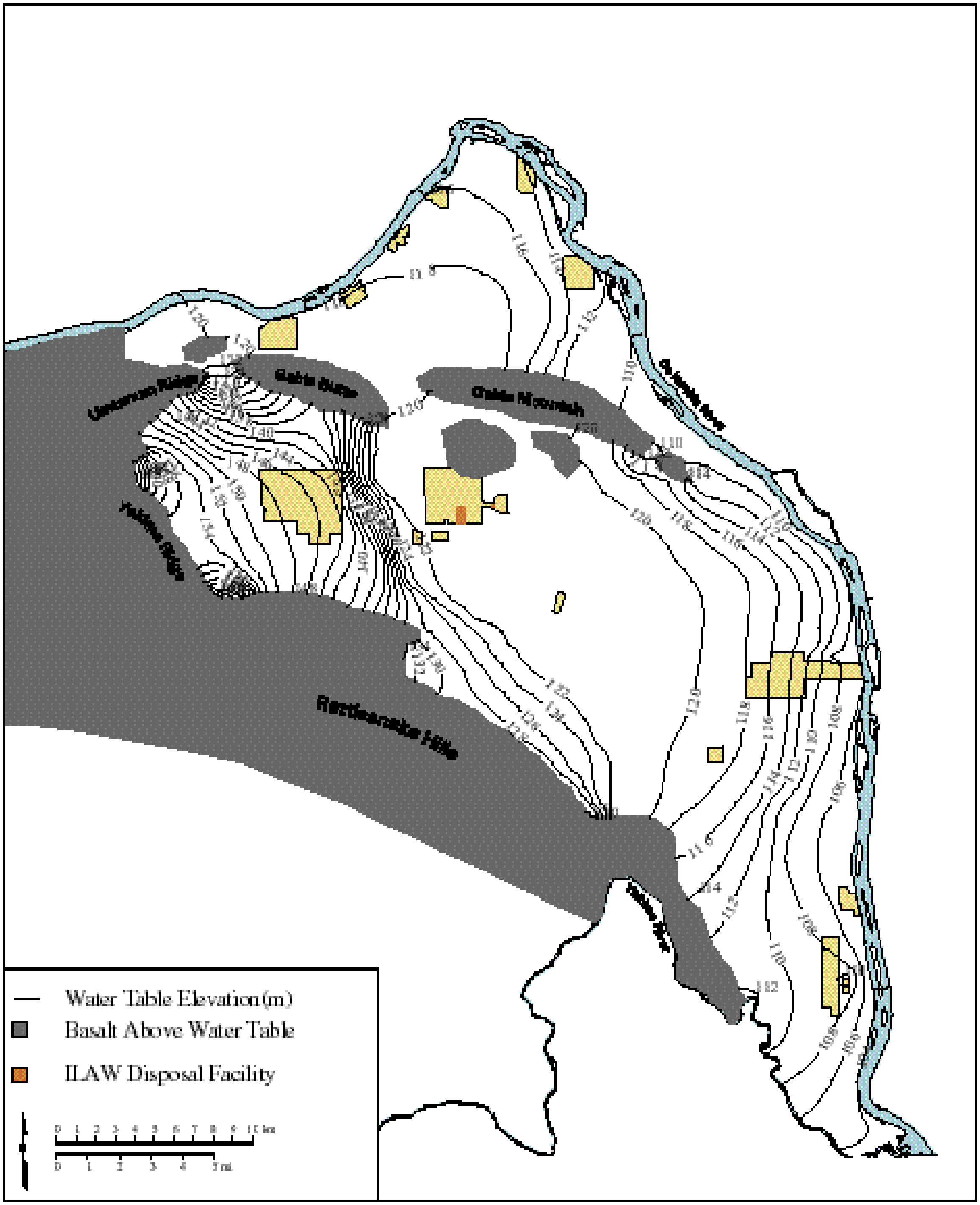

Figure 7.9. Regional-Scale Head Distribution Resulting from Increased (Factor of 3) Regional Natural Recharge

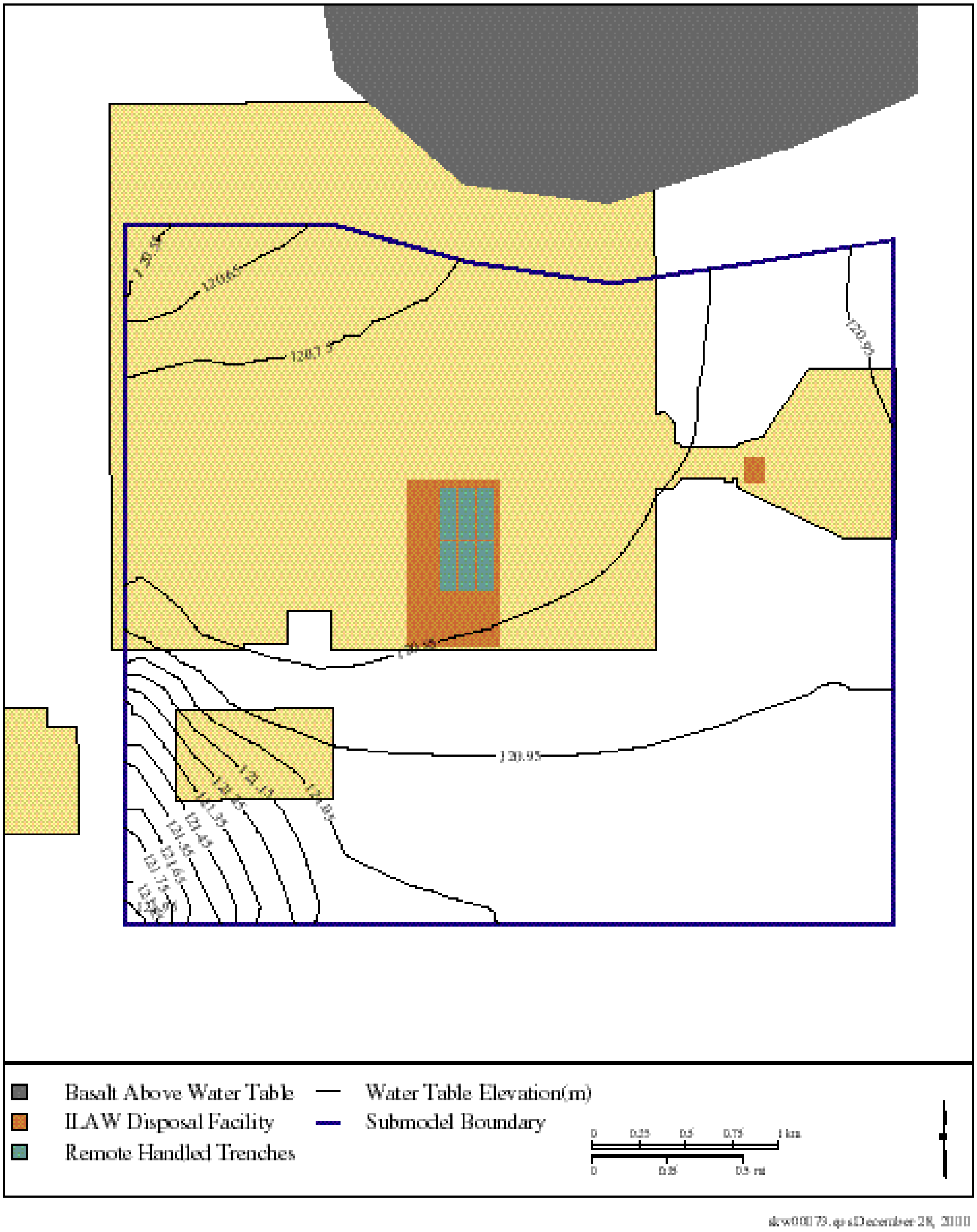

Figure 7.10. Local-Scale Head Distribution Resulting from Increased (Factor of 3) Regional Natural Recharge

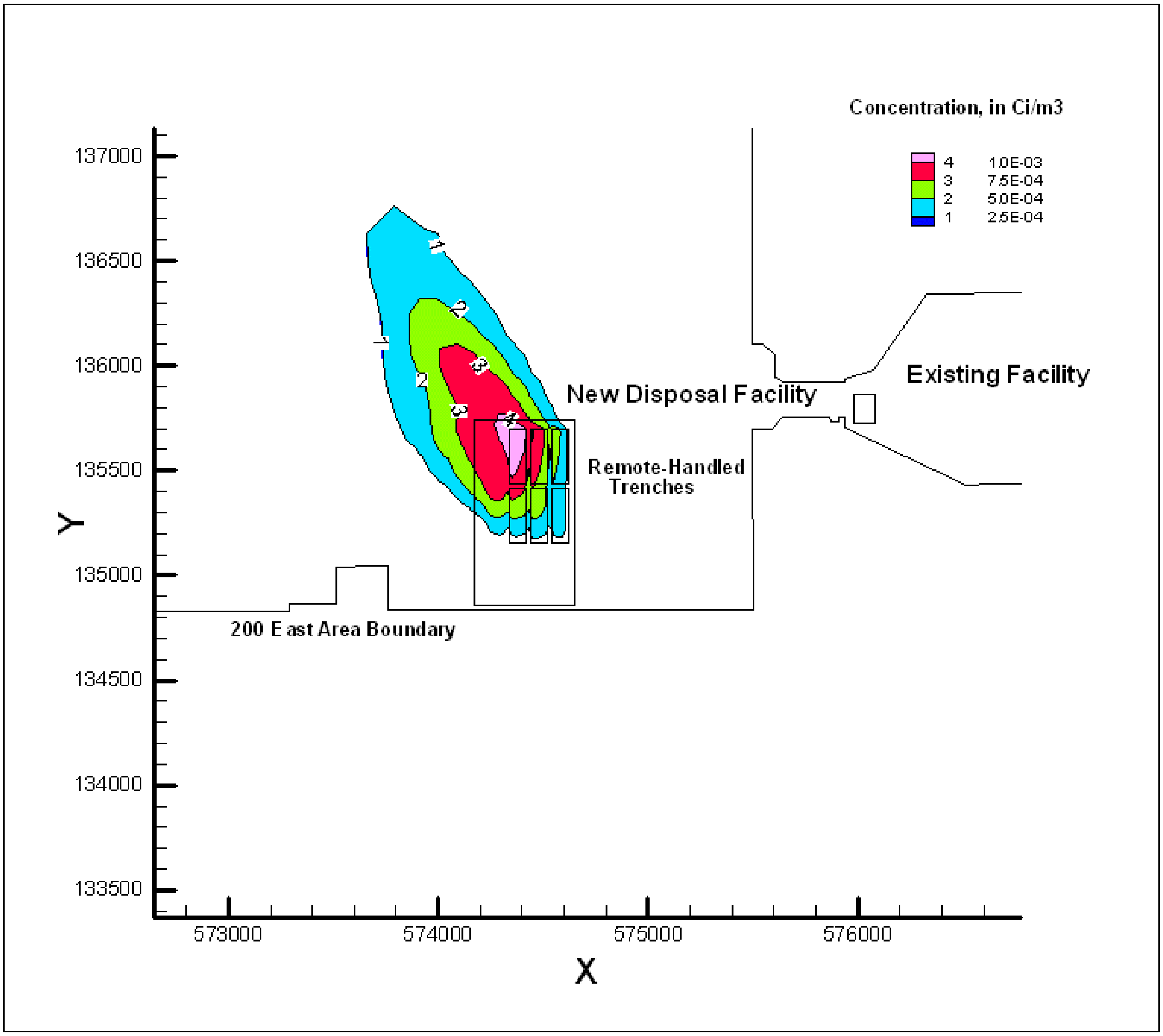

Figure 7.11. Areal Distribution of Contaminant Plume Resulting from the Remote-Handled Trench Concept – Sensitivity to Increased (Factor of 3) Regional Natural Recharge

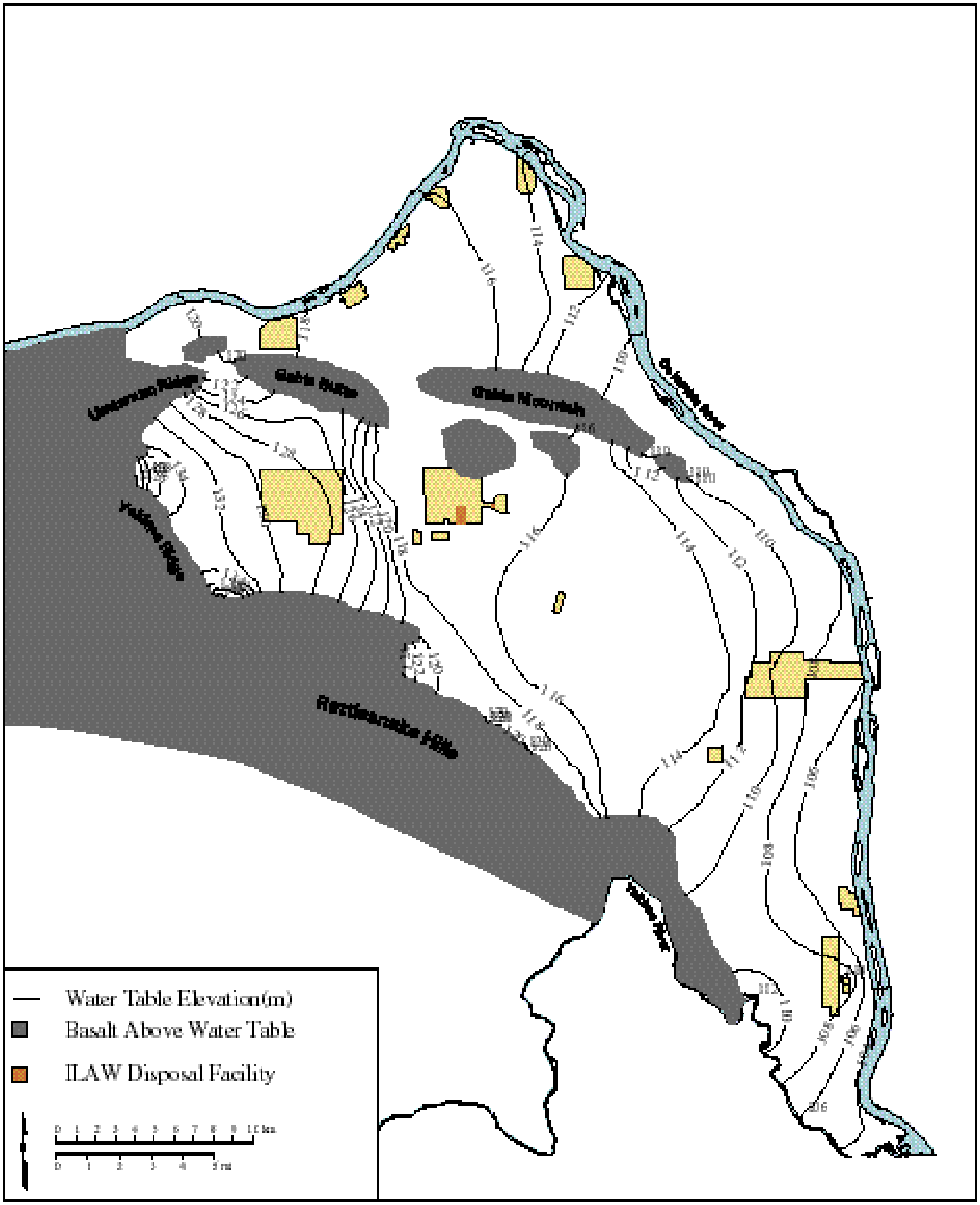

Figure 7.12. Regional-Scale Head Distribution Resulting from Decreased (Factor of 3) Regional Natural Recharge

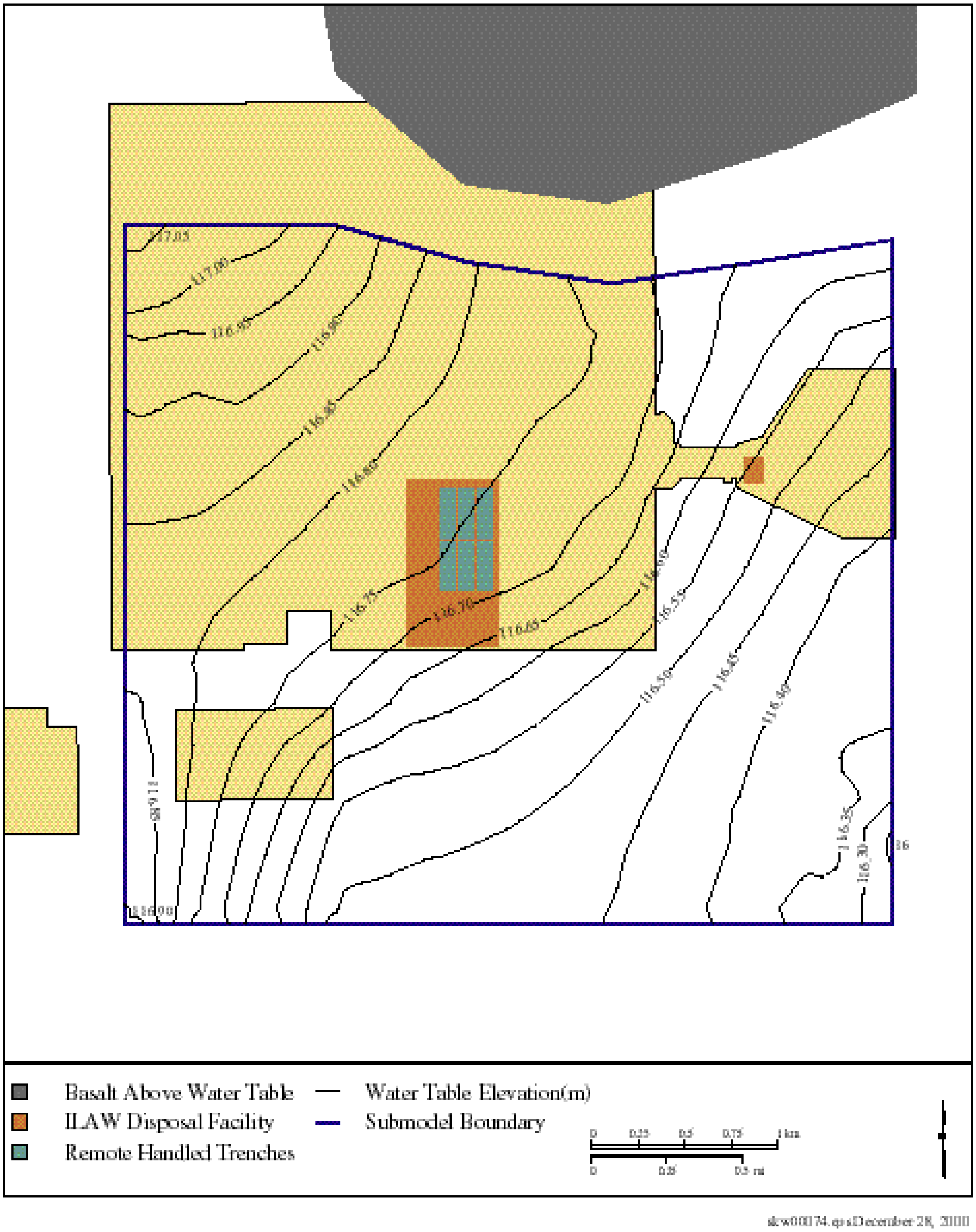

Figure 7.13. Local-Scale Head Distribution Resulting from Decreased (Factor of 3) Regional Natural Recharge

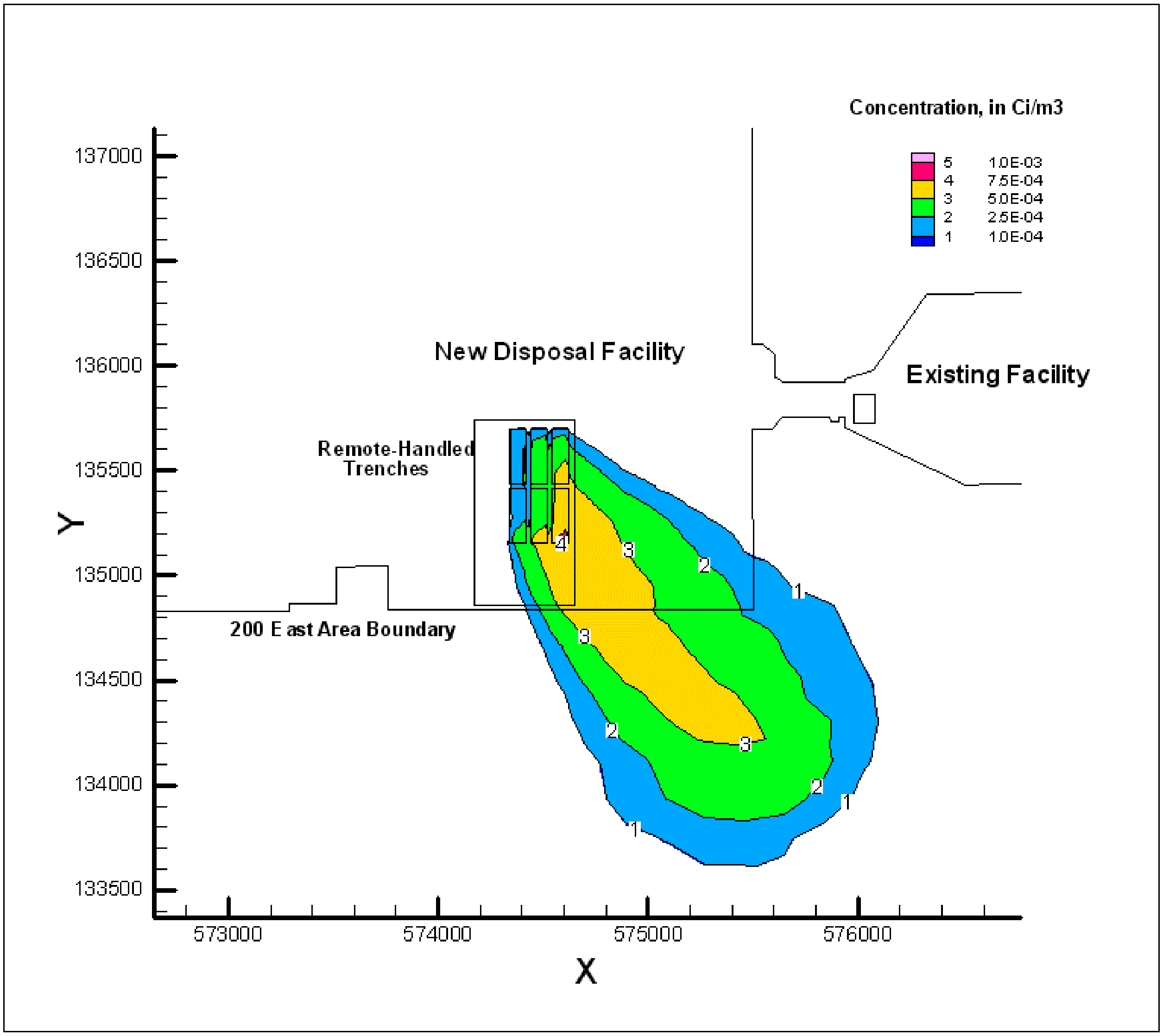

Figure 7.14. Areal Distribution of Contaminant Plume Resulting from the Remote-Handled Trench Concept – Sensitivity to Decreased (Factor of 3) Regional Natural Recharge

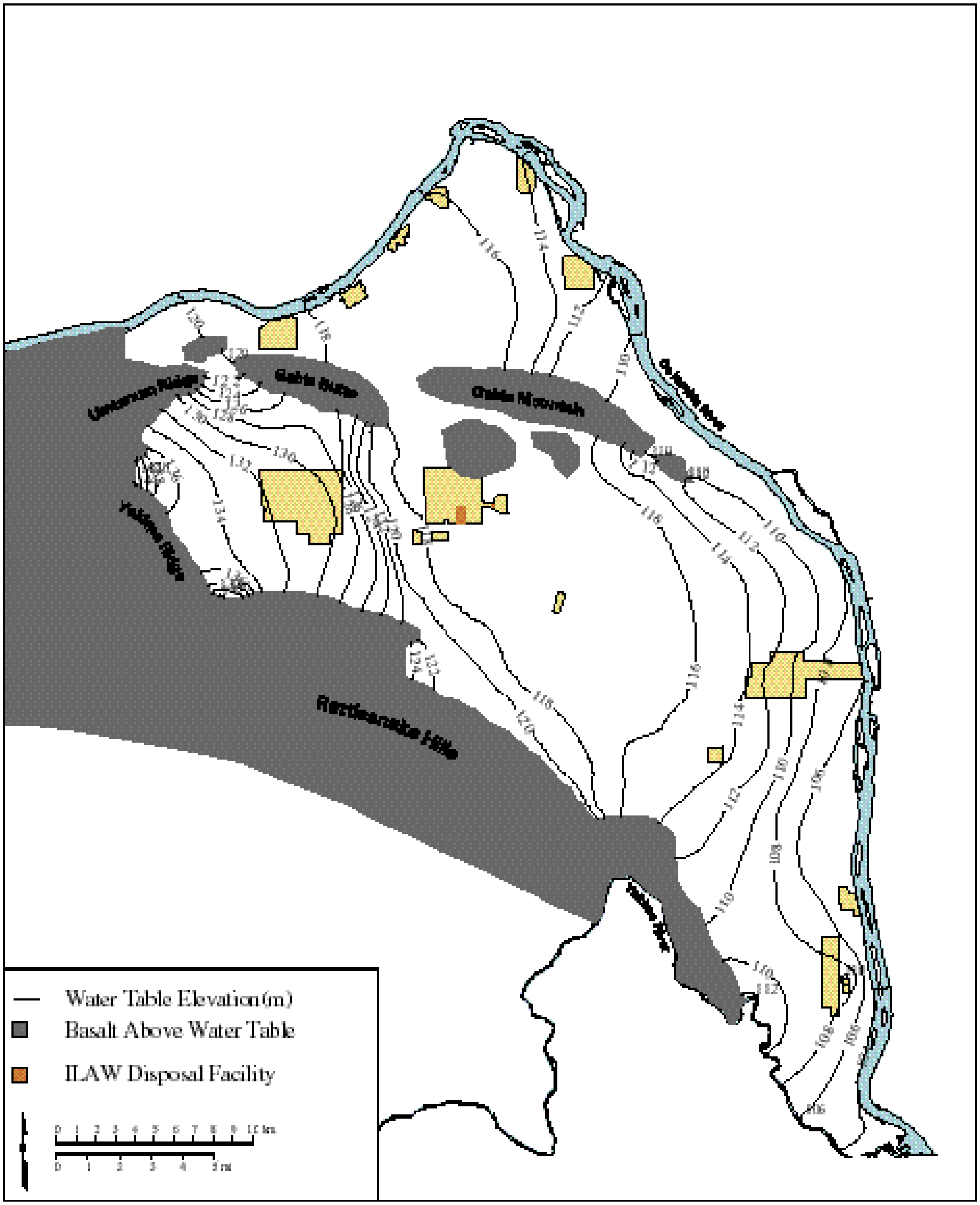

skw00071.eps December 28, 2000

Figure 7.15. Regional-Scale Head Distribution Resulting from Decreased (Factor of 3) Regional Natural Recharge

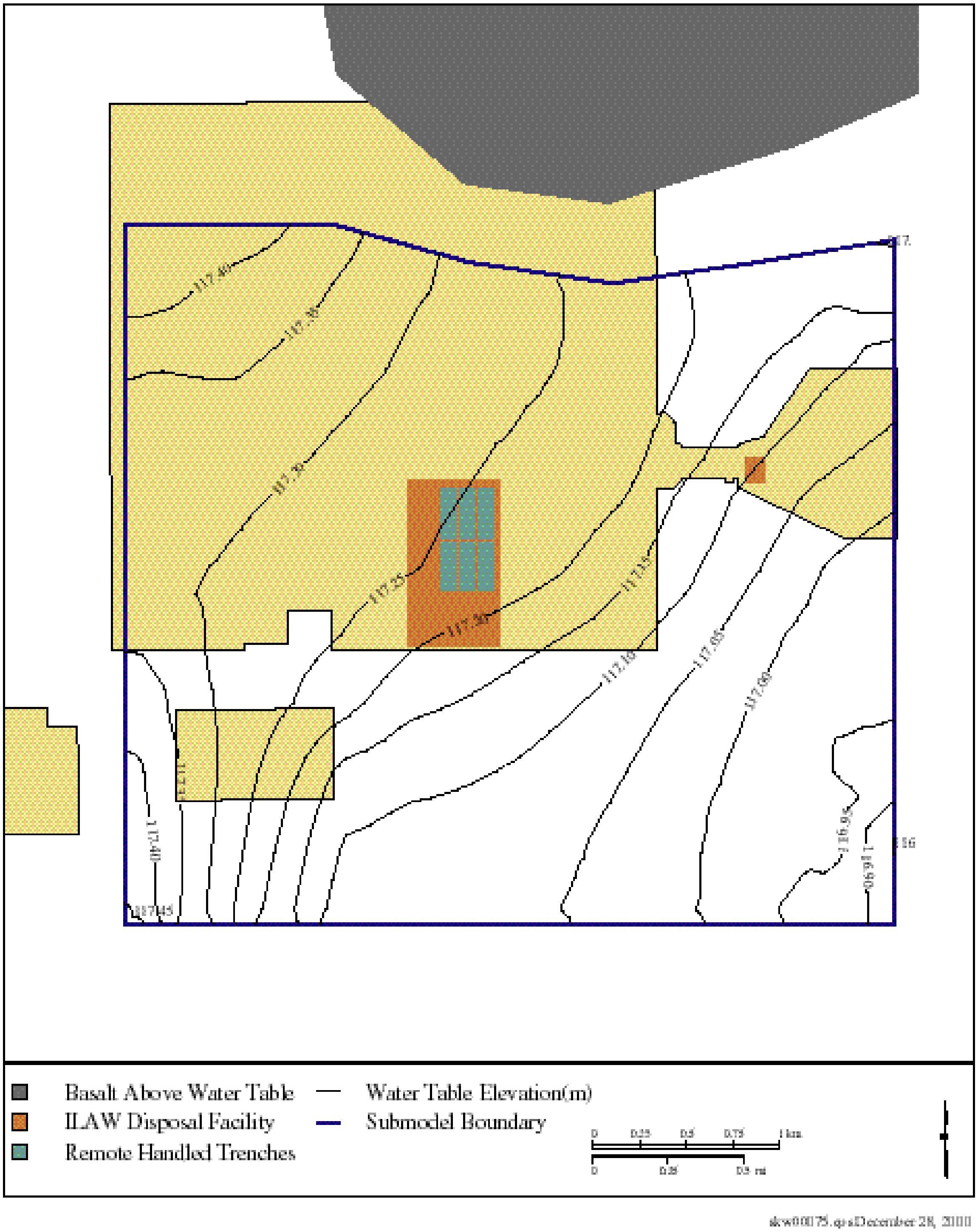

Figure 7.16. Local-Scale Head Distribution Resulting from Decreased (Factor of 2) Regional Boundary Flux

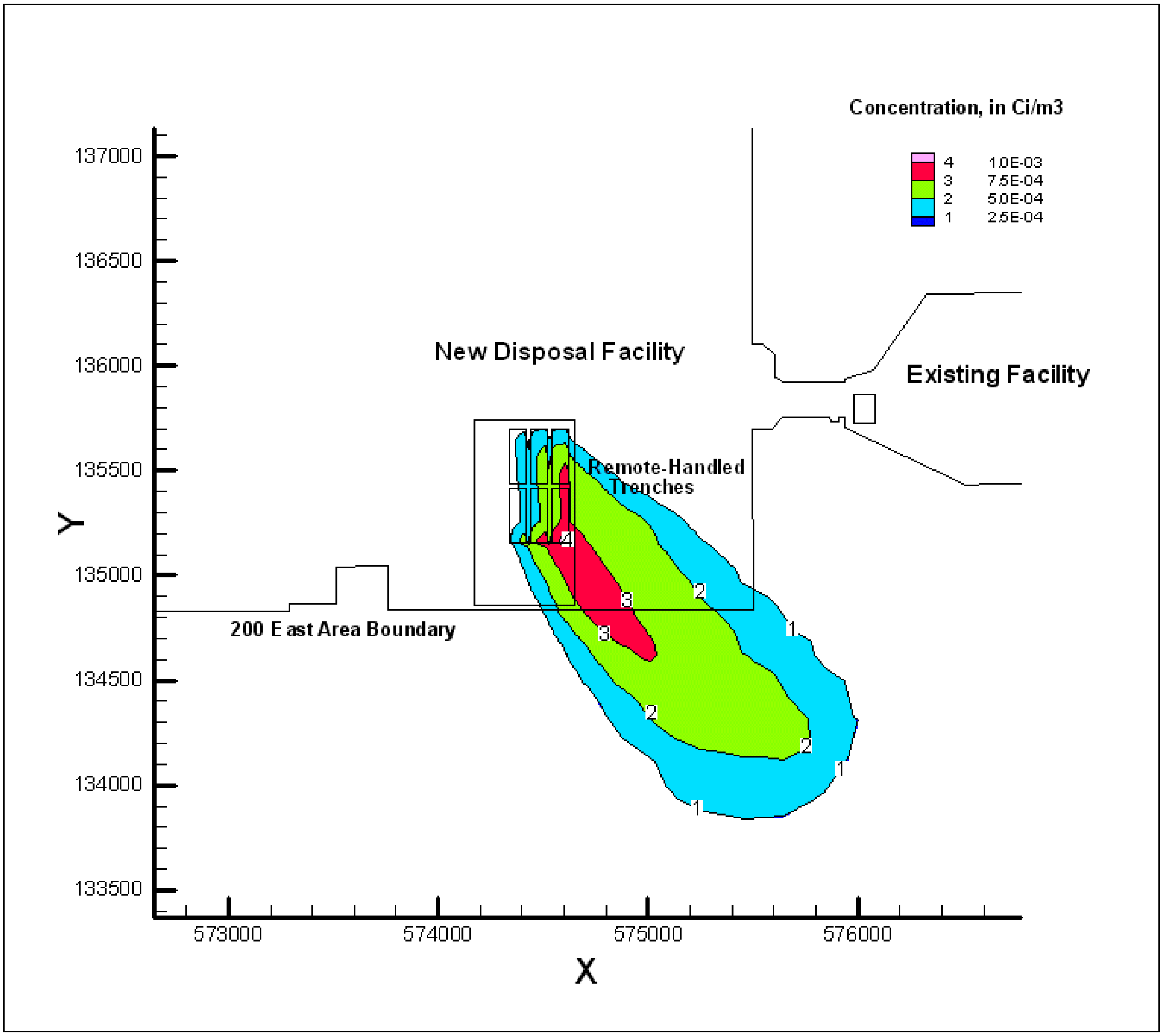

Figure 7.17. Areal Distribution of Contaminant Plume Resulting from the Remote-Handled Trench Concept – Sensitivity to Decreased (Factor of 2) Regional Boundary Flux

8.0 Summary and Conclusions

Calculations of the WIFs in this analysis in general yielded different levels of dilution than those developed in previous calculations of ILAW disposal facility performed by Lu (1996). The differences in the calculated WIFs can be attributed to a number of factors:

The Lu (1996) analysis estimated the water table beneath the facility to be at about the same level considered in this analysis, but assumed the water table would be situated in the Ringold Formation. The current model predicted that the water table would largely be along the edge of a buried channel containing very permeable Hanford formation. The difference in the distribution and hydraulic properties between the two conceptual models has led to higher levels of dilution using the current model. Additional work with the current model will be needed to evaluate the predictability of the WIF as a function of the hydraulic properties of the major hydrogeologic units beneath the facility.

Differences in the conceptual model of the unconfined aquifer used in the current analysis resulted in differences in the simulated direction of flow. The analysis by Lu (1996) predicted an easterly flow direction. The current local-scale model predicts a southeasterly flow direction. This difference in flow direction may be primarily attributable to including the highly permeable ancestral channel of the Columbia River, which contains the Hanford Formation in this analysis. The differences may also be a function of including natural recharge in the current regional-scale and local-scale analysis. Further work with the local-scale model will be needed to evaluate the predictability of the WIF as a function of the direction of flow.

Key factors affecting the current calculations appear to be related to the use of higher estimated hydraulic conductivities and groundwater velocities beneath the facility with the current model. The hydraulic conductivities used by the current model and the previous model used by Lu (1996) for the Ringold Formation are on the same order of magnitude (between 40 and 300 m/day in the current model; between 70 and 245 m/day in the model used by Lu [1996]). However, the current model contains areas of the Hanford formation beneath the facility and as a result has areas of very high permeability (between 2,200 and 30,000 m/day) in the area of the source release.

Uncertainties in the following key factors affecting calculated WIFs were investigated with sensitivity analyses:

- the assumed source-area of release
- the vertical position of the post-closure water table and the associated direction of groundwater flow
- the lateral position of the Hanford-Ringold Formation contact
- the hydraulic properties of Hanford and Ringold sediments.

Results of these analyses suggested that calculated WIFs are linearly related to the source-release area over the range of assumed surface areas of release. Calculated WIFs are also affected by the long-term predicted position of the water table and the resulting estimated distribution of hydraulic properties underlying the ILAW disposal facilities. The new facility is located in an area of the Hanford Site where it is underlain by an ancestral channel of the Columbia River that consists of highly permeable sediments of the Hanford Formation. For the predicted water-table position used in this analysis, the current interpretation places the contact between the Hanford Formation and the underlying less-permeable Ringold Formation along the south edge of the new ILAW disposal facility area.

Assumptions made about long-term regional natural recharge rates and boundary conditions are uncertain and can also change the predicted position of the water table and the position of the contact between the Hanford and Ringold sediments. Higher assumed rates of recharge can increase the water-table elevation and the level of saturation in the Hanford formation sediments leading to lower calculated WIFs (i.e., higher levels of dilution) from releases from the ILAW facilities.

Estimates of the hydraulic properties used in this assessment are based on past calibration of the site-wide model that provides a reasonable approximation of the regional observations and trends. Estimates of these properties on the local-scale model used in this analysis are uncertain and can affect calculated WIFs. Reducing the estimated hydraulic conductivities of the Hanford formation underlying the disposal facilities to those estimated for the Ringold Formation resulted in an order of magnitude increase in the WIFs (i.e., less dilution) from releases from the ILAW disposal facilities.

9.0 References

Bacon, D. H., M. D. White, and B. P. McGrail. 1999. *Subsurface Transport Over Reactive Multiphases (STORM): A General, Coupled, Non-isothermal Multiphase Flow, Reactive, Transport, and Porous Medium Alteration Simulator, Version 2; User's Guide*, PNNL-13108, Pacific Northwest National Laboratory, Richland, Washington.

Cole, C. R., S. K. Wurstner, M. P. Bergeron, M. D. Williams, and P. D. Thorne. 1997. *Three-Dimensional Analysis of Future Groundwater Flow Conditions and Contaminant Plume Transport in the Hanford Site Unconfined Aquifer System: FY 1996 and 1997 Status Report*, PNNL-11801, Pacific Northwest National Laboratory, Richland, Washington.

Fayer, M. J., and T. B. Walters. 1995. *Estimated Recharge Rates at the Hanford Site,* PNL-10285, Pacific Northwest Laboratory, Richland, Washington.

Fayer, M. J. 1999. *Recharge Data Package for the Immobilized Low-Activity Waste 2001 Performance Assessment*, PNNL-13033, Pacific Northwest National Laboratory, Richland, Washington.

Gupta, S. K., C. R. Cole, C. T. Kincaid, and A. M. Monti. 1987. *Coupled Fluid, Energy, and Solute Transport (CFEST) Model: Formulation and User's Manual*, Report BMI/ONWI-660, Battelle Memorial Institute, Columbus, Ohio.

Gupta, S. K. 1996. *Draft User's Manual, CFEST-96 Flow and Solute Transport, Constant/Variable Density, Computationally Efficient, and Low Disk PC/Unix Version*. Consultant for Environmental System Technologies, Irvine, California.

Huyakon, P. S., and S. Panday. 1999. *VAM3DF - Variably Saturated Analysis Model in Three Dimensions for the Data Fusion System: Documentation and User's Guide, Version 2.0*, HydroGeoLogic, Inc., Herndon, Virginia.

Kincaid, C. T., M. P. Bergeron, C. R. Cole, M. D. Freshley, N. L. Hassig, V. G. Johnson, D. I. Kaplan, R. J. Serne, G. P. Streile, D. L. Strenge, P. D. Thorne, L. W. Vail, G. A. Whyatt, and S. K. Wurstner. 1998. *Composite Analysis for Low-Level Waste Disposal in the 200-Area Plateau of the Hanford Site*, PNNL-11800, Pacific Northwest National Laboratory, Richland, Washington.

Kirkbride, R. A. 1999. *Tank Waste Remediation System Operational Utilization Plan*, HNF-SD-WM-SP-012, Rev. 1, Volume I and II, Numatec Hanford Company, Richland, Washington.

Law, A., S. Panday, C. Denslow, K. Fetch, and A. Knepp. 1996. *Hanford Sitewide Groundwater Flow and Transport Model Calibration Report*, BHI-00608, Rev. 0, Bechtel Hanford Inc., Richland, Washington.

Lindsey, K. A. 1995. *Miocene- to Pliocene-Aged Suprabasalt Sediments of the Hanford Site, South Central Washington*, BHI-00184, Bechtel Hanford, Inc., Richland, Washington.

Lu, A.H. 1996. *Contaminant Transport in the Unconfined Aquifer, Input to the Low Level Tank Waste Interim PA*, WHC-SD-WM-RPT-241, Westinghouse Hanford Company, Richland, Washington.

Mann, F. M., C. R. Eiholzer, R. Khaleel, N. W. Kline, A. H. Lu, B. P. McGrail, P. D. Rittmann, and F. Schmittroth. 1995. *Definition of the Base Analysis Case of the Interim Performance Assessment*, WHC-SD-WM-RPT-200, Revision 0, Westinghouse Hanford Company, Richland, Washington, December 1995.

Mann, F. M. 1996. I*NTEG: A Program to Calculate Groundwater Contamination and Human Doses*, WHC-SD-WM-RPT-219, Westinghouse Hanford Company, Richland, Washington.

Mann, F. M., R. J. Puigh II, P. D. Rittmann, N. W. Kline, J. A. Voogd, Y. Chen, C. R., Eiholzer, C. T. Kincaid, B. P. McGrail, A.H. Lu, G. F. Williamson, N. R. Brown, and P. E. LaMont. 1998. *Hanford Immobilized Low-Activity Tank Waste Performance Assessment*, DOE/RL-97-69, Rev. 0, U.S. Department of Energy-Richland Operations Office, Richland, Washington.

Mann F. M., S. H. Finfock, E. J. Freeman, R. J. Puigh III, D. H. Bacon, M. P. Bergeron, B. P. McGrail, and S. K. Wurstner. 2000. White Paper: *Updating Conclusions of 1998 ILAW Performance Assessment*, DOE/ORP-2000-07, Revision 0, U. S. Department of Energy, Office of River Protection, Richland, Washington.

Pickett, W. W. 1998. *Immobilized Low-Activity Waste Interim Storage Facility, Project W-520 Conceptual Design Report [DRAFT]*, HNF-3013, Rev. B, Fluor Daniel Northwest Company, Richland, Washington.

Puigh II, R. J. 1999. *Disposal Facility Data for the Hanford Immobilized Low-Activity Tank Waste*, HNF-4950, Rev. 1, Fluor Federal Services, Richland, Washington, December 1999.

Rawlins, J. A., R. A. Karnesky, R. Khaleel, A. H. Lu, F. M. Mann, B. P. McGrail, W. J. McMahon, M. G. Piepho, P. D. Rittmann, and F. Schmittroth. 1994. *Impacts of Disposal System Design Options on Low-Level Glass Waste Disposal System Performance*, WHC-EP-0810, Revision 0, Westinghouse Hanford Company, Richland, Washington.

Rittmann, P. D. 1993. *GRTPA - A Program to Calculate Human Dose from PORFLOW Output*, WHC-SD-WM-UM-018, Westinghouse Hanford Company, Richland, Washington.

Taylor, W.J. 1999. *Contract No. DE-AC06-99RL14047 – Decision to Change the Immobilized Low-Activity Waste (ILAW) Disposal Baseline to Proceed with the Remote-Handled Trench Alternative*, letter 99-DPD-066 (correspondence control number 9958849), Department of Energy, Richland, Washington.

Thorne, P. D., and M. A. Chamness. 1992. *Status Report on the Development of a Three-Dimensional Conceptual Model for the Hanford Site Unconfined Aquifer System,* PNL-8332, Pacific Northwest Laboratory, Richland, Washington.

Thorne, P. D., and D. R. Newcomer. 1992. *Summary and Evaluation of Available Hydraulic Property Data for the Hanford Site Unconfined Aquifer System*, PNL-8337, Pacific Northwest Laboratory, Richland, Washington.

Thorne, P. D., M. A. Chamness., F. A. Spane Jr., V. R. Vermeul, and W. D. Webber. 1993. *Three-Dimensional Conceptual Model of the Hanford Site Unconfined Aquifer System, FY 93 Status Report,* PNL-8971, Pacific Northwest Laboratory, Richland, Washington.

Thorne, P. D., M. A. Chamness., V. R. Vermeul, Q. C. MacDonald, and S. E. Schubert. 1994. *Three-Dimensional Conceptual Model for the Hanford Site Unconfined Aquifer System, FY 1994 Status Report,* PNL-10195, Pacific Northwest Laboratory, Richland, Washington.

U.S. Department of Energy (DOE). 1994. *Remedial Investigation and Feasibility Study Report for the Environmental Restoration Disposal Facility,* DOE/RL-93-99, Rev. 1, Richland, Washington.

Walters, W. H., M. C. Richmond, and B. G. Gilmore. 1994. *Reconstruction of Radionuclide Concentrations in the Columbia River from Hanford, Washington to Portland, Oregon, January 1950 - January 1971,* BNWD-2225 HEDR, Battelle Pacific Northwest Division, Richland, Washington.

Wood, M. I., R. Khaleel, P. D. Rittmann, A. H. Lu, S. H. Finfrock, R. J. Serne, K. J. Cantrell, and T. H. DeLorenzo. 1995. *Performance Assessment for the Disposal of Low-Level Waste in the 200 West Area Burial Grounds,* WHC-ED-0645, Westinghouse Hanford Company, Richland, Washington.

Wood, M. I., R. Khaleel, P. D. Rittmann, S. H. Finfrock, T. H. DeLorenzo, and D. Y. Garbrick. 1996. *Performance Assessment for the Disposal of Low-Level Waste in the 200-East Area Burial Grounds*, WHC-SD-WM-TI-730, Rev. 0, Westinghouse Hanford Company, Richland, Washington.

Wurstner, S. K., P. D. Thorne, M. A. Chamness, M. D. Freshley, and M. D. Williams. 1995. *Development of a Three-Dimensional Groundwater Model of the Hanford Site Unconfined Aquifer System: FY 1995 Status Report*, PNL-10886, Pacific Northwest Laboratory, Richland, Washington.

Distribution

No. of Copies

OFFSITE

2 DOE/Office of Scientific and Technical Information

2 Wanapum Indian Band
P.O. Box 878
Ephrata, WA 98823
ATTN: R. Buck, Jr.
L. Seelatsee

5 Washington State Department of Ecology
Nuclear Waste Program
1315 West 4th
Kennewick, WA 99336-6018
ATTN: S. Dahl
D.N. Goswami

3 Yakima Indian Nation
P.O. Box 151
Toppenish, WA 98948
ATTN: R. Jim
W. Rigsbee

2 Confederated Tribes of the Umatilla Indian Reservation
P.O. Box 638
Pendleton, OR 97801
ATTN: J.R. Wilkinson
S. Harris

2 Nez Perce Indian Tribe
P.O. Box 365
Lapwai, ID 83540-0365
ATTN: D.L. Powaukee
S.M. Sobczyk

No. of Copies

OFFSITE

2 Oregon Department of Energy
625 Marion St. N.E.
Salem, OR 97310
ATTN: R. Bennett
M.L. Blazek

1 U.S. Ecology
P.O. Box 638
Richland, WA 99352
ATTN: S. Bede

1 Department of Health
Division of Radiation Protection
Waste Management Section
P.O. Box 47827
Olympia, WA 98504-7827
ATTN: Maxine Dunkleman

ONSITE

7 CH2M Hill Group

D. A. Burbank	H4-02
K. C. Burgard	H4-02
A. J. Knepp	H0-22
F. M. Mann (3)	H0-22
G. L. Parsons	H4-02

3 DOE Office of River Protection

C. A. Babel (2)	H6-60
P. E. LaMont	H6-60

No. of Copies		
ONSITE		
9	DOE Richland Operations Office	
	P.F. Dunigan	A5-15
	B.L. Foley	H0-12
	R.D. Hildebrand	H0-12
	R.A. Holten	H0-12
	K.M. Thompson	H0-12
	DOE Public Reading Room	H2-53
1	CH2M Hill	
	L.C. Swanson	H9-02
5	Fluor Federal Services	
	S. W. Finfrock	B4-45
	R. Khaleel	B4-43
	R.J. Puigh (3)	B4-43
1	International Technologies	
	D.A. Myers	G3-21
2	BHI	
	B. H. Ford	HO-19
	G. A. Jewel	HO-21
1	Fluor Hanford	
	M.I. Wood	H8-44

No. of Copies		
ONSITE		
37	Pacific Northwest National Laboratory	
	M.P. Bergeron (10)	K9-36
	R. W. Bryce	K6-75
	C.R. Cole	K9-36
	P.E. Dresel	K6-96
	M.J. Fayer	K9-36
	M.D. Freshley	K9-36
	E. J. Freeman	K9-36
	J. Fruchter	K6-96
	G.W. Gee	K9-36
	V.G. Johnson	K6-96
	C.T. Kincaid	K9-36
	S. Luttrell	K9-96
	B. P. McGrail	K2-38
	P.D. Meyer	K9-36
	S. Reidel	K6-96
	R.J. Serne	K6-81
	R.M. Smith	K6-96
	P.D. Thorne	K9-36
	S.K. Wurstner (5)	K9-36
	Information Release Office (5)	
2	U.S. Environmental Protection Agency	
	D.R. Sherwood	B5-01